REPUBLIC OF CAMEROON

REPUBLIQUE DU CAMEROUN

MINISTRY OF HIGHER EDUCATION

MINISTERE DE L'ENSEIGNEMENT SUPERIEUR

Ecole Nationale Supérieure des Travaux Publics

DEPARTMENT OF CIVIL ENGINEERING

DEPARTEMENT DE GENIE CIVIL

UNIVERSITÀ DEGLI STUDI DI PADOVA

DEPARTMENT OF CIVIL, ARCHITECTURAL AND ENVIRONMENTAL ENGINEERING

INFLUENCE OF SOIL-STRUCTURE INTERACTION ON THE SEISMIC RESPONSE OF BUILDINGS CONSIDERING DIFFERENT TYPES OF SOIL

Thesis submitted in partial fulfilment of the requirement for the degree of Masters in Engineering

Curriculum: Civil Engineering

Presented by:

KWAYEP TCHATAT David Kevin

Student Matriculate number: **15TP20989**

Supervised by:

Prof. Carmelo MAJORANA

Co-supervised by:

Dr. Eng. Guillaume Hervé POH'SIE

Eng. Giuseppe CARDILLO

Academic year: 2019/2020

REPUBLIC OF CAMEROON

REPUBLIQUE DU CAMEROUN

MINISTRY OF HIGHER EDUCATION

MINISTERE DE L'ENSEIGNEMENT SUPERIEUR

Ecole Nationale Supérieure des Travaux Publics

DEPARTMENT OF CIVIL ENGINEERING

DEPARTEMENT DE GENIE CIVIL

UNIVERSITÀ DEGLI STUDI DI PADOVA

DEPARTMENT OF CIVIL, ARCHITECTURAL AND ENVIRONMENTAL ENGINEERING

INFLUENCE OF SOIL-STRUCTURE INTERACTION ON THE SEISMIC RESPONSE OF BUILDINGS CONSIDERING DIFFERENT TYPES OF SOIL

Thesis submitted in partial fulfilment of the requirement for the degree of Masters in Engineering

Curriculum: Civil Engineering

Presented by:

KWAYEP TCHATAT David Kevin

Student Matriculate number: **15TP20989**

Supervised by:

Prof. Carmelo MAJORANA

Co-supervised by:

Dr. Eng. Guillaume Hervé POH'SIE

Eng. Giuseppe CARDILLO

Academic year: 2019/2020

DEDICATION

To my beloved family, **KWAYEP**

ACKNOWLEDGEMENTS

First of all, I thank the Almighty God for giving me the courage, strength and patience to complete this modest work. This thesis is the fruit of the combined efforts of several individuals who contributed either directly or indirectly to its elaboration. It is therefore with gratitude that I address my sincere thanks to:

- The **President of the jury** Prof. **Carmelo MAJORANA** for the honour of accepting to preside this jury;
- The **Examiner** Dr **Deodonne KUNWUNFINE** of this jury for accepting to bring his criticisms and observations to ameliorate this work;
- My supervisors Dr Eng. **Guillaume Hervé POH'SIE** and Eng. **Giuseppe CARDILLO** for all the guidance, the advices and the patience provided to me during this work;
- The Director of the National Advanced School of Public Works (NASPW) of Yaoundé Prof. **NKENG George ELAMBO**, and Prof. **Carmelo MAJORANA** of University of Padua in Italy for all their academic and administrative support during these five years spent at NASPW;
- Prof. **MBESSA Michel**, the head of department of Civil Engineering for his tutoring and valuable advices;
- **All the teaching staff** of NASPW and University of Padua for their good quality teaching and the motivation they developed in us to continue our studies;
- My mother Mrs. **MBAKOP Philomene Brigitte** for the trust, love, unconditional support, valuable advices and efforts invested in me for the obtaining of this degree;
- My father Mr. **KWAYEP TONOU Roger** for the trust, love, unconditional support, valuable advices and efforts invested in me for the obtaining of this degree;
- Eng. **TCHIKAYA Gilles** for his support and valuable advices to achieve the set objectives of this thesis.
- Eng. **MOUSTAPHA HOUSSENI** for his support and guidance to achieve the set objectives of this thesis.
- **All my classmates** and my friends of the 6th batch of MEng in the National Advanced School of Public Works.
- To all people who, from near or far, have given me their heartfelt help in carrying out this work.

GLOSSARY

LIST OF ABBREVIATIONS AND SYMBOLS

EC	Eurocode
FFM	Free Field Motion
FIM	Foundation Input Motion
RC	Reinforced Concrete
SAP	Structural Analysis Program
SLS	Serviceability Limit State
SSI	Soil-Structure-Interaction
ULS	Ultimate limite state
A	Area of the cross section
A_c	Area of the concrete cross section
A_{min}	Minimum section area
A_{net}	Net area of the cross section
A_s	Area of the steel reinforcement section
A_{sw}	Cross sectional area of the shear reinforcement
B	Foundation half width
C	Modulus of subgrade reaction of the soil
C_{min}	Minimum concrete cover
$C_{min,b}$	Minimum cover due to bond requirement
$C_{min,dur}$	Minimum cover due to environmental conditions
Cs	Ordinate obtained from the design spectrum at period T
D	Embedment depth
$F_{Ed,Sup}$	Design support reaction
F_b	Shear force
G	Shear modulus
G1k	Structural load of the building
G2k	Non-structural load apply on the building
Hu	Transfer function
I_{xx}	Moment of inertia of the section along x axis
I_{yy}	Moment of inertia of the section along y axis
K_j	Static stiffness
L	Foundation half length
M_{sd+}	Positive moment at mid-span in hyperstatic condition

M_{sd-}	Negative moment at support in hyperstatic condition
M_{Ed}	Bending moment at support
M_{Rd}	Resisting moment
M_{Sd}	Soliciting bending moment
T	Period of the structure with fixed base
$\check{T}$	Period of the structure with flexible base
T_B	Lower limit of the period of the constant spectral acceleration branch
T_C	Upper limit of the period of the constant spectral acceleration branch
T_D	Value defining the beginning the constant displacement response range of the spectrum
T_x	Fictitious period along x
T_{yy}	Fictitious period along y
V_{app}	Apparent velocity
V_s	Shear velocity
W	Weight of the structure
a_g	Design ground acceleration
a_{0k}	Dimensionless frequency
b	Width of the element
b_t	Mean width of the tension zone
b_w	Smallest width of the cross section in the tensile area
c	Concrete cover
fcd	Design resisting strength of the concrete
f_{ctm}	Tensile strength of the concrete
f_y	Design yielding strength of the steel
f_{yd}	Design yielding strength of the steel
f_{yk}	Characteristic yield strength
f_{ywd}	Design yield strength of the shear reinforcement
g_k	Permanent load applied on the building
h	Structure height
k_x	Lateral stiffness of the foundation
k_{yy}	Rotational stiffness of the foundation
k_z^i	Individual spring stiffness
S	Soil factor
Sl,max	Maximum longitudinal spacing
St,max	Maximum transversal spacing

$S_e(T_{is}, \xi_{is})$	Spectral acceleration corresponding to the isolated period on the elastic spectrum of the project
$S_e(\mathrm{t})$	Elastic response spectrum
u_{FIM}	Foundation input motion
u_g	Free field motion
σ	Contact pressure
σ_{adm}	Admissible pressure on the soil
γ_c	Partial factor for concrete
γ_s	Partial safety factor for steel
λ	Slenderness
λ_{lim}	Limit value of slenderness
ν	Poisson's ratio
θ	Angle of concrete compression struts to the beam axis
ρ_w	Shear reinforcement ratio
$\rho_{w,min}$	Minimum shear reinforcement ratio
σ_c	Stress in the concrete
σ_s	Stress in the reinforcement
α_j	Dynamic modifier
β_f	Foundation damping that ranges between 0% and 25%
β_i	Structural damping
β_s	Hysteretic damping
β_x	Translational damping
β_{yy}	Rotational damping
ω	Seismic wavelength frequency
α	Adhesion coefficient
η_j	Embedment modifier

ABSTRACT

The main objective of this work was to study the effect of soil structure interaction (SSI) on the seismic response of a building considering different types of soil condition. To achieve this goal, an evaluation of the behaviour of a building with three types of soil namely shale, dense sand and soft clay was done. A literature review was carried out to highlight the basic principles related to soil-structure interaction, the methods used to study it and its effects on the seismic demands of buildings. The methodology adopted consisted first in a site recognition and the collection of geometric data of the building prototype. After, the case study which is an irregular G+6 storey office building with two (02) basements was analysed and designed under static loads according to European standards. The underneath soil was modelled using Winkler springs approach to depict soil flexibility. Then, the building was subjected to the Loma Prieta earthquake of USA in 1989 using SAP 2000 (Structural Analysis Program) version 22. The results are presented and compared in terms of vibration period, lateral deformation, inter-storey drift, storey shear and base shear for the different types of soil condition. The results showed that as stiffness of the subsoil decreases, the effects of soil-structure interaction become more dominant and detrimental to the seismic behaviour of reinforced concrete buildings. SSI leads to an increase of the vibration period, lateral deformation, inter-storey drift, storey shear and base shear in the superstructure especially in the case of dense sand and soft clay. The results led to a criterion indicating that considering SSI in dynamic design for buildings on medium and soft soil is essential.

Keywords: Soil-Structure Interaction, seismic response, types of soil, Winkler method.

RESUME

L'objectif principal de ce travail est d'étudier l'effet de l'interaction sol-structure (ISS) sur la réponse sismique d'un bâtiment en considérant différents types de sol. Pour atteindre cet objectif, une évaluation du comportement d'un bâtiment reposant sur trois types de sol à savoir du schiste, du sable dense et d'une argile molle a été faite. Une revue de la littérature a été effectuée pour mettre en évidence les principes de base liés à l'interaction sol-structure, les méthodes utilisées pour l'étudier et ses effets sur les exigences sismiques des bâtiments. La méthodologie adoptée a consisté d'abord en une reconnaissance du site et la collecte de données géométriques du prototype de bâtiment. Ensuite, le cas d'étude, qui est un immeuble irrégulier à usage de bureaux de type R+6 avec deux (02) sous-sols, a été analysé et conçu sous des charges statiques selon les normes européennes. Le sol sous-jacent a été modélisé en utilisant l'approche des ressorts de Winkler pour décrire la flexibilité du sol. Ensuite, le bâtiment a été soumis au tremblement de terre de Loma Prieta qui a été enregistré aux Etats-Unis en 1989 en utilisant SAP 2000 (Structural Analysis Program) version 22. Les résultats sont présentés et comparés en termes de période de vibration propre, de déformation latérale, de déplacement inter-étage, du cisaillement d'étage et du cisaillement de base pour les différents types de sol. Les résultats ont montré que lorsque la rigidité du sol de fondation diminue, les effets de l'interaction sol-structure deviennent plus dominants et nuisibles au comportement sismique des bâtiments en béton armé. L'ISS conduit à une augmentation de la période de vibration propre, de la déformation latérale, du déplacement inter-étage, du cisaillement d'étage et de l de base dans la superstructure, en particulier dans le cas d'un sable dense et d'une argile molle. Les résultats ont conduit à un critère indiquant que la prise en compte de l'ISS dans la conception dynamique des bâtiments sur des sols à souplesse moyenne et grande est essentielle.

Mots clés : Interaction sol-structure, réponse sismique, types de sol, méthode de Winkler.

LIST OF FIGURES

LIST OF TABLES

TABLE OF CONTENT

GENERAL INTRODUCTION

Earthquakes are among the most devastating natural disasters which humans have faced over history. Since civilization has developed, and demand for all kind of buildings and other type of structures has increased, with the development of civilization during the last century, buildings and infrastructures have increased exponentially in number and size, which inherently has increased the risks related to earthquakes.

Since the design of earthquake resistant buildings started assumption made that supports are fixed and traditionally soil-structure interaction effects were ignored in seismic design of structures, since they were believed to only have favourable effects. The lengthening of the period shifts the structure response to the spectral branch of lower accelerations which implies a reduction of inertia forces in the structure. However, along modern response spectrum analysis principles, soil structure interaction effects are recognized to not necessarily have beneficial but even may have very detrimental effects for the response of the superstructure. The global trend shift towards Earthquake resistance design in the seismic engineering branch implies an increasing focus on displacements rather than on inertia forces, which makes proper consideration of soil structure interaction a critical factor.

The effects of soil-structure interaction have been subjective to research for about half a century, but are still under discussion. Code provisions relating to soil-structure interaction nowadays are still very limited and straight forward procedures to account for soil structure interaction in design are not included in most codes.

The aim of this work is to evaluate and quantify the effect of soil-structure interaction on the seismic response of a reinforced concrete building considering different types of soil condition.

To attain this objective, the work is divided in three chapters. The first chapter is about the state of the art and will permit to master the basic concepts related to SSI. The second chapter entitled methodology will present the steps adopted to achieve the objective of this work. Finally, at chapter three the results of the comparison of the seismic demands for the different types of soil will be presented.

CHAPTER 1: LITTERATURE REVIEW

Introduction

All the civil engineering structure consist of structural elements which are directly supported on ground. Conventional structural design methods neglect SSI effects. However, in dynamic analysis of a building structure, the base support condition is very essential for calculating its dynamic behaviour and useful for estimating structural responses and distribution within structural members. Unfortunately, the application of SSI for building is hindered by a literature that is often difficult to understand, and codes that contain limited guidance. This chapter is intended to provide background for the implementation of SSI by presenting the SSI principles, and the methods used to study it. Then the effects of SSI on the seismic performance of buildings will be presented.

1.1 Soil as support of structures

Soil is an aggregation of particles that may range very widely in size .It is the by-product of mechanical and chemical weathering of rock .Some of these particles are given specific names according to their sizes, such as gravel, sand ,silt, clay and so on.

1.1.1. Foundation subsoil

We are concerned with placing the foundation on either soil or rock .This material may be under water as for certain bridge and marine structure, but more commonly we will place the foundation on soil or rock near the ground surface.

Soil may be described as residual or transported. Residual soil is formed from weathering of parent rock at the present location. It usually contains angular rock fragments of varying size in the soil-rock interface zone. Transported soils are those formed from rock weathered at one location and transported by wind, water, ice or gravity to the present site. The terms residual and transported must be taken in the proper context, for many current residual soils are formed from transported soil deposits of earlier geological periods, which indurated into rocks. Later uplifts have exposed these rocks to a new onset of weathering .Exposed limestone ,sandstone ,and shale are typical of indurated transported soil deposits of earlier geological eras that have been uplifted to undergo current weathering and decomposition back to soil to repeat geological cycle (Bowles,1996).

Residual soils are usually preferred to supports foundations as they tend to have better engineering properties. Soils that have been transported particularly by wind or water are often

of poor quality .These are typified by small grain size, large amounts of pore space, potential for the presence of large amounts of pore water and they often are highly compressible. Note, however, exceptions that produce poor quality residual soils and good quality transported soil deposits commonly exist. In general, each site must be examined on its own merits.

1.1.2. Elastic properties of soil

Hooke's generalized stress-strain law is commonly used in solving geotechnical problems of stress and settlement .The stress-strain modulus Es, poison's ration ν, and the modulus of subgrade reaction Ks are the elastic properties of most interest. These values are commonly used in computing estimates of foundation settlements (Bowles,1996).

The stress strain modulus can be obtained from the slope of stress-strain curves from triaxial tests. It is often estimate from field test. Typical values ranges for several soils are given in table 1.1. The Poisson's ratio is used in both pressure and settlement studies and is defined as the ratio of axial compression εv to lateral expansion εl strain. Table 1.2 gives values range for the Poisson's ratio for certain types of soil .The subgrade modulus, also known as the modulus of subgrade reaction, is a stiffness parameter typically used in defining the support conditions of footings and mat foundations. Physically, however, it is defined as the contact bearing pressure of the foundation against the soil that will produce a unit deflection of the foundation. The use of the parameter implies a linear elastic response, and therefore in design, the pressure generate by the subgrade modulus is always limited by the allowable bearing pressure of the soil (Bowles,1996).

Table 1.1. Value range for the elastic stress-strain modulus Es for selected soils (Bowles,1996)

Soil	Es,MPA
Clay	
Very soft	2-15
Soft	5-25
Medium	15-50
Hard	50-100
Sandy	25-250
Glacial till	
Loose	10-150
Dense	150-720
Very dense	500-1440
Sand and gravel	
Loose	50-150
Dense	100-200
Shale	150-5000
Silt	2-20

Table 1.2. Value range for the Poisson's ratio for selected soils (Bowles,1996)

Poisson's ratio	Soil type
0.4-0.5	Most clay soil
0.45-0.5	Saturated clay soils
0.3-0.4	Cohesionless-medium and dense
0.2-0.35	Cohensionless-loose to medium

1.2. Soil-structure interaction

Usually in the seismic design of ordinary building, soil structure interaction is neglected and the dynamic response of the structure is evaluated under the assumption of a fixed base response. However during seismic loading the soil undergoes deformations which are imposed to the foundation. The question naturally arises of knowing if the motion in the vicinity of the structure is altered by the presence of the structure and how the structure response is modified

by the compliance of the supporting soil. This interaction between the structure and the soil is named soil-structure interaction.

1.2.1. Numerical methods in the SSI analysis

SSI problems have been solved using numerous approaches in literature. Experimental analyses such as shaking table and centrifugal tests have been attempted but they revealed to be expensive. Practically, the techniques used are the direct approach and the sub-structural approach.

1.2.1.1. Direct approach

The direct approach evaluates SSI by modelling a limited soil domain along with the foundation system, superstructure, transmitting boundaries along the perimeter of the soil domain, and interface elements between the foundation system and soil as shown in figure 1.1. Therefore, the direct solution considers the complete soil-structure system and solves this problem in one step. For this method, it is necessary to evaluate the input ground motion at the base of the numerical model consistent with the desire seismic design hazard level. This input ground motion is typically obtained using deconvolution or using outcrop motions available. However, since the availability of outcrop motions is limited, site response analyses are usually performed to get this input ground motion using deconvolution. Commercially available finite element programs such as ABAQUS, ANSYS, and LS-DYNA, or the open-source finite element program, OpenSees, can perform nonlinear analysis considering SSI and using the direct approach. Other programs such as SASSI2000 can execute multi-step linear analysis considering SSI with the direct approach.

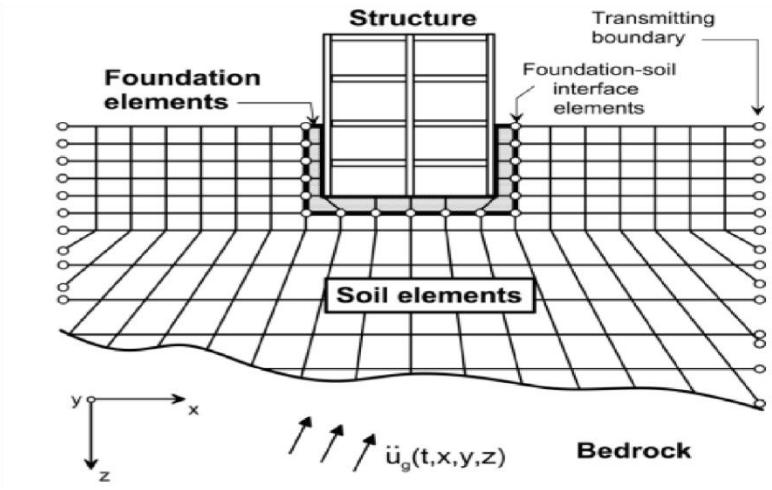

Figure 1.1. Schematic illustration of a direct analysis of SSI (NIST, 2012).

The transmitting boundary, defined as a special consideration of the external fictitious boundary of the soil model to eliminate wave reflections and to apply seismic excitations, is a requirement of this approach. Lysmer et al. (1969) proposed a simple viscous local boundary modelling, which comprises two series of dashpots oriented normal and tangential to the boundary of FE mesh. This approach has the advantage that it can consider nonlinear behaviour of soil and superstructure. If the system is treated as being fully linear, the solution can be carried out in the frequency domain. But if the structure foundation subsystem is modelled as a nonlinear system the solution should be carried out in the time domain. In the latter case, the coupled nonlinear equations of motion are solved using standard step-by-step numerical integration procedures (Arefi, 2008).

By using the direct approach, kinematic and inertial interaction effects are automatically included in the numerical model. Nevertheless, this approach is computationally demanding and time-consuming, so direct analyses for SSI are seldom used in practice. The substructure approach is more often implemented in design offices for the seismic design of buildings considering SSI.

1.2.1.2. Sub-structural approach

The substructure approach is a multi-step procedure for which it is necessary to determine the seismic motion of the foundation or foundation input motion (FIM) without any structure, evaluate the dynamic stiffness of the foundation as a function of frequency for a steady state harmonic excitation as well and finally perform dynamic analysis of the structure using the dynamic stiffness and the seismic motion applied at the base of the structural model.

By partitioning the soil system into a simpler sets as in figure 1.2, the three main steps in the substructure method are presented. The first step is to evaluate the foundation input motion (FIM), which is the motion that would occur on the base slab if the structure and foundation had no mass; the second step consist to determine the impedance function that describes the stiffness and damping characteristics of the foundation-soil system; and the final step is a dynamic analysis of the structure supported on a compliant base that is represented by impedance. It includes both geotechnical analysis which are foundation input motion and subgrade impedances, and structural analysis.

Numerous studies (Kutanis et al. 2001; Carbonari et al. 2011; Allotey et al. 2008; Liu et al. 2015) have been performed using the substructure method to assess the seismic response of structural systems while considering soil–structure interaction. This method has a lot of conveniences for both modelling and computation. However, since this method is based on

the principle of superposition, any predictions would only be accurate for linear soil and structural behaviours, while approximations of soil non-linearity by means of iterative wave propagation analyses, would allow the superposition to be applied to moderately non-linear systems (Wolf, 1998).

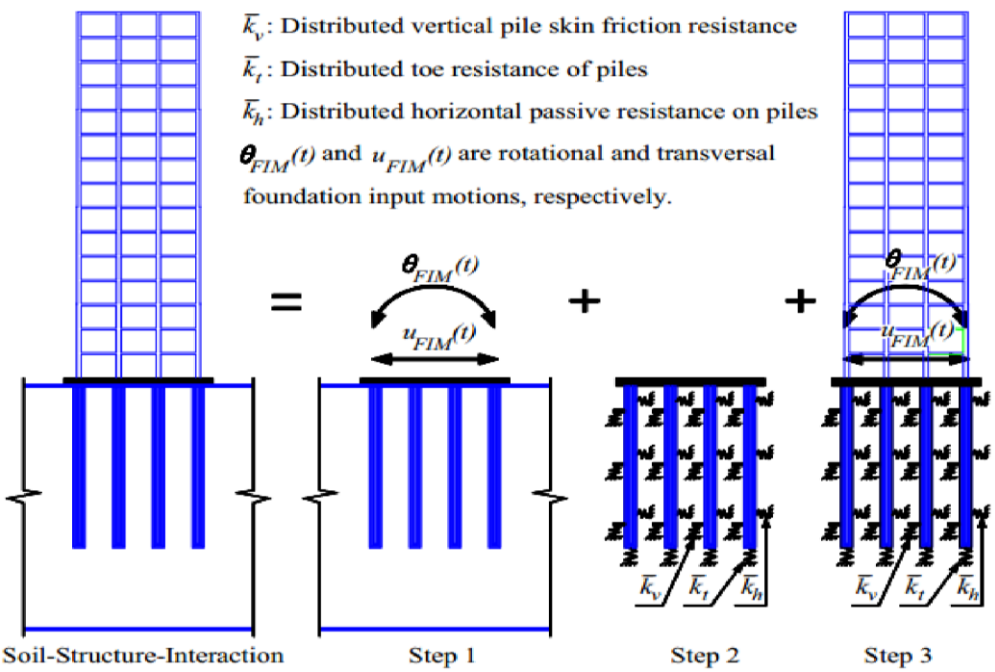

Figure 1.2. Substructure method for modelling the soil–pile–structure interaction (Moustapha, 2019).

1.2.2. Soil-structure interaction components

The earthquake design loads applied to the foundation arise from the inertia forces developed in the superstructure and from the soil deformations, caused by the passage of seismic waves, imposed on the foundations. These two phenomena are referred in the technical literature as inertial and kinematic interaction.

1.2.2.1. Inertial interaction

Inertial interaction results from the inertia developed in the structure as its own vibration produces base shear, moment, and torsional excitation. These forces generate displacements and rotations at the soil-foundation interface.

a. Soil-structure system behaviour

Inertial forces obtained from the analysis of a structure with fixed base are different from a structure with flexible base. In fact, soil flexibility modifies the response of structure due to the period lengthening and damping increase. To appreciate the inertial interaction effect, a

non-dimensional parameter has been proposed by Bielak (1974) and Veletsos et al (1975) as shown in expression 1.1.

$$\frac{h}{Vs\,T} \tag{1.1}$$

Where:

h is the structure height;

Vs is the shear wave velocity;

T is the period of the structure.

The term in relation 1.1 represents the structure-to-soil stiffness ratio and is the most important parameter controlling the significance of inertial interaction. Studies done by Stewart et al showed that the SSI effects are generally negligible for $h/(VsT) < 0.1$, which occurs in flexible structures (e.g., moment frame buildings) located on competent soil or rock. For typical building structures on soil and weathered rock sites, $h/(V_sT)$ is less than 0.1 for moment frame structures, and between approximately 0.1 and 0.5 for shear wall and braced frame structures.

b. Impedance functions

Impedance functions represent the stiffness and damping characteristics of the foundation-soil system under dynamic loads. For a complete 3-D model, six dynamic impedances are needed, three translational and three rotational, in order to evaluate the dynamic equilibrium equation of a rigid foundation. These impedances are a function of the foundation geometry, the soil properties, and frequency of the structure-foundation-soil system.

Many analytical solutions for impedance functions have been developed for rigid circular and rectangular footings on the surface or embedded within the soil. These solutions were evaluated for a uniform, elastic, or visco-elastic half space. Pais et al (1988), Gazetas (1991), and Mylonakis et al. (2006) reviewed impedance functions for rigid rectangular footings resting on the surface of a half-space. These analytical solutions describe translational stiffness and damping along axes x, y, and z, and rotational stiffness and damping about those axes. These equations for stiffness are a function of the foundation dimensions, soil shear modulus, G,

Poisson's ratio of the soil, ν, dynamic stiffness modifiers, αj, and the embedment modifiers, ηj. The general expression for evaluating the dynamic stiffness, *K*j, can be expressed using equation 1.2.

$$k_j = K_j \alpha_j \eta_j \qquad (1.2)$$

Where:

K_j is the static stiffness;

α_j is the dynamic modifier;

η_j is the embedment modifier;

j is an index denoting the mode of vibration (translation or rotation).

Equations for evaluating stiffness, embedment factors and dynamic correction factors sated by Pais et al. (1988) are shown in table 1.3 and table 1.4. Figure 1.4 presents the geometry of the foundation entering in the evaluation of these stiffnesses.

Table 1.3. Elastic solutions for static stiffness of rigid footings at the ground surface and embedment correction factors (NIST 2012).

Degree of freedom	Static Stiffness	Embedment modifier
Translation along z-axis	$K_{z,sur} = \frac{GB}{1-v}\left[3.1\left(\frac{L}{B}\right)^{0.75} + 1.6\right]$	$\eta_z = \left[1.0 + \left(0.25 + \frac{0.25}{L/B}\right)\left(\frac{D}{B}\right)^{0.8}\right]$
Translation along y-axis	$K_{y,sur} = \frac{GB}{2-v}\left[6.8\left(\frac{L}{B}\right)^{0.65} + 0.8\left(\frac{L}{B}\right) + 1.6\right]$	$\eta_y = \left[1.0 + \left(0.33 + \frac{1.34}{1+L/B}\right)\left(\frac{D}{B}\right)^{0.8}\right]$
Translation along x-axis	$K_{x,sur} = \frac{GB}{2-v}\left[6.8\left(\frac{L}{B}\right)^{0.65} + 2.4\right]$	$\eta_y \approx \eta_z$
Torsion about z-axis	$K_{z,sur} = GB^3\left[4.25\left(\frac{L}{B}\right)^{2.45} + 4.06\right]$	$\eta_z = \left[1.0 + \left(1.3 + \frac{1.32}{L/B}\right)\left(\frac{D}{B}\right)^{0.9}\right]$
Torsion about y-axis	$K_{yy,sur} = \frac{GB^3}{1-v}\left[3.73\left(\frac{L}{B}\right)^{2.4} + 0.27\right]$	$\eta_{yy} = \left[1.0 + \left(0.25 + \frac{1.32}{L/B}\right)\left(\frac{D}{B}\right)^{0.9}\right]$
Torsion about x-axis	$K_{xx,sur} = \frac{GB^3}{1-v}\left[3.2\left(\frac{L}{B}\right) + 0.8\right]$	$\eta_{xx} = \left[1.0 + \frac{D}{B}\left(\frac{1.6}{0.35 + L/B}\right)\left(\frac{D}{B}\right)^2\right]$

Table 1.4. Dynamic correction factor for static stiffness of rigid footings (NIST, 2012).

Degree of freedom	Dynamic Modifier
Translation along z-axis	$a_z = 1.0 - \left[\frac{\left(0.4 + \frac{0.2}{L/B}\right){a_o}^2}{\left(\frac{10}{1+3(L/B-1)}\right) + {a_o}^2}\right]$
Translation along z-axis	$a_y = 1.0$
Translation along z-axis	$a_x = 1.0$
Torsion about z-axis	$a_{zz} = 1.0 - \left[\frac{\left(0.33 + 0.03\sqrt{L/B-1}\right){a_o}^2}{\left(\frac{0.8}{1+0.3(L/B-1)}\right) + {a_o}^2}\right]$
Torsion about y-axis	$a_{yy} = 1.0 - \left[\frac{0.55{a_o}^2}{\left(0.6 + \frac{1.4}{(L/B)^3}\right) + {a_o}^2}\right]$
Torsion about x-axis	$a_{xx} = 1.0 - \left[\frac{\left(0.55 + 0.01\sqrt{L/B-1}\right){a_o}^2}{\left(2.4 - \frac{0.4}{(L/B)^3}\right) + {a_o}^2}\right]$

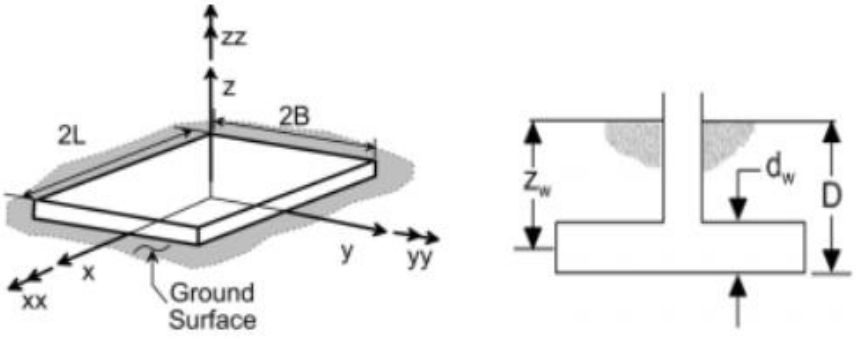

(a) (b)

Figure 1.3. Foundation geometry :(a) Rigid footing at ground surface, (b) embedded footing (NIST, 2012).

Other formulations are available in literature such as the Newmark-Rosenblueth method, the Deleuze method. All these methods strictly apply for rigid foundations, but other formulations exist for flexible structural elements.

1.2.2.2. Kinematic interaction

Ground motion induces soil deformation known as free-field motion. However, stiff foundation embedded in the soil will not follow that free-field motion. Kinematic interaction is this inability of the foundation to conform to the deformations of the free field ground motion (Kramer,1996).

a. Base-slab averaging

Base slab averaging results from the adjustment of the ground motion within the foundation footprint due to the stiffness and strength of the foundation system. Motions of surface foundations are modified relative to the free-field when seismic waves are incoherent. Incoherence of the incident waves at two different points means that they have variations in their phase angle. The effect is greater at higher frequencies and is caused by different ray paths and local heterogeneity in the geologic media through which seismic waves travel (Goyez, 2017). Therefore, base-slab averaging is caused by waves which have an incidence angle relative to the vertical, or which are incoherent in time and space. In the presence of incoherent wave fields, translational base-slab motions are reduced relative to the free-field, and rotational motions are introduced. The reduction in translational motion is generally the most important result (NIST, 2012).

There are many analytical equations for predicting the relationship between the foundation input motion (FIM) and the free-field motion (FFM) for the case of inclined, otherwise coherent, shear waves. A model was suggested by Mylonakis et al. in 2006, which considers wave passage effects to evaluate transfer functions, *Hu*. This model relates the seismic wavelength frequencyω, the shear velocity V_s, the apparent velocity V_{app}, the displacement of the foundation input motion, u_{FIM}, and the free-field motion, u_g, by using equations 1.3 to 1.6.

$$U_{FIM} = \text{Hu Ug} \tag{1.3}$$

$$\text{Hu}=\frac{Sin(a_0^k\left(\frac{Vs}{Vapp}\right))}{a_0^k\left(\frac{Vs}{Vapp}\right)}\ , a_0^k \leq \frac{\pi}{2}\frac{Vs}{Vapp} \tag{1.4}$$

$$\text{Hu}=\frac{\pi}{2},\ a_0^k \geq \frac{\pi}{2}\frac{Vs}{Vapp} \tag{1.5}$$

$$a_0^k=\frac{\omega Be^A}{Vs} \tag{1.6}$$

Where:

a_0^k is the dimensionless frequency;

Be^A is defined as function of the foundation area A and is expressed by using equation 1.7.

$$Be^A = \sqrt{\frac{A}{4}} \tag{1.7}$$

From array studies (Ancheta et al., 2011), *Vapp* ranges from approximately 2.0 km/s to 3.5 km/s, so a reasonable estimation of the velocity ratio, *Vapp/Vs*, for typical soils is approximately 10.The transfer function between u_{FIM} and u_g based on equations 1.1 to 1.4 is illustrated in the figure 1.4 Using this model, wave passage alone causes relatively modest base-slab reductions in ground motion.

Veletsos et al in 1997 developed several transfer functions between translational and torsional foundation motions and the free field ground motion. These functions are strongly dependent upon a parameter, κa, related to lagged coherency and wave inclination. By matching model predictions to observed variations between foundation input and free-field ground motions from instrumented buildings, Kim et al in 2003 developed a semi-empirical model for κa which is presented in equation 1.8.

$$\kappa_a = 0.00065 \times V_s,\ 200 < V_s < 500\ ^m/_s \tag{1.8}$$

Transfer functions calculated with this semi-empirical approach for upper and lower limits of κ*a* are shown in figure 1.4.

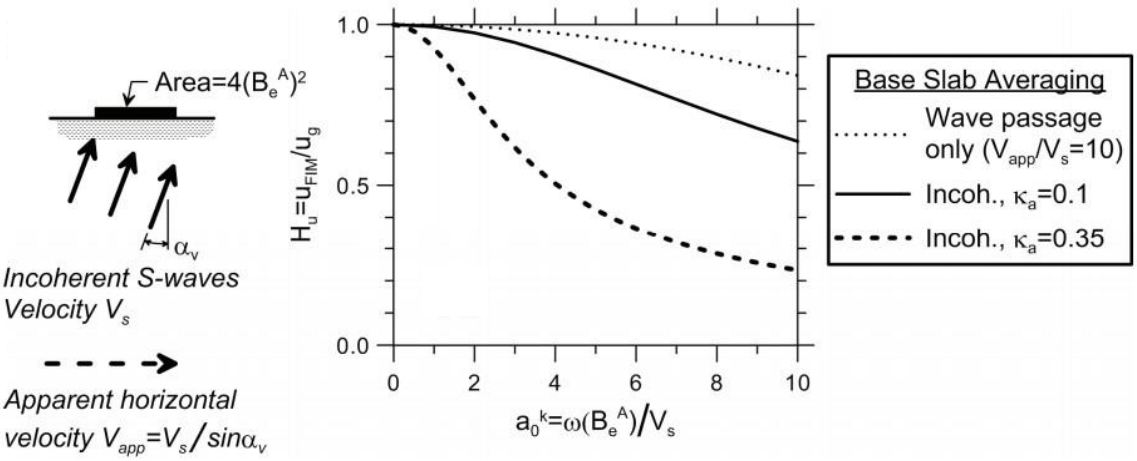

Figure 1.4. Base slab averaging effects (NIST, 2012).

b. Embedment effects

For a structure that has a basement level, foundation-level motions are further reduced as a result of ground motion reduction with depth below the free surface. Analytical solutions are

available to consider embedment effects for rigid cylinders embedded in a uniform soil of finite or infinite thickness. NIST (2012) presents studies conducted by Kausel et al. (1978) and Day (1978) to describe FIM at the base of embedded cylinders as a function of FFMs. The FFM for these cylinders showed a reduction in its translation mode when subjected to vertically propagating coherent shear waves because of ground motion reductions with depth and wave scattering. In addition, as a result of differential displacements imposed to the cylinders over their embedment depth, rotations in the vertical plane are developed. As a result of the aforementioned studies, transfer functions for translational and rotational motions, *Hu* and *Hyy*, were adapted for rectangular foundations as shown in equations 1.9 to 1.12.

$$H_u = \frac{U_{FIM}}{U_g} = \cos\left(\frac{D}{B_e} a_0^k\right) = \cos\left(\frac{D\,\omega}{V_S}\right), \frac{D\,\omega}{V_S} < 1.1 \quad (1.9)$$

$$H_u = 0.45\,, \frac{D\,\omega}{V_S} > 1.1 \quad (1.10)$$

$$H_{yy} = 0.26\left[1 - \cos\left(\frac{D\,\omega}{V_S}\right)\right], \frac{D\,\omega}{V_S} < \frac{\pi}{2} \quad (1.11)$$

$$H_{yy} = 0.26\,, \frac{D\,\omega}{V_S} > \frac{\pi}{2} \quad (1.12)$$

Where:

D is the embedment depth;

Vs is the average effective profile velocity.

All these equations need to be carefully used because most of them were calibrated for specific foundation conditions, soil types, and wave propagation directions, so their application is limited to those unique scenario (Goyez, 2017).

The above equations suggested for evaluating translational and rotational transfer functions are plotted in figure 1.5. It can be seen from that figure 1.5 there is a significant reduction in the FFM at high frequencies, at approximately 70% of the fundamental frequency of the soil column. By further inspection of figure 1.5, it is observed that the effect of the embedment on the de-amplification of the ground motions is greater in comparison with base-slab averaging. On the other hand, the rotational transfer function, Hyy, increases with frequency.

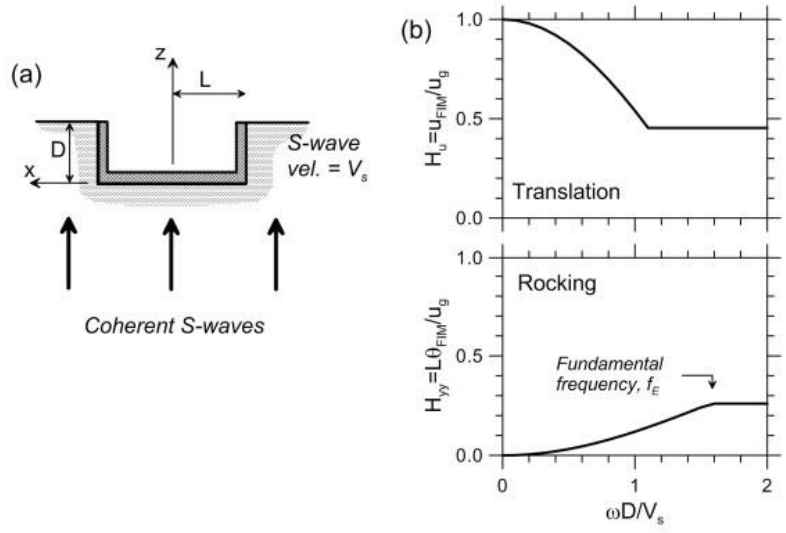

Figure 1.5. Foundation subjected to shear waves: (a) schematic geometry (b) Transfer function for foundation subjected to translation and rocking (NIST,2012)

1.2.3. Effects of SSI on building performance

Many researches showed that SSI has non-negligible effects on the seismic demands of buildings. In fact, SSI changes the building vibration characteristics and seismic demands including the base shear, lateral deformation, storey drifts, moment at beam ends and force of inner columns.

1.2.3.1. Period lengthening

Soil flexibility can be a source of energy dissipation that affects the dynamic properties of the structure-foundation-soil system. As discussed above, a rigid base is the most common support assumption used in practice for modelling structures. This support condition assumes that the soil foundation interface is infinitely rigid. On the other hand, a flexible base considers the deformability of the foundation system and the soil, and it leads to an increase of the system period.

A schematic illustration of the fixed and flexible base conditions for a single-degree-of-freedom structure with a force concentrated at the top can be seen in the figure.1.6 The lateral deflection $\tilde{\Delta}$ of the structure with a fixed base presented in the figure 1.6(a) is caused by its translational displacement; however, the lateral deflection, $\tilde{\Delta}$, of this structure with a flexible base illustrated in figure 1.6 b is not just function of its translational displacement, but also the rotation of the foundation system. The undamped period of vibration, T, for the structure with a fixed base can

be calculated as function of the circular frequency ω, mass, m, and stiffness, k, using the equation (1.13) (Clough & Penzien, 1993):

$$T=\frac{2\pi}{w}=2\pi\sqrt{\frac{m}{k}} \qquad (1.13)$$

For the case of the flexible base, vertical kz, horizontal kx, and rotational springs kyy represent the flexibility of the soil-foundation system (see figure 1.6.b). The undamped period of vibration, $\tilde{T}$, for a structure with a flexible base can be estimated as a function of the structure height, h, spring constants at the foundation (kz, kx, and kyy), k, and T using the equation suggested by Veletsos et al (1974) expressed in equation 1.13. This period ratio is greater than unity based on the degree of flexibility of the structure-soil-foundation system.

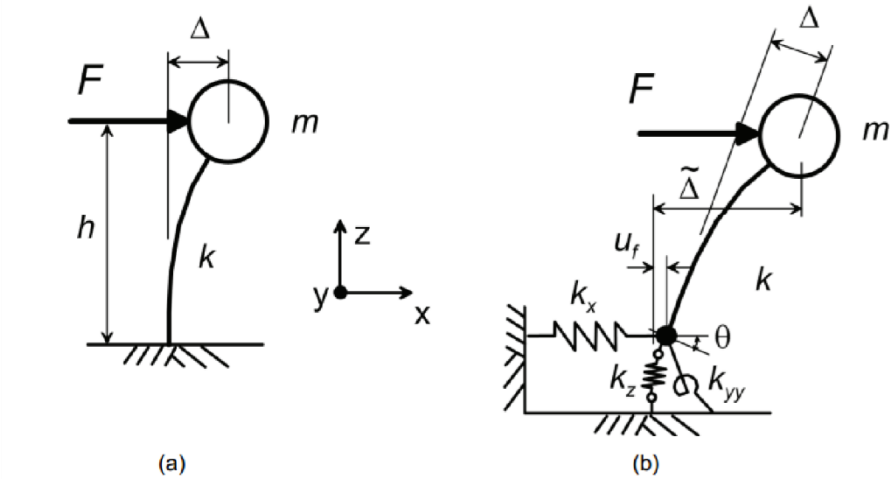

Figure 1.6. Schematic illustration of deflections caused by lateral force applied to: (a) structure with fixed base, (b) structure with flexible base (NIST, 2012).

1.2.3.2. System damping

The change in damping is one of the effects of the inertial interaction. There are two main sources of foundation damping that are the hysteric and radiation damping. Hysteretic damping is caused by the hysteric behaviour of soil under seismic excitation while radiation damping is originated by the radiation of the reflected wave-field away from the foundation. The damping of a flexible base system is greater compared to the structural damping due to the contribution of the foundation damping as shown in equation 1.14.

NIST (2012) presents works done by many researchers to develop analytical models for the evaluation of the foundation damping. Most of these models are frequency-dependent. One exception is the expression suggested by Wolf (1985) using a circular foundation resting on a halfspace, which ignores the frequency dependence of the foundation stiffness terms and assumes a linear foundation radiation damping. Similar to a previous study presented by Roësset (1980) considering frequency dependence, the expression initially suggested by Wolf's can be expressed using equation 1.14.

$$\beta_f = \left[\frac{(\frac{\tilde{T}}{T})^{n_s} - 1}{(\frac{\tilde{T}}{T})^{n_s}}\right] \beta s + \frac{1}{(\frac{\tilde{T}}{T})^{n_x}} \beta x + \frac{1}{(\frac{\tilde{T}}{T_{yy}})^{n_{yy}}} \beta yy \qquad (1.14)$$

Where:

β_s is the hysteric damping evaluated from information in the literature;

β_x is the translational damping;

β_{yy} is the rotational damping.

ns, nx, nyy are exponents that are equal to 2 for linear viscous damping and otherwise T_x *and* T_{yy} are the fictitious period defined by equation 1.15 and 1.16 respectively.

$$T_x = 2\pi \sqrt{\frac{m}{k_x}} \qquad (1.15)$$

$$T_{yy} = 2\pi \sqrt{\frac{mh^2}{k_{yy}}} \qquad (1.16)$$

From the increase in the damping it is obvious that when using a general acceleration response spectrum, consideration of SSI effects will reduce the response of the flexible base system.

1.2.3.3. Shear force distribution

As discussed above, SSI tends to increase the period and the damping of the system which leads to a change of the base shear given from the response spectrum as shown in the figure 1.7. The effect of SSI on base shear is related to the slope of the spectrum. Base shear tends to increase when the slope is positive and decrease when the slope is negative. For the common case of buildings with relatively long periods on the descending portion of the spectrum, the use of flexible base shear in lieu of fixed base shear typically results in the

reduction of the base shear demand. Conversely, inertial SSI can increase the base shear in relatively short-period structures.

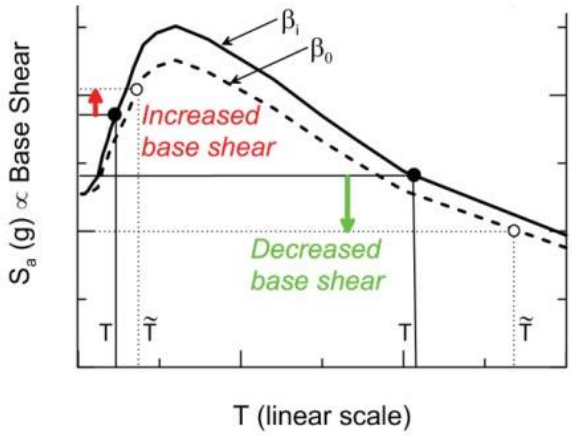

Figure 1.7. Illustration of the SSI effect on base shear due to the period lengthening and change in damping (NIST, 2012).

SSI also influences how the base shear is distributed in the superstructure. Several researchers as Hokmabadi et al (2015), Abdelraheem (2014) and Bargheri et al (2018) studied the effect of SSI on the distribution of shear force in the structural elements of a building and concluded that although SSI reduced the shear forces but the amount and trend of this reduction was not the same at every level. In fact, in the structure analysed by Hokmabadi & Fatahi (2015) the maximum shear force experienced in the first level of the 15 storey superstructure supported by the pile-raft foundation reduced by 38% compared to the fixed-based structure under the impact of the 1994 Northridge earthquake, whereas the seventh level experienced virtually no reduction in the generated shear force (less than 10%). As a consequence, practicing engineers should realise that the reduction ratio for the maximum base shear due to SSI cannot be generalized to all levels of the superstructure because it could result in an unsafe design.

1.2.3.4. Lateral deformation and inter-storey drift.

Overall lateral deformation and inter-storey drift are the most used damage parameters in the performance-based seismic design approach. The increase in the lateral deformation of the building can change the performance level of the structure and is particularly important in tall, slender, and closely spaced structures that can be subjected to pounding when relative displacements are large (Kramer 1996). Moreover, increase in the total deformation of the structure, and in turn secondary P- Δ effect, influences the total stability of the structure as well as the performance of the non-structural elements. Storey drift ratio is the

maximum relative displacement of each floor divided by the height of the same floor and is strictly connected to the damage suffered by both structural and non-structural elements. In general, SSI leads to an increase of the lateral deflection.in the superstructure.

Conclusion

In this first chapter, we were interested in understanding the basic concepts related to SSI. It is found that for a structure resting on a soft soil, the dynamic response will be different for that of a flexible base condition due to the interactions between the structure, the foundation, and the soil underlying and surrounding the foundation. Various numerical methods are available to study the behaviour of structures on soft soil. However, the application of simple methods, such as the Winkler approach, is preferred in practical SSI problems rather than the direct method. Although not widely used in practice, engineering guidelines are available in seismic codes like Eurocode 8 and NEHRP for simple evaluation of SSI effects. In general, SSI effects can be summarized as follows: increase of the natural period of the system, increase in damping, increase in the rate of the lateral displacement, and change in the force demands of the structure. Our analysis will be based on a new building and the methodology that will be adopted is presented in the next chapter.

CHAPTER 2: METHODOLOGY

Introduction

The methodology is a part allowing to establish the procedure of the research in order to attain the fixed objectives. In other words, it will be question of describing the different constitutive elements of our research. In this work, the first step consists in a site recognition through a documentary research followed by the data collection. Then, the norms used and the design procedure for elements such as beam, column, retaining wall and foundation will be presented. The method of consideration of the interaction between soil and structure, the ground motion selection and the numerical simulation procedure will also be discussed. At the end, the parameters such as period, lateral displacement, inter-storey drift, storey shear and base shear used as comparison criteria are going to be brought forth and explained.

2.1. Site recognition

The site recognition will be carried out from a documentary research whose essential goal is to know the location of the site, the climate, the hydrology and socio-economic parameters in the region.

2.2. Data collection

The architectural plans will be the main data collected. These plans will define the geometry of the building and highlight the distribution of structural elements.

2.3. Actions and combination of actions

The norms that will be used for the design of elements are the Eurocode 0, basis of structural design Eurocode 1, actions on structure, Eurocode 2, design of concrete structures, Eurocode 7, geotechnical design and Eurocode 8 design for earthquake resistance. These European standards define the actions and the combination of actions for the design.

2.3.1. Actions

Different types of actions can be applied on a structure. This analysis is focused on a building structure and the different kinds of actions which are considered are permanent actions, imposed actions and seismic action.

2.3.1.1. Permanent actions

This kind of actions is constituted by the self-weight of structural and non-structural elements. The weight of the structural elements is obtained by multiplying the specific weight of concrete

by the section of the elements. The self-weight of the non-structural elements are extracted form Eurocode 1.

2.3.1.2. Imposed actions

Imposed actions are those arising from occupancy. It includes the normal use by people, the furniture and moveable objects and others. According to the Eurocode 1, different use categories of areas exist. Therefore, those ones are presented in the table A1 of the annex A. Based on these different categories the different values of loads recommended by this norm are presented in the table A2 of the Annex A.

2.3.1.3. Seismic action

These are actions due to earthquake ground motions and according to the Eurocode 8, the reference method for determining the seismic effect is the modal response spectrum analysis using the linear elastic model of the structure and the design response spectrum.

Seismic actions are going accounted in the analysis by the definition of an elastic response spectrum defined in the Eurocode 8 by expressions 2.1 to 2.4.

$0 \leq T \leq T_B$: $$S_e(t) = a_g.S\left[1 + \frac{T}{T_B}(\eta 2.5 - 1)\right] \quad (2.1)$$

$T_B \leq T \leq T_C$: $$S_e(t) = a_g.S.\eta 2.5 \quad (2.2)$$

$T_C \leq T \leq T_D$: $$S_e(t) = a_g.S.\frac{T_C}{T} \quad (2.3)$$

$T_D > T$: $$S_e(t) = a_g.S.\eta 2.5\left[\frac{T_C T_D}{T^2}\right] \quad (2.4)$$

Where:

$S_e(t)$ is the elastic response spectrum;

T is the vibration period of a linear single degree of freedom system;

a_g is the design ground acceleration on type A ground;

T_B is the lower limit of period of the period of the constant spectral acceleration branch;

T_C is the upper limit of the period of the constant spectral acceleration branch;

T_D is the value defining the beginning the constant displacement response range of the spectrum;

S is the soil factor that depends on the ground type;

η is the correction factor given by $\eta = \sqrt{10/(5+\xi)}$;

ξ is the viscous damping ratio.

The general shape of the elastic response spectrum defined by the Eurocode 8 is presented in figure 2.1.

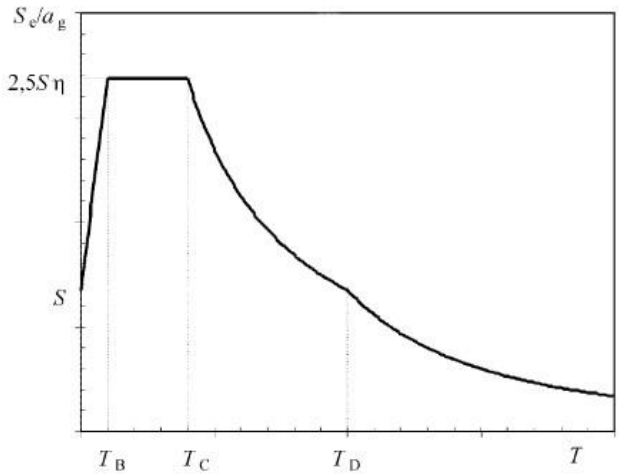

Figure 2.1. Shape of the elastic response spectrum (EC8 Part 1)

This elastic spectrum depends on many inputs notably the ground type, the importance class of the buildings, the peak ground acceleration of the region and the damping ratio of the structure which are going to be described in the following paragraphs.

The ground type has a great influence on the seismic waves when it travels on the soil so it can modify his spectra. Eurocode 8 considers seven different ground types, accounting by a ground factor S, depending on their mechanical properties (average value of propagation velocity of S waves, Standard penetration test blow count and undrained shear strength of the soil or cohesive resistance). These different ground types are presented in the table A3 of the annex and the variation of the elastic spectrum in function of the ground type is presented in figure 2.2.

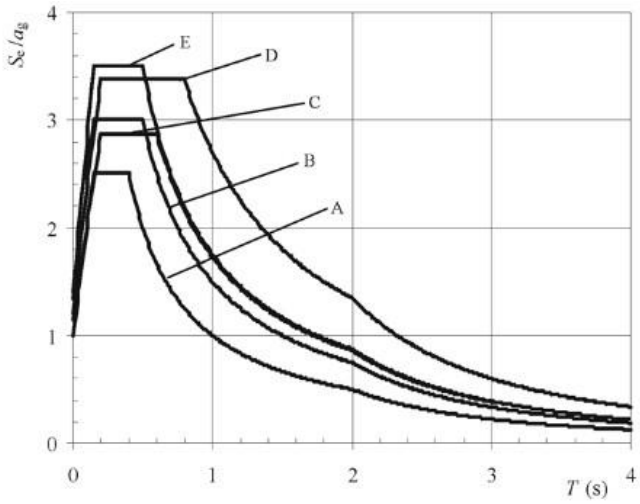

Figure 2.2. Shape of the elastic response spectrum for different ground types (Djeukoa, 2018)

The importance class permits the classification of the building considers the consequence of the collapse for human life, on their importance for public safety and civil protection in the immediate post-earthquake, on the social and economic consequences of collapse. Each class is characterized by an importance factor $\gamma 1$. There are four classes of building as presented in table A4 of the annex.

Peak ground acceleration values are generally available for different hazard zone in the national annex, usually through a hazard map. This value has to be corrected by the importance factors corresponding to the importance class of the buildings.

The damping ratio depends on the material used and the structural type of the building. For a concrete building, the Eurocode 8 uses a default damping ratio ξ of 5%. The correction factor is obtained by equation 2.5.

$$\eta = \sqrt{\frac{10}{5+\xi}} \tag{2.5}$$

2.3.2. Combination of actions

A combination of actions defines a set of values used for the verification of the structural reliability for a limit state under the simultaneous influence of different actions. In the case of a building, they are defined by the fundamental combination, used for the Ultimate Limit State (ULS) associated with collapse or other similar forms of structural failure is presented in equation 2.6.

$$\sum_{j\geq 1} \gamma_{G,i}\ G_{k,j} + \gamma_{Q,1}\ Q_{K,1} + \sum_{i\geq 1} \gamma_{Q,1}\ \Psi_{0,i}\ Q_{k,i} \quad (2.6)$$

Where the coefficients $\gamma_{G,j}$ and $\gamma_{Q,i}$ are partials factors which minimize the action which tends to reduce the solicitations and maximize the one which tends to increase it. The recommended values preconized by the Eurocode 0 for the structural and Geotechnical (STR and GEO) verifications are:

$\gamma_{G,j,sup} = 1.35$ and $\gamma_{G,j,inf} = 1.0$

$\gamma_{Q,1,sup} = 1.50$ and $\gamma_{Q,1,inf} = 0$

$\gamma_{Q,i,sup} = 1.50$ and $\gamma_{Q,i,inf} = 0$

The Characteristic combination (rare), used for non-reversible serviceability limit states (SLS) to be used in the verifications with the allowable stress method is presented in equation 2.7.

$$\sum_{j\geq 1} G_{k,j} + Q_{K,1} + \sum_{i\geq 1} \Psi_{0,i}\ Q_{k,i} \quad (2.7)$$

The seismic combination, used for the ultimate and serviceability limit state related to the seismic action is presented in equation 2.8.

$$\sum_{j\geq 1} G_{k,j} + E + \sum_{i\geq 1} \Psi_{2,i}\ Q_{k,i} \quad (2.8)$$

Ψ are the combination factors that is function of the category of the building. The recommended values by the Eurocode 0 are presented in the table A6 of the annex A.

Where:

$G_{k,j}$ is the characteristic value of the permanent action j;

$Q_{k,1}$ is the characteristic value of the leading variable action 1;

$Q_{k,i}$ is the characteristic value of the accompanying variable action i;

E is the combination of the effects of the horizontal component of the seismic action.

2.4. Static Design

The static analysis of the building is done by the definition of the concrete cover, the design and the verification of one continuous beam, one columns line element, and a retaining wall at the basement. The interaction between the soil and the structure is also defined in other to take into account the soil properties in the design of the foundation.

2.4.1. Durability and cover to reinforcement

To ensure the required design working life of the structure, it is necessary to protect each structural element against the environmental action. For concrete structures, the Eurocode 2 ensured this protection by the definition of a concrete cover taking into account the structural class of the structure and the exposure class. This concrete cover is defined as the distance between the surface of the reinforcement closest to the nearest concrete surface and the nearest concrete surface as shown in figure 2.3.

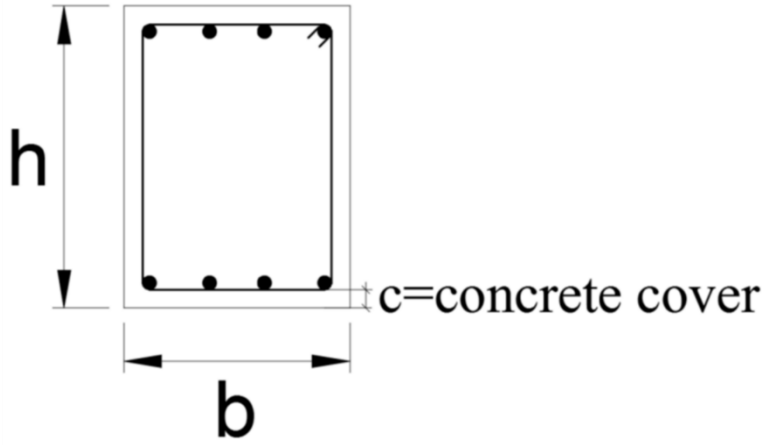

Figure 2.3. Illustration of the concrete cover (Djeukoa, 2018)

The nominal value of the concrete cover is defined as a minimum cover C_{min} plus an allowance in design for deviation. The minimum cover C_{min} is define by equation 2.9.

$$C_{min} = \max\left(C_{min,b}; C_{min,dur} + \Delta C_{dur,\gamma} - \Delta C_{dur,st} - \Delta C_{dur\,add}; 10mm\right) \quad (2.9)$$

Where:

$C_{min,b}$ is the minimum cover due to bond requirement, equal to the diameter of the bars or the equivalent diameter in the case of bundled bars;

$\Delta C_{dur,\gamma}$ is the additive safety element with a recommended value of 0 mm;

$\Delta C_{dur,st}$ is the reduction of minimum cover for use of stainless steel;

$\Delta C_{dur\,add}$ is the add reduction of minimum cover for use of additional protection;

$C_{min,dur}$: is the minimum cover due to environmental conditions obtain from the table A4 of the annex A in function of the exposure and the structural class of the building.

The nominal value of the concrete cover is then expressed by equation 2.10.

$$C_{nom} = C_{min} + \Delta C_{dev} \quad (2.10)$$

Where:

ΔC_{dev} is the allowance in design for deviation with a recommended value of 10 mm;

C_{min} is the minimum concrete cover.

2.4.2. Beam element design methodology

The beam design is composed of an ultimate limit state (ULS) design and a serviceability limit state verification (SLS).

2.4.2.1. Ultimate Limit State Design

The ULS design of this element will be done for the bending moment and the shear force solicitations.

a. Bending moment design

The bending moment solicitations obtained, the determination and the verification of the steel reinforcement can be done.

i. Longitudinal steel reinforcement of the beams

Knowing the solicitation curve, the steel reinforcement is compute for a rectangular section with the height h, the width b and the effective depth d.The section of steel at each point of the beams is estimated using the formula 2.11.

$$A_s = \frac{M_{Ed}}{0.9 d f_{yd}} \quad (2.11)$$

The section obtained has to verify the detailing of beams prescribed by the Eurocode2 which defines the maximum and the minimum reinforcement areas by the equations 2.12 and 2.13.

$$A_{S,min} = \max(0.26 \frac{f_{ctm}}{f_{yk}} b_t\, d; 0.0013 b_t\, d) \quad (2.12)$$

$$A_{S,\,max} = 0.004\, A_c \quad (2.13)$$

Where:

b_t is the Mean width of the tension zone;

d is the is the effective depth of the section;

f_{ctm} is the tensile strength of the concrete.

ii. Verification of the steel reinforcement

The steel reinforcement section defined, the effective area of the steel reinforcement is obtained by computing the number of bars necessary and the corresponding area. The verification of the section is done by calculating the resisting bending moment of the section using the position of the neutral axis inside the section.

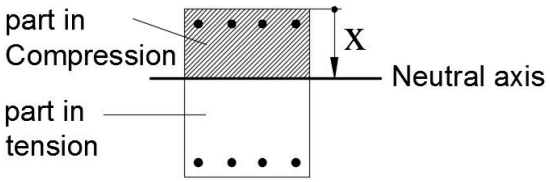

Figure 2.4. Neutral axis position inside a section (Djeukoa, 2018)

This neutral axis is obtained from the equation 2.14.

$$x = \frac{d}{2\,\beta_2} - \sqrt{\left(\frac{d}{2\,\beta_2}\right)^2 - \frac{M_{Ed}}{\beta_2\beta_2.b.f_{cd}}} \qquad (2.14)$$

Where:

d is the effective depth of the section b is the width of the section;

f_{cd} is the design compressive strength of the concrete;

$\beta_1\, and\, \beta_2$ is a correction factor equal to 0.81 and 0.41 respectively.

This resisting moment is then given by the relation 2.15.

$$M_{Rd} = A_{Sreal}.\, f_{yd}.\, (d - \beta_2.\, x) \qquad (2.15)$$

Where:

A_{Sreal} is the effective area of the steel section;

f_{yd} is the design yielding strength of the steel.

b. Shear verification

In order to take over the shear force inside the beam, Transversal steel reinforcement has to be insert inside the section as shown in figure 2.5.

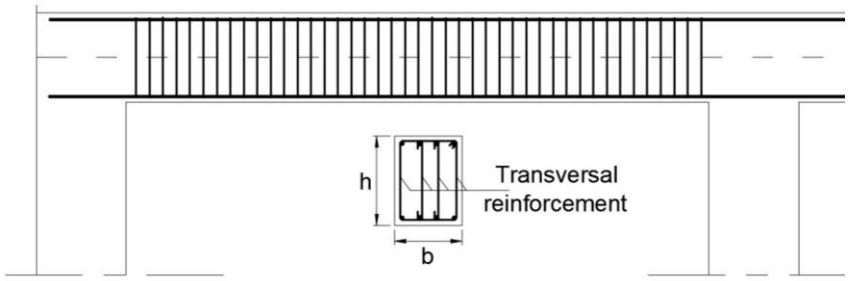

Figure 2.5. Longitudinal and transversal beam section with transversal reinforcement (Djeukoa, 2018)

From the envelope curve of the shear solicitation, the necessity of the shear reinforcement is verified by comparing the acting shear V_{Ed} to the design shear resistance of the member without shear reinforcement $V_{Rd,C}$ which is defined by equation 2.16.

$$V_{Rd,C} = max\left\{\left[C_{Rd,c}k(100\rho_l f_{ck})^{\frac{1}{3}} + k_1\sigma_{cp}\right] b_w d; \left(V_{min} + k_1\sigma_{cp}\right)b_w d\right\} \quad (2.16)$$

Where:

f_{ck} is the characteristic strength of the reinforcement;

d is the is the effective depth of the section;

b_w is the smallest width of the cross section in the tensile area.

$$\sigma_{cp} = \frac{N_{Ed}}{A_C} < 0.2 f_{cd}[N/mm^2] \quad (2.17)$$

N_{Ed} is the axial force in the cross section due to loading or prestressing (in N);

A_C is the area of the concrete cross section.

$$k = 1 + \sqrt{\frac{200}{d}} \leq 2.0 \quad (2.18)$$

With d in mm.

If no design shear reinforcement is required, the minimum shear reinforcement is applied according to the detailing of that member.

For members where the design shear reinforcement is required, the shear resistance is the minimum of V_{rds} and V_{rdmax} defined by the equations 2.19 and 2.20.

$$V_{Rd,} = \alpha_{cw} b_w z v_1 f_{cd} / (cot\theta + tan\theta) \quad (2.19)$$

$$V_{Rd,s} = \frac{A_{sw}}{S} z f_{ywd} cot\theta \quad (2.20)$$

Where:

f_{ywd} is the design yield strength of the shear reinforcement;

v_1 is a reduction factor for concrete cracked in shear ($v_1 = 0.6$ for $f_{ck} \leq 60 N/mm^2$);

α_{cw} is a coefficient taking account of the state of stress in the compression cord;

$\alpha_{cw} = 1$ for non-prestressed structures;

S is the spacing of the stirrups.

A_{sw} is the cross sectional area of the shear reinforcement with a maximum value is given by the relation 2.21.

$$\frac{A_{sw,\max} f_{ywd}}{b_w S} \leq \frac{1}{2} \alpha_{cw} v_1 f_{cd} \quad (2.21)$$

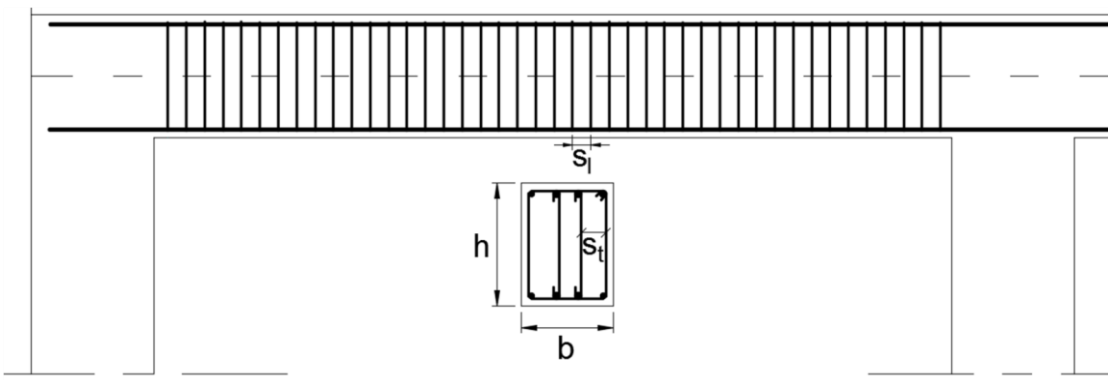

Figure 2.6. Illustration of the maximum longitudinal spacing and maximum transversal spacing of the legs (Djeukoa, 2018)

These limitations is given respectively in the equations 2.22 to 2.24.

$$s_{l,max} = 0.75d(1 + cot\alpha) \quad (2.22)$$

$$s_{t,max} = 0.75d \leq 600mm \quad (2.23)$$

$$\rho_{w,min} = \left(0.08\sqrt{f_{ck}}\right)/f_{yk} \quad (2.24)$$

With the shear ratio reinforcement ratio computed as shown in equation 2.25 as:

$$\rho_w = A_{sw}/(s.\, b_w.\, sin\alpha) \quad (2.25)$$

2.4.2.2. Serviceability Limit State Verification

The common serviceability limit states are the stress limitation, the crack and the deflection control. Only the stress limitation is presented on this work.

The verification of the allowable stress on the beam is done at the characteristic (rare) combination and permits to avoid inelastic deformation of the reinforcement and longitudinal cracks in concrete. The stress value is function of the modular ratio in short terms and long terms expressed by equations 2.26 and 2.27 respectively.

$$n_0 = \frac{E_S}{E_C} \tag{2.26}$$

$$n_\infty = n_0\,(1 + \varphi_L * \rho_\infty) \tag{2.27}$$

Where $\varphi_L = 0.55$ for shrinkage of concrete and the parameter $\rho_\infty = 2 \div 2.5$

The neutral axis position is computed for an uncracked concrete by the equation 2.28.

$$x = \frac{-n(A_S'+A_S)+\sqrt{[n(A_S'+A_S)]^2+2bn(A_S'd'+A_Sd}}{b} \tag{2.28}$$

Where A_S' ,A_s are the upper and lower steel reinforcement inside the section respectively. b, d' and d are geometrical characteristics of the section.

The moment of inertia of the uncracked section is given by equation 2.29.

$$J_{cr} = \frac{bx^3}{3} + nA_s(d-x)^2 + nA_s^{'}(x-c)^2 \tag{2.29}$$

The stress in the concrete and in the steel reinforcement in tension are then obtained using the Equation 2.30 and 2.31.

$$\sigma_S = \frac{M_{ED}\,(d-x)}{J_{cr}}\ \text{x}\ n_\infty \tag{2.30}$$

$$\sigma_S = \frac{M_{ED}\,x}{J_{cr}} \tag{2.31}$$

The Eurocode 2 limitation of these stresses as presented in the equations 2.32 and 2.33.

$$\sigma_c \leq k_1 * f_{ck} \tag{2.32}$$

$$\sigma_s \leq k_3 * f_{yk} \tag{2.33}$$

With $k_1 = 0.6$ and $k_3 = 0.8$.

2.4.3. Column design methodology

For the column design, a 3D modelling of the building in software SAP 2000 will be done. Also, different loads arrangements will be considered to obtain the envelope curve for each solicitation .The preliminary design is done and the design at ULS for the axial force, the bending moment and the shear and the verification is done for the slenderness.

2.4.3.1. Preliminary design process

The preliminary design of the column is based on the axial load resistance to determine the minimum area section. 60% of the concrete resistance is used to take over the axial force in the preliminary design of columns is seismic areas.

2.4.3.2. Bending moment-axial force verification

The envelope of the bending moment and the axial force solicitations obtained, the design is done through the M-N interaction diagram. For each level, we have to ensure that the maximum M-N solicitation belong to the M-N interaction diagram of the section considered.

a. First point

The interaction diagram is a diagram that shows all the limit situation that can determine the failure of the section. The points which are lying onto the diagram represent the limit configuration: beyond them, failure occurs. This diagram is computed by determining some significant points: the procedure is presented below considering a rectangular section presented in figure 2.7.

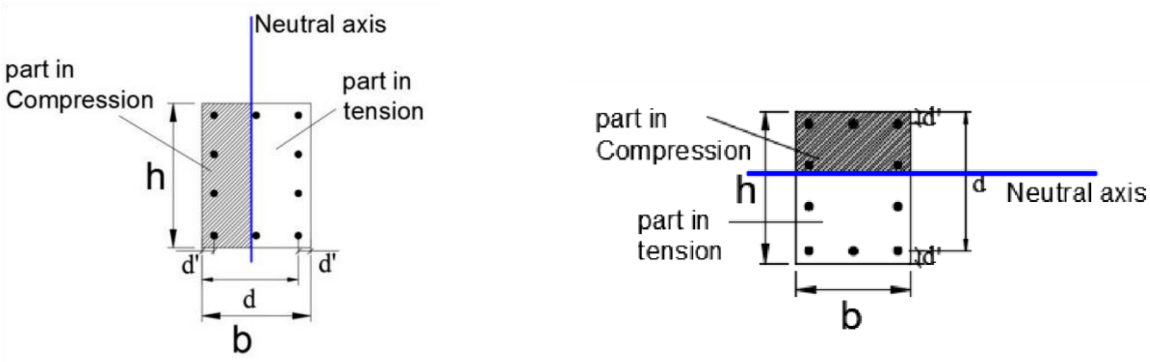

Figure 2.7. Rectangular section to illustrate the computation of the M-N diagram for different direction of the neutral axis (Djeukoa, 2018)

The section is completely subjected to tension, hence, the concrete is not reacting. We impose $\varepsilon_s = \varepsilon_{su}, \varepsilon_s{}' = \varepsilon_{syd}$ then the stress inside the element correspond to the design yielding strength of the steel reinforcement and the limit axial force and bending moment are obtained from the equations 2.34 and 2.35.

$$N_{Rd} = f_{yd}As + f_{yd}A's \quad (2.34)$$

$$M_{RD} = f_{yd}A_s\left(\frac{h}{2} - d'\right) - f_{yd}A'_s\left(\frac{h}{2} - d'\right) \quad (2.35)$$

b. Second point

At the second point, the section is completely subjected to tension. We impose that; the strains, $\varepsilon_s = \varepsilon_{su}$, $\varepsilon_c = 0$. The upper steel yielding condition is verified. If the steel has not yielded, then ε_s' is determined. Equations 2.34 and 2.35 are used for the computation of the limit axial force and the bending moment.

c. Third point

Here failure is due to concrete and the lower reinforcements have yielded. We assume, $\varepsilon_s \geq \varepsilon_{syd}$, $\varepsilon_c = \varepsilon_{cu2}$ and the position of the neutral axis is determined. Yielding condition of the upper steel reinforcement is verified. If the steel is yielded or not is determined by determining ε_s' in order to determine the corresponding stress. The limit axial force and bending moment corresponding to the third point are computed by using equation 2.36 and 2.37 respectively.

$$N_{Rd} = -\beta_1.b.x.f_{cd} + A_sf_{yd} - A_s'f_{yd} \quad (2.36)$$

$$M_{RD} = f_{yd}A_s\left(\frac{h}{2} - d'\right) + f_{yd}A'_s\left(\frac{h}{2} - d'\right) + \beta_1.b.x.f_{cd}\left(\frac{h}{2} - \beta_2.x\right) \quad (2.37)$$

d. Fourth point

We impose that the failure is due to concrete and the lower reinforcement reaches exactly $\varepsilon_s = \varepsilon_{syd}$. Likewise, we determine the neutral axis position and the strain ε_s'. Equations 2.36 and 2.37 are used to compute the limit axial force and bending moment corresponding to fourth point.

e. Fifth point

We impose that the failure is due to concrete and the lower reinforcement reaches exactly $\varepsilon_s = 0$. Then the neutral axis position is equal to the effective depth of the section. The limit axial force and bending moment are obtained from the equations 2.38 and 2.39 respectively.

$$N_{Rd} = -\beta_1.b.x.f_{cd} + A_s'f_{yd} \quad (2.38)$$

$$M_{RD} = f_{yd}A_s'\left(\frac{h}{2} - d'\right) + \beta_1.b.x.f_{cd}\left(\frac{h}{2} - \beta_2.x\right) \quad (2.39)$$

f. Sixth point

We impose that concrete is uniformly compressed and assume the strains $\varepsilon_s = \varepsilon_c \geq \varepsilon_{c2}$. Limit values of axial force and bending moment are computed by using equations 2.40 and 2.41 respectively.

$$N_{Rd} = -b.h.f_{cd} - A'_s f_{yd} - A_s f_{yd} \quad (2.40)$$

$$M_{RD} = f_{yd}A'_s\left(\frac{h}{2} - d'\right) - f_{yd}A_s\left(\frac{h}{2} - d'\right) \quad (2.41)$$

The steel reinforcement of the column is considered taking into account the limitations of the Eurocode 2 that are presented in equations 2.42 and 2.43.

$$A_{s,min} = max\left(\frac{0.10N_{ED}}{f_{yd}}; 0.002A_c\right) \quad (2.42)$$

$$A_{s,max} = 0.04A_c \quad (2.43)$$

Where:

N_{Ed} is the design axial compression force;

f_{yd} is the design yield strength of the longitudinal reinforcement.

2.4.3.3. Shear verification

Just like the beam, the procedure goes same. Provisions given by the Eurocode 2 requires a minimum diameter of 6mm or one quarter of the maximum diameter of the longitudinal bars. The maximum spacing of the transverse reinforcement is given by the equation 2.44.

$$S_{cl,max} = \min\ (20\emptyset_{l,min}; b; 400mm) \quad (2.44)$$

Where:

$\emptyset$ is the minimum diameter of the longitudinal bars;

B is lesser dimension of the column.

The factor of 0.6 is used to reduce the maximum spacing in sections within a distance equal to the larger dimension of the column bars.

2.4.3.4. Slenderness verification

The need for slenderness verification arises from whether or not second order effects are to be accounted for. Eurocode 2 recommendations are outlined with equation 2.45.

$$\lambda_{lim} = 20.A.B.C/\sqrt{n} \quad (2.45)$$

Where:

$A = \frac{1}{1+0,2\varphi_{ef}}$ where φ_{ef} is the effective creep ratio; If not known, A=0.7;

$B = \sqrt{1+2\omega}$ where $\omega = A_s f_{yd}/A_C f_{cd}$ is the mechanical reinforcement ratio;

C=1.7−r_m with r_m =M_{01}/M_{02} is the moment ratio; equal to 1 for unbraced system;

n=$N_{Ed}/A_c f_{cd}$ is the relative normal force.

The expression in 2.46 is the one used for the estimation of slenderness.

$$\lambda = l_0/i \qquad (2.46)$$

Where:

l_0 is the effective length of the element (l_0 =0.7l);

i is the gyration radius of the uncracked concrete given by equation 2.47;

$$i = \sqrt{\frac{I}{A}} \qquad (2.47)$$

I is the moment of inertia and A is the area of the section.

2.4.4. Retaining wall design process

Retaining wall is a structure designed and constructed to resist the lateral pressure of soil. There are several type of retaining walls like gravity wall, reinforced retaining wall, Buttressed retaining wall, cantilevered wall and so on.

In the present work, we will consider a reinforced concrete wall. After determining lateral earth pressures by using equations 2.48 and 2.49 geotechnical analysis and structural design of wall is done.The total lateral earth pressure is given by equation 2.50.

Sk,surcharge =Ka x W x H (2.48)

Sk,ground= 0.5 x Ka x γ x H² (2.49)

Lateral earth pressure= Sk,surcharge+ Sk,ground (2.50)

Where:

Sk,ground is Ground horizontal force;

Sk,surcharge is Surcharge horizontal force provided by the surcharge on the embankment;

W is the uniform surcharge load;

H is the height of the embedded part of the wall.

Ka is factor of horizontal active earth pressure which is compute by using equation 2.51.

$$Ka=\frac{1-sin\Phi}{1+sin\Phi} \quad (2.51)$$

Notice that Φ is the angle of shearing resistance.

Geotechnical analysis consist to verify sliding and overturning. In the other side structural design permits to get the required steel reinforcement and to check the resistance of the concrete wall against normal force using equation 2.52.

$$Nrd=\frac{\alpha \text{ x } Br \text{ x} fcd}{0.9} \quad (2.52)$$

Where:

$\alpha=\frac{0.65}{1+\frac{0.2\ x\lambda}{30}}$ with λ the slenderness ratio of the wall.

The required steel is get after the computation of the bending moment in the longitudinal and in the transverse direction of the wall by using the previous equation 2.11.

2.4.5. Foundation design methodology

The adopted foundation is a raft foundation. A raft foundation is a continuous slab which covers the whole plan area of the structure. It is used when the supporting soil has a low bearing capacity and compressible. Many types of mat foundations exit. For heavily loaded raft require the foundation to be strengthen by beams to form a ribbed slab.

2.4.5.1. Geotechnical design of the raft

The slab is designed by the conventional rigid method. The pressure developed by the total vertical load of applied on the raft should less than the allowable pressure of the soil as expressed in relation 2.53.

$$\sigma=\frac{Q}{A}<\sigma_{adm} \quad (2.53)$$

Where:

σ is the contact pressure;

σ_{adm} is the admissible pressure on the soil;

Q is the total vertical arriving at the foundations;

A is the surface of the mat.

The soil pressure will be computed by using the software SAP2000.

2.4.5.2. Structural design of the raft

The raft is made of panels and strengthening beams. The panel are designed as a plate thick element. The panels will be modelled in SAP2000 as a plate resting on Winkler's springs. The stiffness of the springs is obtained from the modulus of subgrade reaction of the soil times the area of the meshing square using relation 2.54. The modulus of subgrade reaction is obtained by the geotechnical report of the site of the study case.

$$k = C \times A \qquad (2.54)$$

Where:

C is the modulus of subgrade reaction of the soil;

A is the mesh area.

The effective depth along direction x and direction y is given according to equation 2.55 and 2.56 respectively.

$$d_x = d - c_{nom} - 3\emptyset/2 \qquad (2.55)$$

$$d_y = d - c_{nom} - \emptyset/2 \qquad (2.56)$$

Where:

d is the total depth of the slab;

c_{nom} is the concrete cover;

$\emptyset$ is the diameter of the bars used as reinforcement.

The computation of the reinforcement area is done for one-meter length using equation 2.13 with the mean value of the effective depth along x and y. The strengthening beams are designed as inverted beams. The depth of the beam H follows the relation 2.57.

$$H \geq L/10 \qquad (2.57)$$

The moment at mid span, the moment at a support and the shear can be after running the analysis in the software.

2.5. Analysis criteria

The results of the study will be analysed on four parameters that are: the period of the three first vibration modes of the structure, the lateral deformation, the inter-storey drift, the base shear and the storey shear.

2.5.1. Soil springs

The adopted method to represent the soil-foundation-structure interaction is the sub-structure approach. This approach required to use linear springs associated to the structure as shown in figure 2.8.

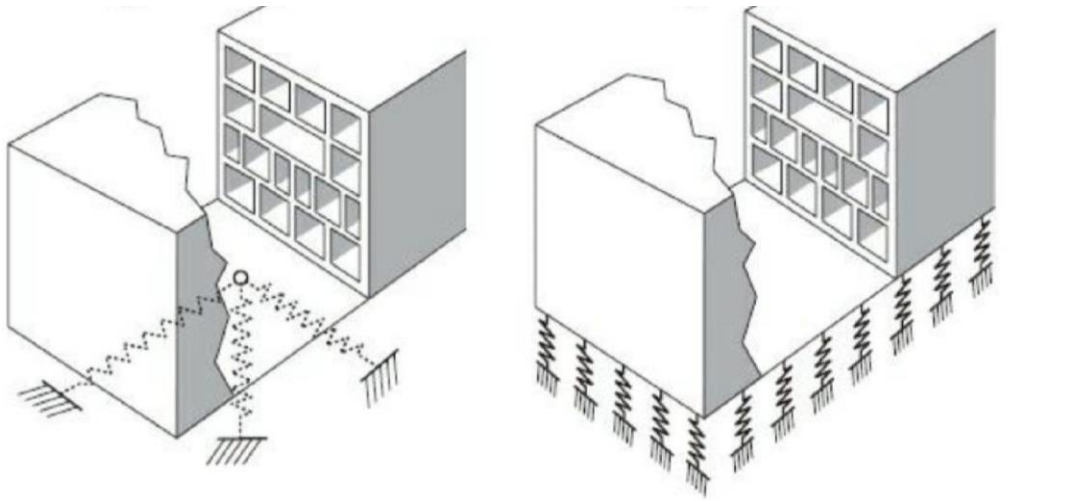

(a) (b)

Figure 2.8. Soil modelling by a linear springs system: (a) concentrated spring (b) distributed springs (Djeukoa, 2018)

In the present work, we will consider a distributed spring system. The characteristics of these springs being function the soil properties and the interaction surface between the soil and the building.

In the case of a rectangular foundations located on the surface or embedded within a uniform soil the computing of the stiffness k_j is given by equation 2.58.

$$k_j = K_j \alpha_j \eta_j \qquad (2.58)$$

Where:

K_j is the static stiffness for vibration mode j;

α_j is the dynamic stiffness modifier;

η_j is the embedment modifier.

The stiffness in x, y and z directions is given by equation 2.59, 2.60 and 2.61 respectively

$$K_x = \frac{GB}{2-\nu}\left[6.8\left(\frac{L}{B}\right)^{0,65} + 2.4\right] \quad (2.59)$$

$$K_y = \frac{G}{2-\nu}\left[6.8\left(\frac{L}{B}\right)^{0,65} + 0.8\left(\frac{L}{B}\right) + 1.1\right] \quad (2.60)$$

$$K_z = \frac{GB}{1-\nu}\left[3.1\left(\frac{L}{B}\right)^{0,7} + 1.6\right] \quad (2.61)$$

Where:

G is the shear modulus;

ν is the Poisson ratio;

L is the foundation half-length;

B is the foundation half width.

Factor η_j is used to increase K_j for the effects of embedment along x, y and z directions is obtained using equation 2.62 and 2.63:

$$\eta_x=\eta_y=\left[1.0 + \left(0.33 + \frac{1.34}{1+\frac{L}{B}}\right)\left(\frac{D}{B}\right)^{0.8}\right] \quad (2.62)$$

$$\eta_z=\left[1.0 + \left(0.25 + \frac{0.25}{\frac{L}{B}}\right)\left(\frac{D}{B}\right)^{0.8}\right] \quad (2.63)$$

Where D is the foundation depth.

It is very important to notice that the side soil around a basement wall is take into account by increasing the dynamic stiffness using the embedment modifier.

The dynamic stiffness modifiers are independent of the depth and is computed as shown in equation 2.64.

$$\alpha_x = \alpha_y = \alpha_z = 1 \quad (2.64)$$

For flexible foundations, distributed springs should allow the foundation to deform in a natural manner given the loads imposed by the superstructure and the spring reactions. For vertical springs, this can be accomplished by calculating the vertical translational stiffness, as described above, and normalizing it by the foundation area to compute stiffness intensity. The new

stiffness of individual spring K_Z^i can be taken as the normalized stiffness times the tributary area dA as expressed in equation 2.65.

$$K_Z^i = \frac{k_z}{4BL} \mathrm{dA} \qquad (2.65)$$

2.5.2. Ground motion selection

The structural model will be subjected to the 1989 Loma Prieta earthquake of USA acceleration record .The peak ground acceleration is equal 0,367g.

This record is downloaded from the website of the Pacific Earthquake Engineering Research Centre (PEER). The time history of the Kobe is shown in the figure 2.9.

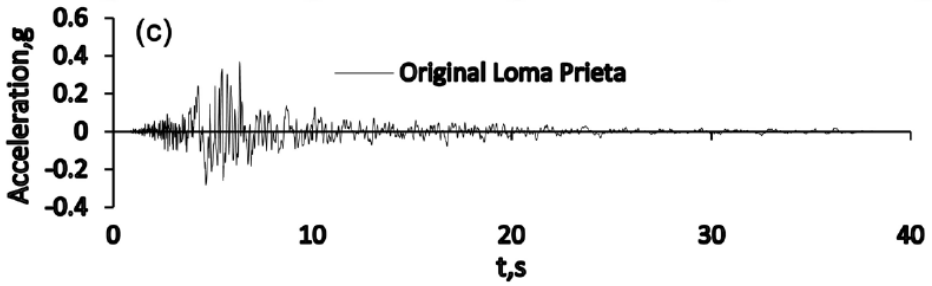

Figure 2.9. Horizontal component of the 1989 Loma earthquake (NIST, 2012).

2.5.3. Modelling of the structure

The study is performed with the software SAP 2000 (Structural Analysis Program) version 22 which is a structural design software through the finite elements method especially dedicated to the analysis of the stability and the resistance of structures. The load induced by the slabs are distributed and directly applied on the beams as well as the linear loads provided by the external wall as distributed frame loads.

The beams and the columns of the structure are modelled as frame elements. The connection between these elements is done through the insertion of joints between the two elements. A diaphragm constraints is assign to each joints of the same level to ensure the rigid floors at each level of the structure.

Four models will be developed, the first model with a fixed base and the third others integrate soil-structure interaction through the insertion of linear springs with translational stiffness at the base of the structure.

The elastic response spectrum of the earthquake is inserted in the software as a function and its application to the structure is done through the definition of the loads cases that use the response spectrum function and the direction of the action The software allows to take into account the eccentricity of the seismic force and then the accidental torsional effect is accounted, as preconized in the Eurocode 8, by defining three seismic loads cases in each directions and the seismic force considered is the envelope of these loads cases.

2.5.4. Vibration period

The fundamental period of a building is an intrinsic property of the structure. In seismic zone, the spectral acceleration of a building is function of this period of the structure then this property of the structure can increase or reduce this spectral acceleration and then become an important parameter in the response of a structure. Some empirical formulas permit to estimate this period. It's the case of the one defined by the Eurocode 8 for buildings with heights up to 40m expressed in equation 2.66.

$$T_1 = c_t H_4 \qquad (2.66)$$

Where:

c_t is a coefficient that depends on the moment resisting type of the structure;

H is the total height of the building above the foundations in meter.

The real values of this properties of the building can be obtained through a dynamic analysis of the structure and this parameter is associated to a mode shapes (vibration modes) and a mass participating ratio. The mode shape of the structure describes the configurations into which a structure will deform naturally while the mass participation ratio indicated the contribution of this mode shapes to the structural response. The vibration mode hence indicated the deformations modes of the structure.

2.5.5. Storey lateral displacement response

The storey displacement is the absolute value of displacement of the storey under action of the lateral forces. It permits also a proper estimation of the separation distance between buildings. Figure 2.10 shows the displacement of the last storey of a building.

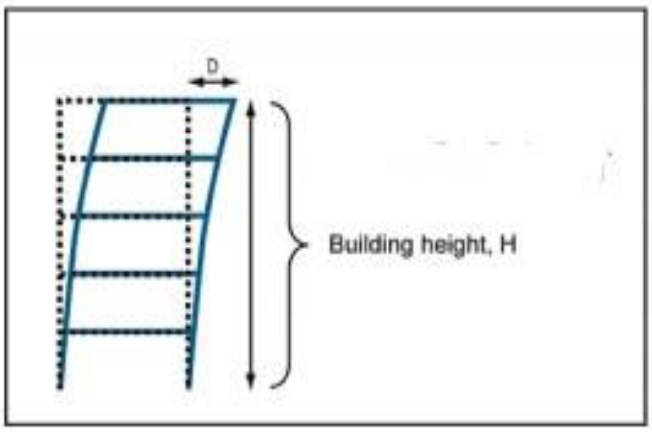

Figure 2.10. Storey displacement of the building (Djeukoa, 2018).

The static deflections due to earthquake, similar to those caused by wind loads have an important effect on the structural integrity of the components of the buildings. These should be limited so as not cause any distress in structural frames, members, or connections, as well as such architectural components as partitions, cladding and windows.

The total displacements must be controlled to mitigate the effects of secondary P-Δ effects and overall stability of the building. In seismic design, this displacement can affect both the structural elements that are part of the lateral force resisting system and structural elements that are not part of the lateral force resisting system. This parameter is better evaluated through the inter-storey drift ratio presented in the next part.

2.5.6. Storey drift ratio

Storey drift ratio is the maximum relative displacement of each floor divided by the height of the same floor and is an important parameter that will be evaluated. Inter-storey drift represents the most important parameter to be analysed as it is strictly connected to the damage suffered by both structural and non-structural elements. The inter-storey drift has been employed as an index to evaluate the deformation capacity of a building and to further determine its performance. This parameter is evaluated as the difference of the average lateral displacements at the top and the bottom of a storey.

The limitation of the inter-storey drift by the Eurocode 8 for buildings having non-structural elements of brittle material attached to the structure is given by the equation 2.67.

$$d_r \nu \leq 0.005h \qquad (2.67)$$

Where:

d_r is the inter-storey drift defined by equation 2.68.

$$d_r = d_{i+1} - d_i \qquad (2.68)$$

d_{i+1} is the deflection at the (i+1) level;

d_i is the deflection at the (i) level;

ν is a reduction factor that depends on the importance class of the building.

The storey drift in the model with fixed base will be compared to the soil structure interaction models with different types of soil.

2.5.7. Storey shear

The total seismic force is distribute over the height of the structure by considering the response of the structure during an earthquake. The resulting shear force at any level is called storey shear. The storey shear depends on the dynamic characteristics of the structural deformation, the mass at that level, and the amplitude of oscillation. The envelope of maximum shears is presented in figure 2.11. The storey shear in the model with fixed base will be compared to the soil structure interaction models with different types of soil.

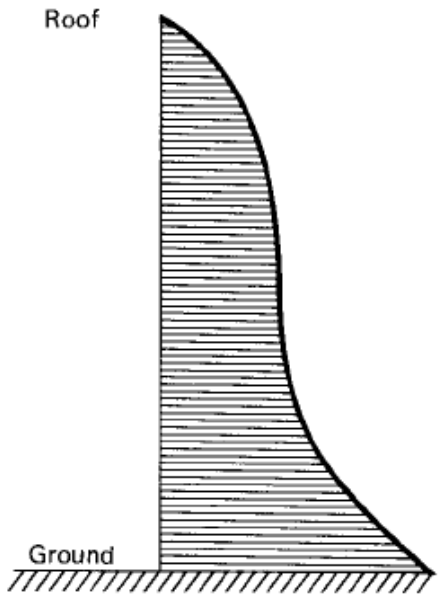

Figure 2.11. Envelope of maximum shears (Bungale, 1988).

2.5.8. Base shear

Using Newton's second law of motion, the total lateral seismic force, also called the base shear is determined by the relation 2.69.

$$V=Ma \qquad (2.69)$$

Where:

V is the total horizontal seismic over the height of the building also called the base shear;

M is the mass of the building;

a is the maximum acceleration of the building.

Since,

$$M=W/g \quad (2.70)$$

Where:

W is the building weight;

g is the gravity acceleration.

So the base shear in x-direction and y-direction can be computed using the equations 2.71 and 2.72 respectively.

$$V_x=Ma_x \quad (2.71)$$

$$V_y=Ma_y \quad (2.72)$$

Where:

V_x is the base shear in the x-direction;

V_y is the base shear in the y-direction;

a_x is the component of the acceleration in x-direction;

a_y is the component of the acceleration in y-acceleration.

The base shear in the model with fixed base will be compared to the soil structure interaction models with different types of soil.

Conclusion

This chapter had as objective to present the different codes, the different procedures that will be used in this work and the seismic performance on which will be based the analysis. The analysis will be performed using a structural analysis software SAP 2000 version 22 while the different designs will be done manually through the software Excel applying the European standards. After all the different procedures have been well described, the case study will be presented, analysed statically in the software SAP 2000 following the process presented in this section and finally the fixed base models and the flexible base models for different types of soil conditions will be compared using the previous analysis criteria.

CHAPTER 3: PRESENTATION AND INTERPRETATION OF RESULTS

Introduction

The methodology presented previously is applied on a case study and the results are highlighted here. This chapter will consist in a preliminary part in the presentation of the case study and the different loads and material properties considered for its analysis. This will be followed by a static analysis in order to determine the different sections of the structural elements of the superstructure and the substructure. Then, the computation of springs stiffness that depict the soil flexibility for the different types of soil condition is presented. The results of the comparison of the seismic demands in terms of vibration periods, lateral deflection, inter-storey drift, shear storey and base shear for the different types of soil are also presented and interpreted.

3.1. General presentation of the site

Here, we present the study area through its location, geology, relief and soil, climate, hydrology, population and socio-economic activities.

3.1.1. Geographic location

Douala is the largest port in the country and one of the most important in Central Africa, located on the Atlantic Ocean, at the bottom of the Gulf of Guinea, at the mouth of the Wouri. The city stretches along both banks of the shore. Since October 2017, a second bridge stretches across the river to connect the two banks.

3.1.2. Climate

Douala's climate is equatorial, it is characterized by an almost constant temperature of around 26°C and very heavy rainfall, particularly during the rainy season from June to October. The air is almost constantly saturated with humidity, 99% relative humidity in the rainy season, but 80% in the dry season. This rainfall causes frequent flooding, which also contributes to the development of diseases such as cholera and malaria.

3.1.3. Economic parameters

The city of Douala has established itself as the country's economic capital through its port, which has enabled the development of nearly 80% of Cameroon's industrial activity. The port alone accounts for more than 95% of the country's port traffic. The port of Douala-Bonaberi is still the main maritime gateway for Cameroon and the Central African Economic Community, CEMAC. The main products exported are wood (from Cameroon and the Central African.

3.1.4. Climate

Douala's climate is equatorial, it is characterized by an almost constant temperature of around 26°C and very heavy rainfall, particularly during the rainy season from June to October. The air is almost constantly saturated with humidity, 99% relative humidity in the rainy season, but 80% in the dry season. This rainfall causes frequent flooding, which also contributes to the development of diseases such as cholera and malaria.

3.1.4. Economic activities

The city of Douala has established itself as the country's economic capital through its port, which has enabled the development of nearly 80% of Cameroon's industrial activity. The port alone accounts for more than 95% of the country's port traffic. The port of Douala-Bonaberi is still the main maritime gateway for Cameroon and the Central African Economic Community, CEMAC. The main products exported are wood (from Cameroon and the Central African Republic), fruit (especially bananas) and petrol. The country's largest companies have set up their headquarters in Douala rather than in Yaoundé. The city is also home to the African Banana and Plantain Research Centre.

3.2. Presentation of the project

In this part, we will present and describe the case study and present the general characteristics of the materials to be used.

3.2.1. Building configuration

The building is a 06-storey structure above grade with two basement levels. The building measures 24.95 m tall from ground surface to the roof. The area of the basement floors are 424.76 m², whereas the area of other floors (above level 0) is smaller. 3D architectural views are shown respectively in the figure 3.1 .The horizontal force-resistance system consists of a reinforced concrete shear wall core and a concrete retaining wall . The gravity system consists of cast in place concrete slab supported on concrete beams and columns. The plan view of the level 2 is plotted in the figure 3.2 and a section of a building in figure 3.3 .The plan views of other levels are presented in annex B.

(a)

(b)

Figure 3.1. 3D architectural view: (a) front view ;(b) back view.

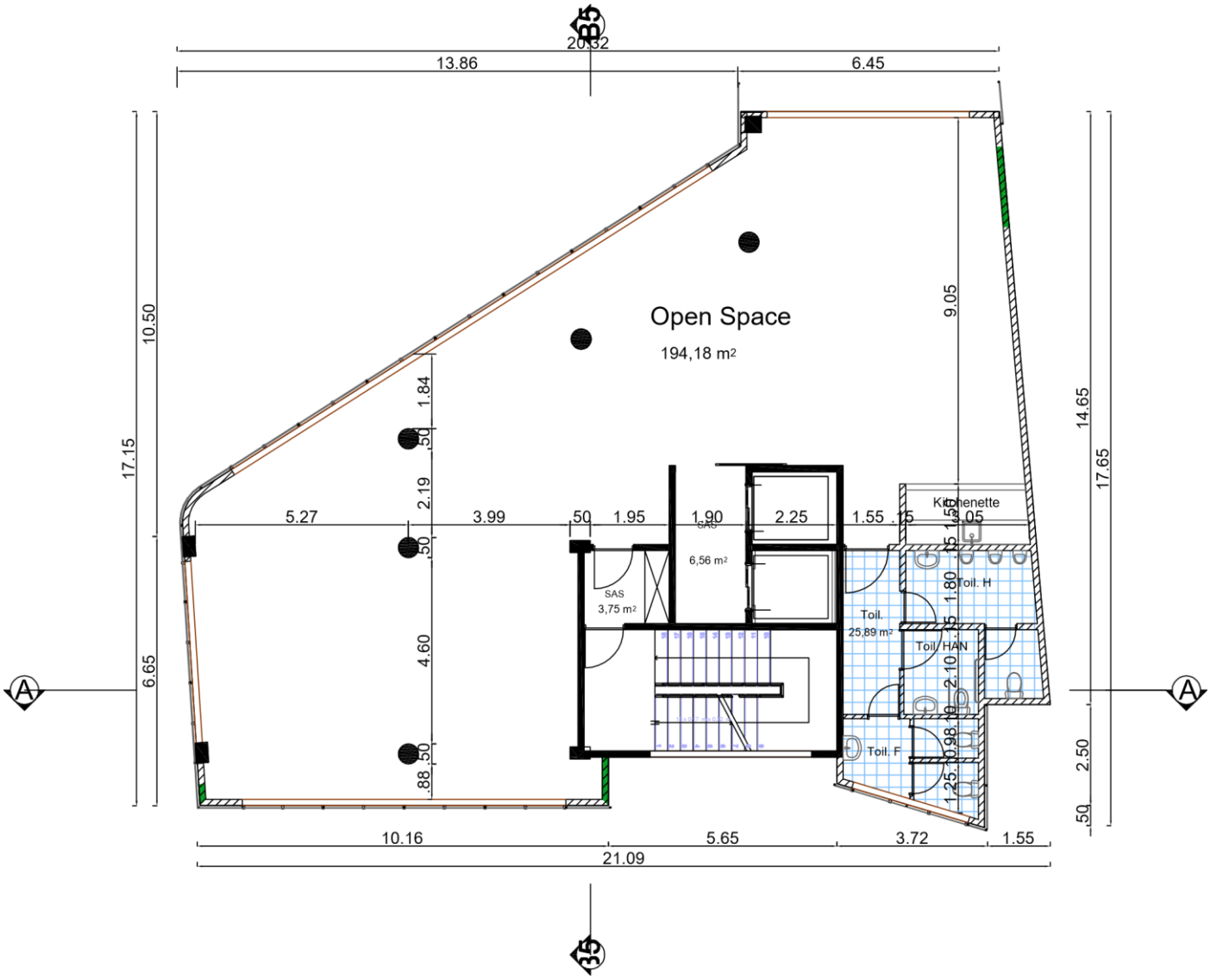

Figure 3.2. Plan view of the level 2

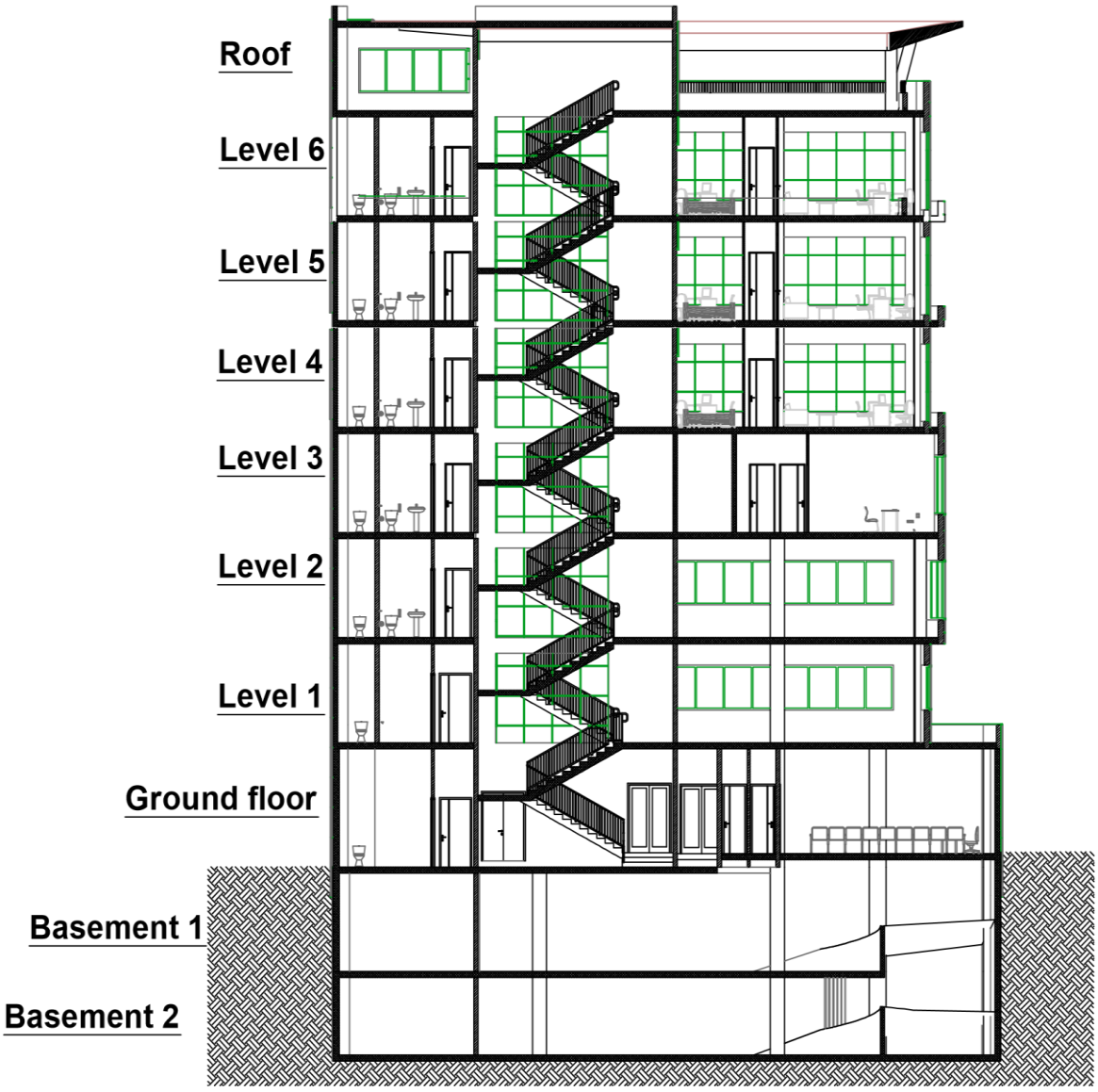

Figure 3.3. Cut section A-A

3.2.2. Material properties

For the analysis and the design, the concrete class adopted for the superstructure is C25/30 and the longitudinal steel reinforcement is Fe400B. For the transversal reinforcement, we consider a characteristic yield strength of 235 N/mm². The main characteristics of these materials for linear analysis and design of the structure are given in table 3.1 for the concrete and table 3.2 for the steel reinforcement.

Table 3.1. Concrete characteristics

Property	Value	Unit	Definition
Class	C25/30	-	Concrete class
f_{ck}	25	N/mm^2	Characteristic compressive strength at 28 days
$f_{cm} = f_{ck} + 8$	33	N/mm^2	Mean value of concrete cylinder compressive strength
γ_c	1,5	-	Partial safety factor for concrete
$fcd = \frac{\alpha_{CC}\, f_{ck}}{\gamma_c}$	14,16	N/mm^2	Design value of compressive strength
$fctm = 0.3\ (0.3\ f_{ck})^{\frac{2}{3}}$	2.56	N/mm^2	Mean value of axial tensile strength of concrete
$f_{ctd} = \frac{0.7\ \text{fctm}}{\gamma c}$	1.2	N/mm^2	Design resistance in traction
$E_{cm} = 22000 \times (f_{cm}/10)^{0.3}$	31476	N/mm^2	Secant modulus of elasticity
ν	0,5	-	Poisson ratio
G	13115	N/mm^2	Shear modulus
γ	25	kN/m^3	Specific weight of concrete

Table 3.2. Longitudinal reinforcement characteristics

Property	Value	Unit	Definition
Class	B400B		Steel class
f_{yk}	400	N/mm^2	Characteristic yield stress
γ_s	1,15	-	Partial safety factor for steel
γ	78,5	kN/m^3	Specific weight of steel
ν	0,3	-	Poisson ratio

3.3. Actions on the building

The vertical loads acting on the elements of the superstructure are recorded and presented thereafter.

3.3.1. Permanent loads

The slab self-weight is the only permanent structural load acting on the building s. The value is obtained by multiplying the specific weight of the concrete by the thickness of the slab. In our case the slab is 16 cm thick except at the floor in basement 1 where the slab is 20cm thick, so G_{1K} is 5 kN/m^2 for the basement 1 and 4kN/m² for the rest of the building. For permanent non-structural load the value is the same from basements to floor7 and decreases at the roof floor as presented in table 3.3 and table 3.4.

Table 3.3. Permanent non-structural loads for floors 1 to 7 and basements.

Nature	Designation	Value	Units
G_{2K}	Screed	1,4	kN/m^2
G_{2K}	False sealing	0,5	kN/m^2
G_{2K}	Tiles	0,5	kN/m^2
G_{2K}	Partition wall	1,2	kN/m^2
	Total	3,6	kN/m^2

Table 3.4. Permanent non-structural loads for the roof floor.

Nature	Designation	Value	Units
G_{2K}	Waterproof	0,12	kN/m^2
G_{2K}	Concrete in the form of slope	2,2	kN/m^2
G_{2K}	False sealing	0,5	kN/m^2
	Total	2,82	kN/m^2

For the linear load provided by external of the building with of 15 cm thickness the load G_k for each floor is provided in table 3.5.

Table 3.5. Permanent non-structural loads for the roof floor.

Nature	Height of the floor	value	units
Gk-ground floor	3,70	9,62	kN/m
Gk-level 1to level 6	3,00	7,80	kN/m

3.3.2. Imposed loads

According to EC 2 the imposed loads for offices (use category B) q_k is equal to 2.0 kN/m^2 and for parking area with light vehicles (category F) q_k is equal to 2.5 kN/m^2.

To the ground floor up to the floor at level 6 imposed load is equal to 2.0 kN/m^2. The last floor is not accessible except for maintenance (use category H) so the imposed load can be taken as 1.0 kN/m^2.

3.4. Static design of the case study

The static design of the building is done under the vertical static action meaning considering only the permanent and the imposed loads. It consists of the design of one beam, one column, a part of the retaining wall and the foundation as well. The chosen beam and column element are considered as representative of the other elements of the structure. Before the design phase of these structural elements, we need to define the loads and the concrete cover in order to fulfil the durability requirements of the structure.

3.4.1. Concrete cover for durability

Applying the procedure presented in the section 2.4.1 and considering a structural class S4 and the exposure class XC1, a minimum concrete cover obtained is equal to:

$$C_{min} = \max(16; 15; 10) = 16\ mm$$

Applying the equation 2.11 for a nominal cover $C_{nom} = 26mm$. So, we will consider a concrete cover $c = 30mm$.

3.4.2. Design of beam

The horizontal structural elements of the considered building are composed of the beams which support the slab.

3.4.2.1. Description of the studied beam

The principal chosen beam for the design is highlighted in the figure 3.4 and has different influence area according to the span.

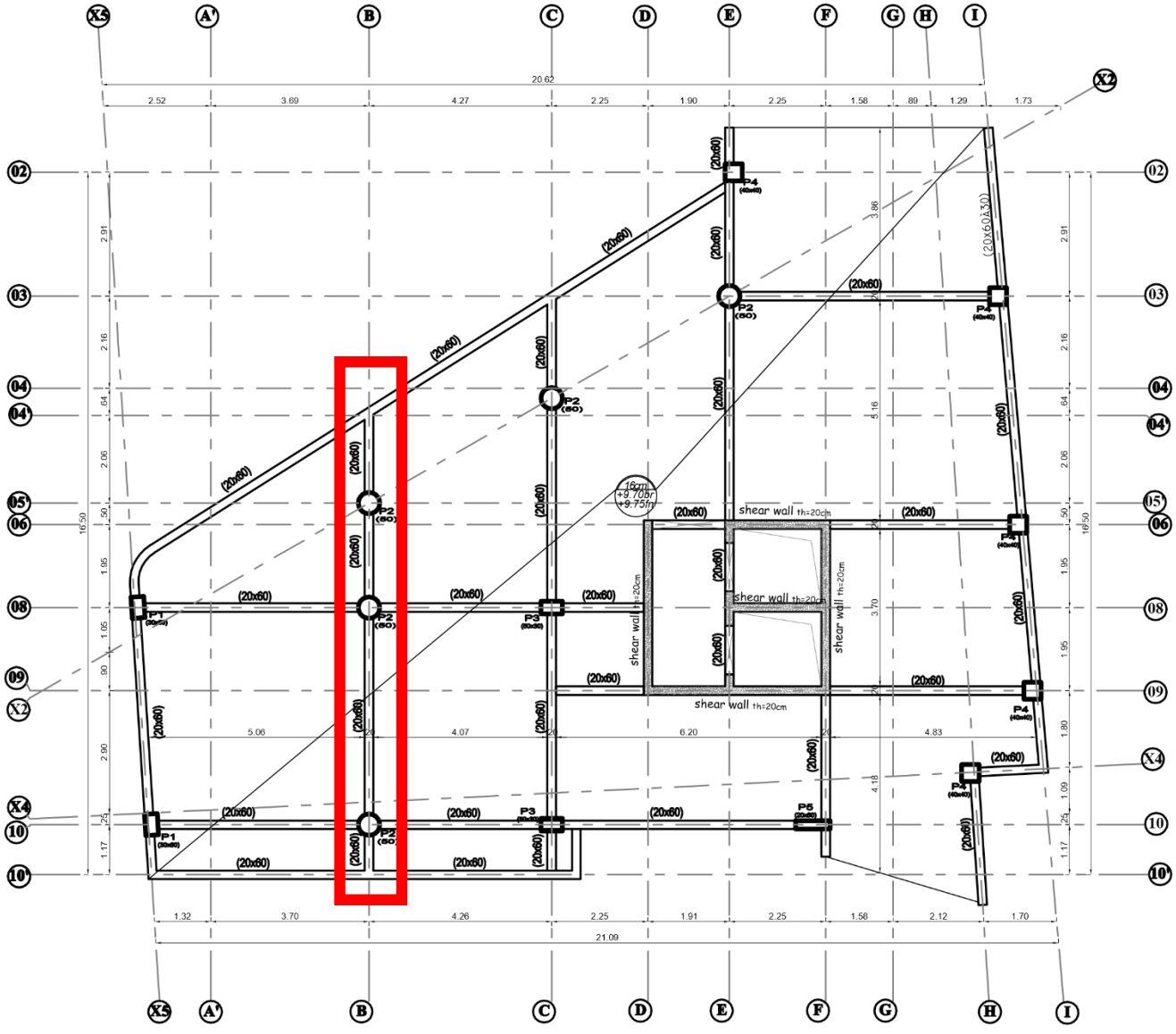

Figure 3.4. Choice of the beam for the design.

The schematic view of the beam is presented in figure 3.5.

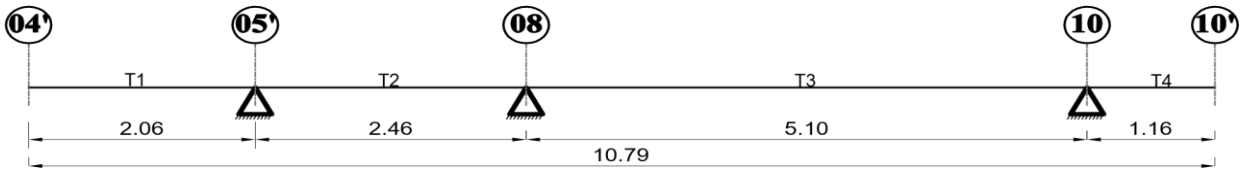

Figure 3.5. Schematic view of the beam

The preliminary section is obtained by assuming the value of the section height and the section depth. The section height is obtained from the maximum span as: $h \geq \frac{5.10}{12} = 0{,}42$ and $b = 20 \sim 30$ cm.

We can take as initial value $h = 60\ cm$ and $b = 20\ cm$. This section, is modelled in the software as frame element with the different restraints as supports as shown in the figure 3.6.

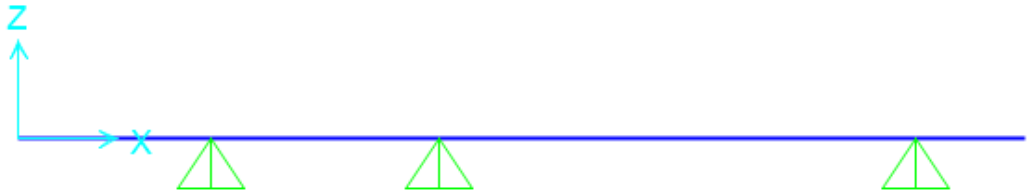

Figure 3.6. Beam model in SAP2000

From this model, six loads arrangements are defined for the design of the beam and are presented in the figure3.7.

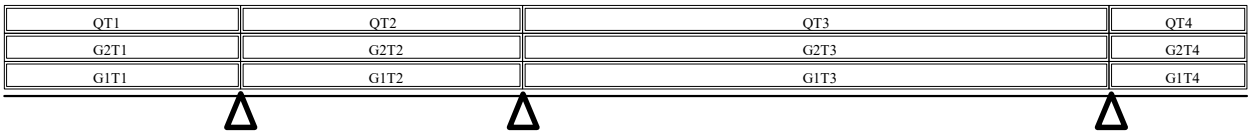

Load combination T1T2T3T4

Load combination T2T4

Load combination T1T2T4

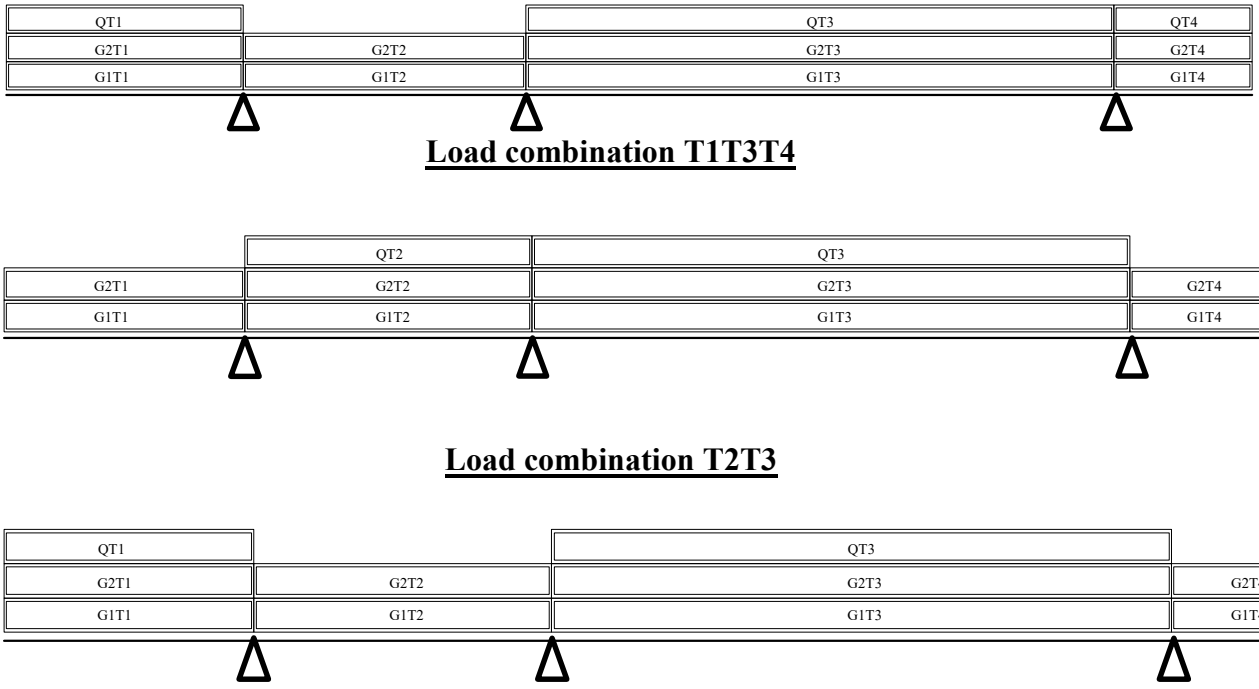

Figure 3.7. Loads combinations on the beam

From the different load arrangements, solicitations are extracted, the ULS design and the SLS verification can be performed.

3.4.2.2. Ultimate limit state design

The six loads arrangements inserted in the software SAP 2000 permitted to obtain solicitations curves along the beam for the bending moment and the shear force represented in the figure 3.8 and the figure 3.9.

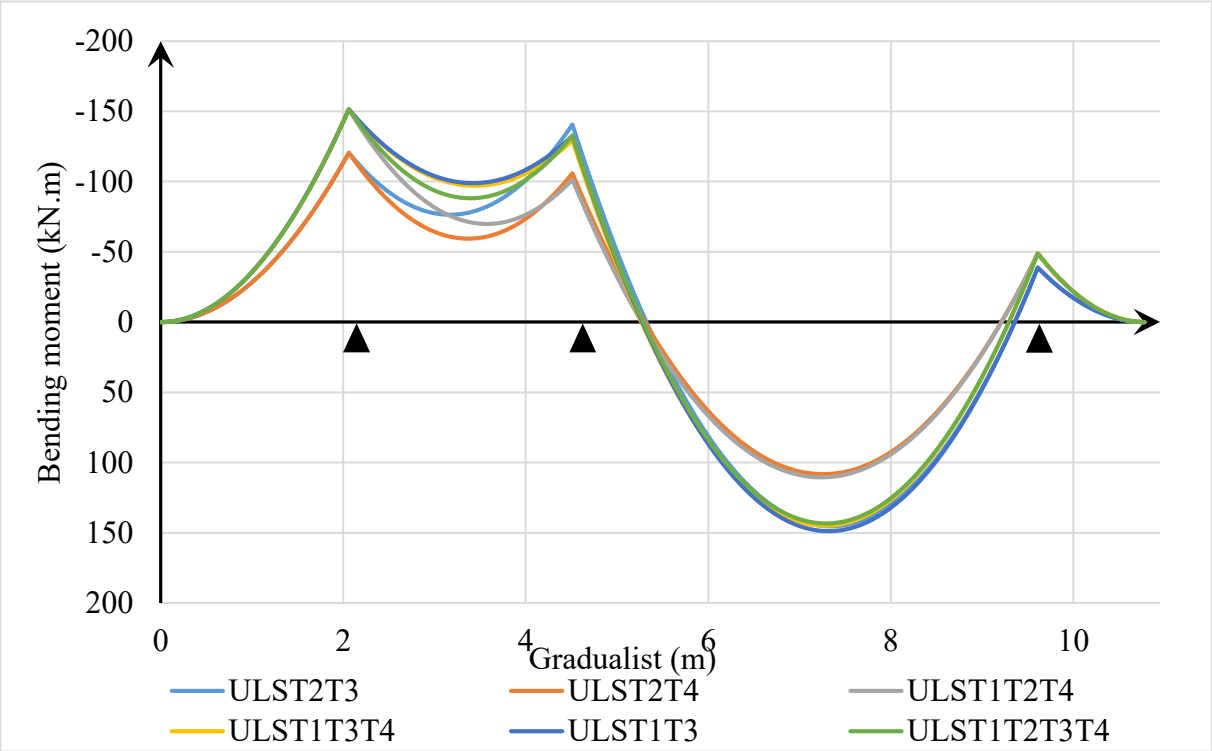

Figure 3.8. Bending moment curves on the beam.

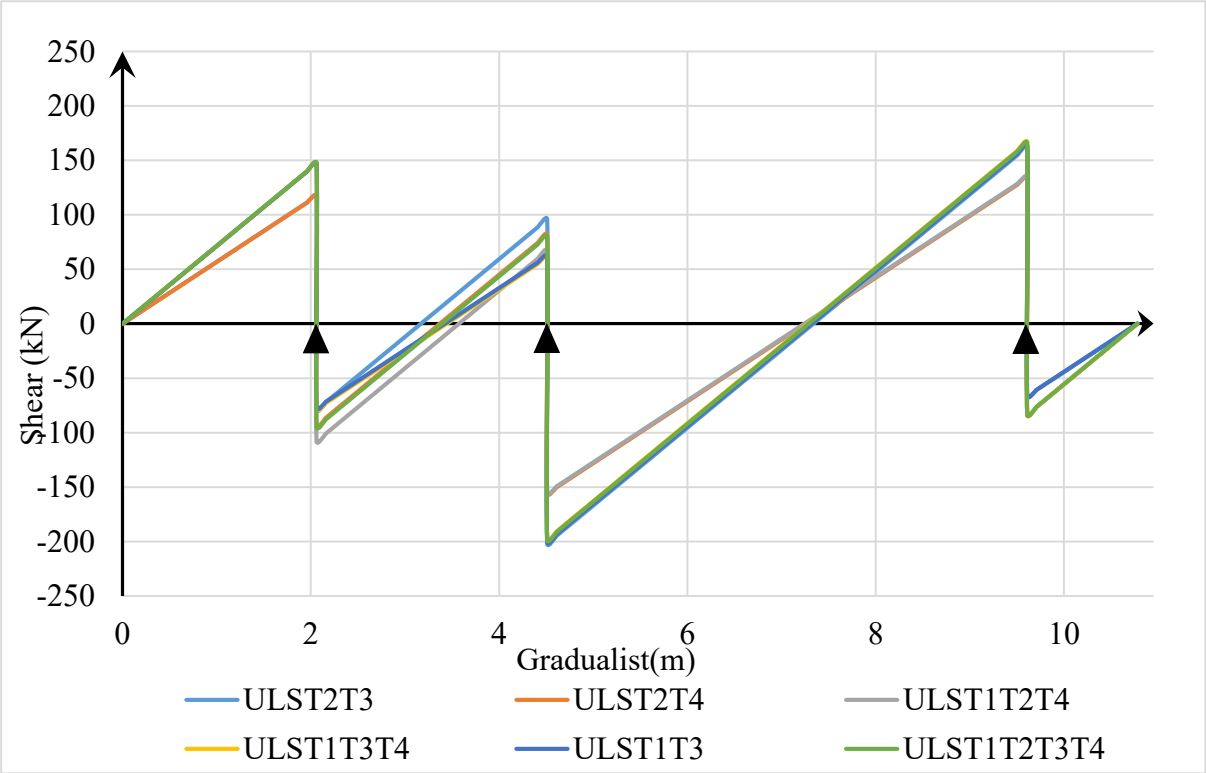

Figure 3.9. Shear solicitations curves on the beam.

These solicitation curves permit to obtain the envelope curves represented in the figure 3.10 and the figure 3.11.

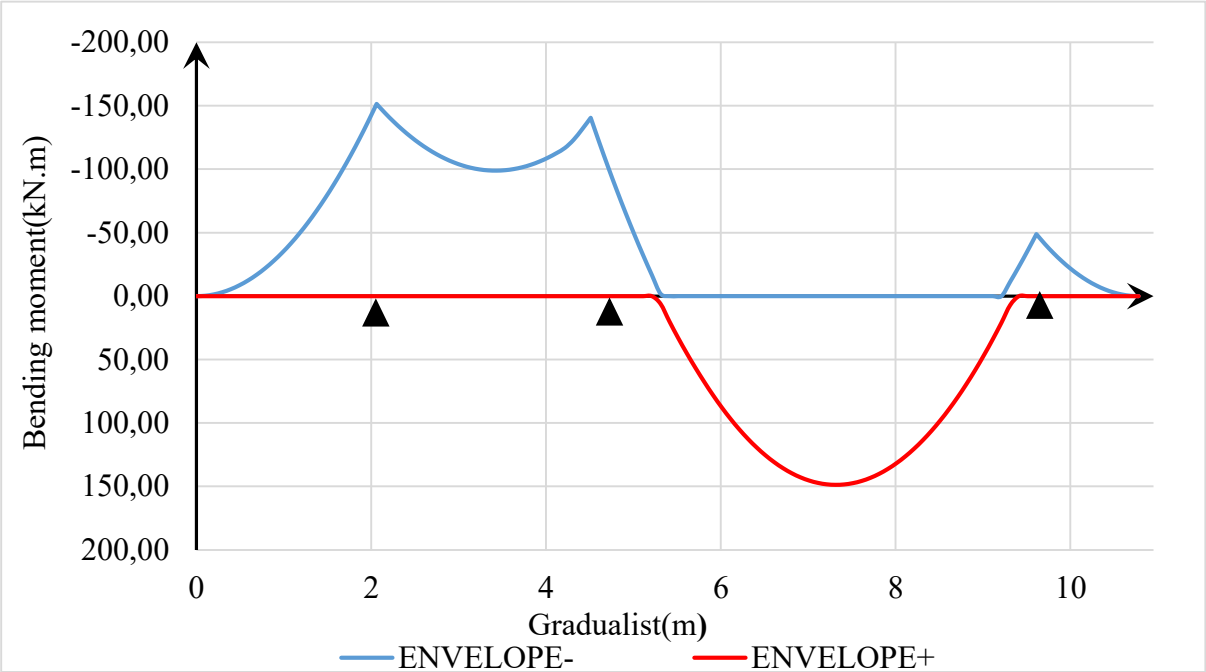

Figure 3.10. Envelope curve of bending moment on the beam

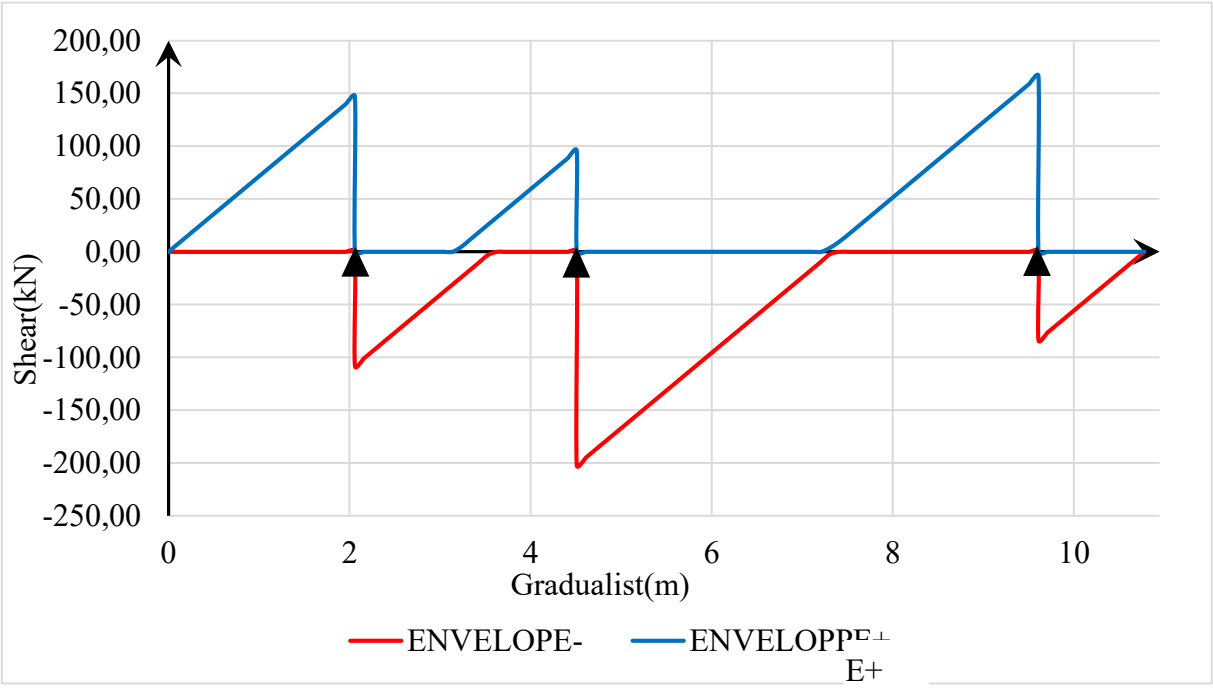

Figure 3.11. Envelope curve of shear on the beam

The steel reinforcement is evaluated using the equation 2.11 and the section obtained is verified for the detailing of member presented in the equations 2.12 and 2.13. At the end, the steel section is evaluated and verified for a beam section of *20 cm* × *60 cm* and the results obtained is presented in the figure 3.12.

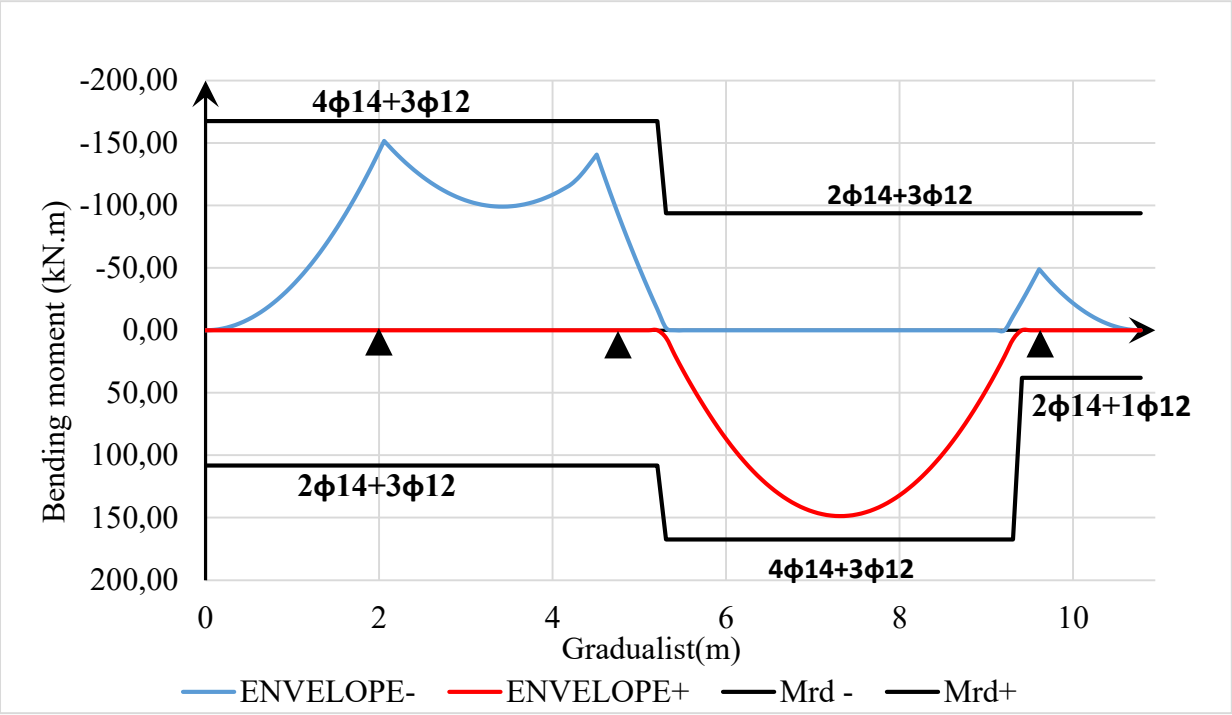

Figure 3.12. Recapitulative curve of the bending moment verification of the beam.

For the transversal reinforcement, considering a diameter of 6 mm the design procedure presented on the section 2.4.2.1.b permits to obtain the spacing of the stirrups necessary to resist to the envelope of the shear solicitations. Figure 3.13 presents a recapitulative of these stirrups spacing along the beam.

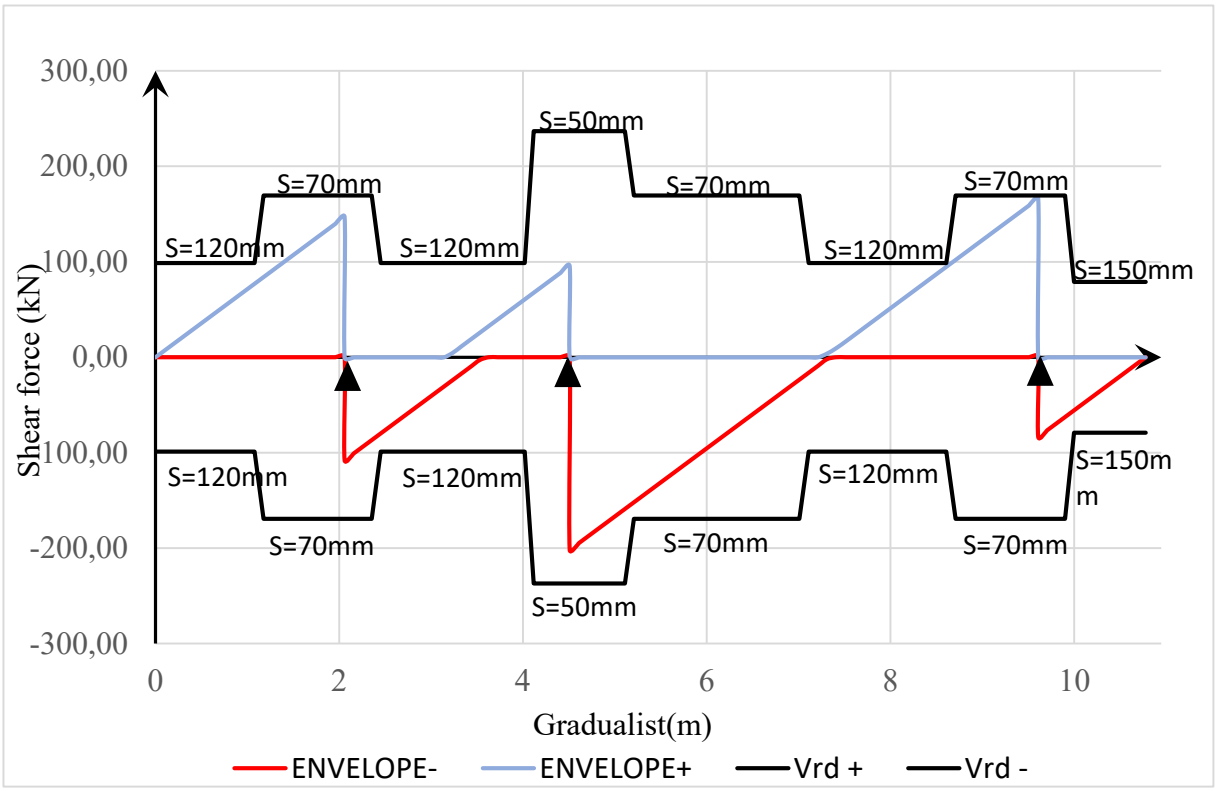

Figure 3.13. Recapitulative curve of the shear verification of the beam.

3.4.2.3. Serviceability limit state

The six load arrangements inserted in SAP 2000 at the characteristic (rare) combination permit to obtain the solicitation curves presented in the figure 3.14.

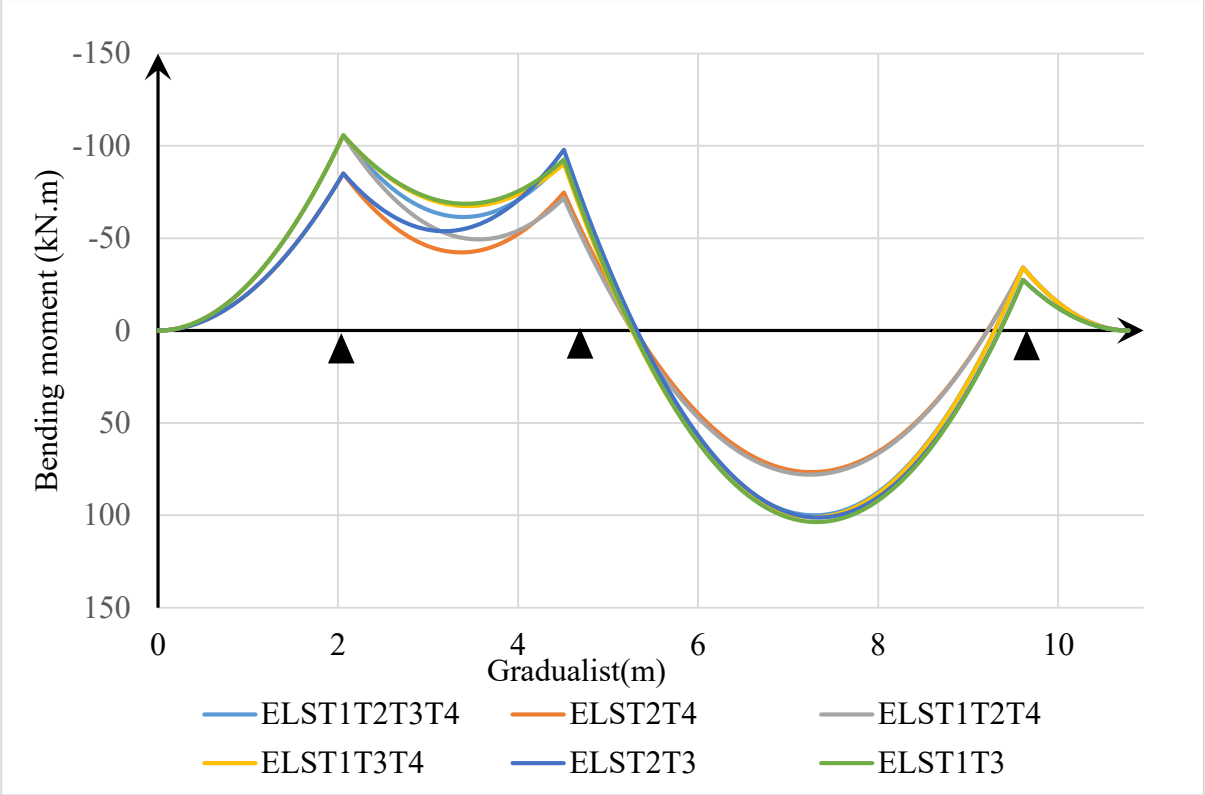

Figure 3.14. Bending moment curves on the beam at SLS

These solicitations permit to obtain the envelope curve presented in the figure 3.15

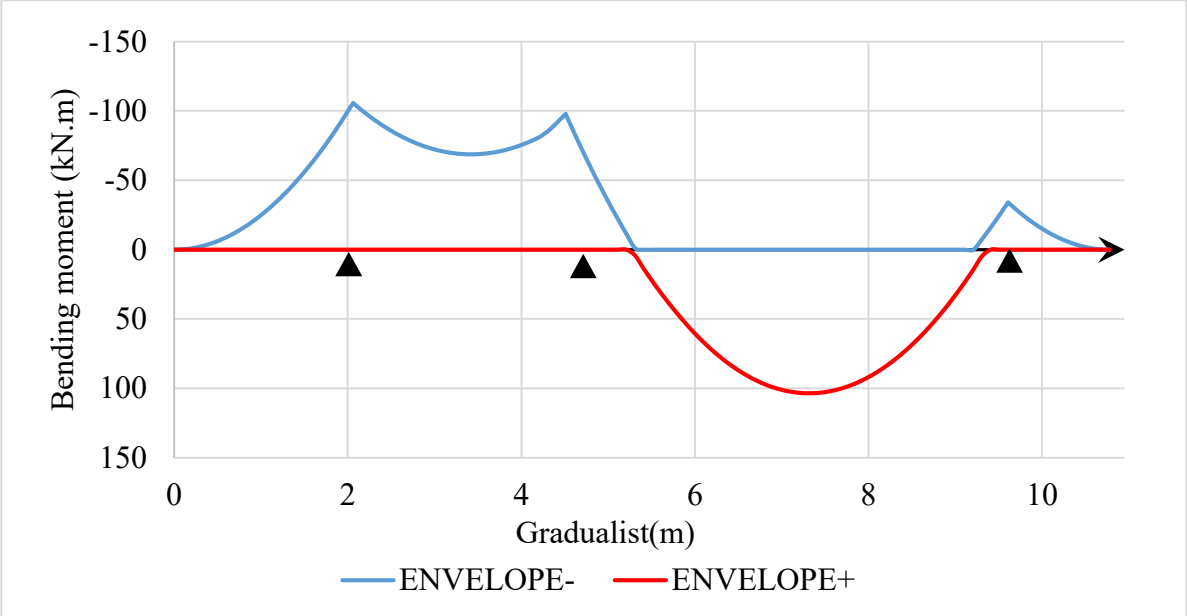

Figure 3.15. Envelope curve of the bending moment solicitation at serviceability limit.

With this envelope curve for bending moment at serviceability limit state the stress in the concrete and in the reinforcement are obtained using the equations 2.30 and 2.31. The limit value on the stress is evaluated from the equations 2.32 and 2.33 using the recommended values of the Eurocode 2, means taking $k_1 = 0.6$ and $k_3 = 0,8$. Figure 3.16 shows a comparison of the stress inside the concrete and the steel reinforcement to the admissible stress.

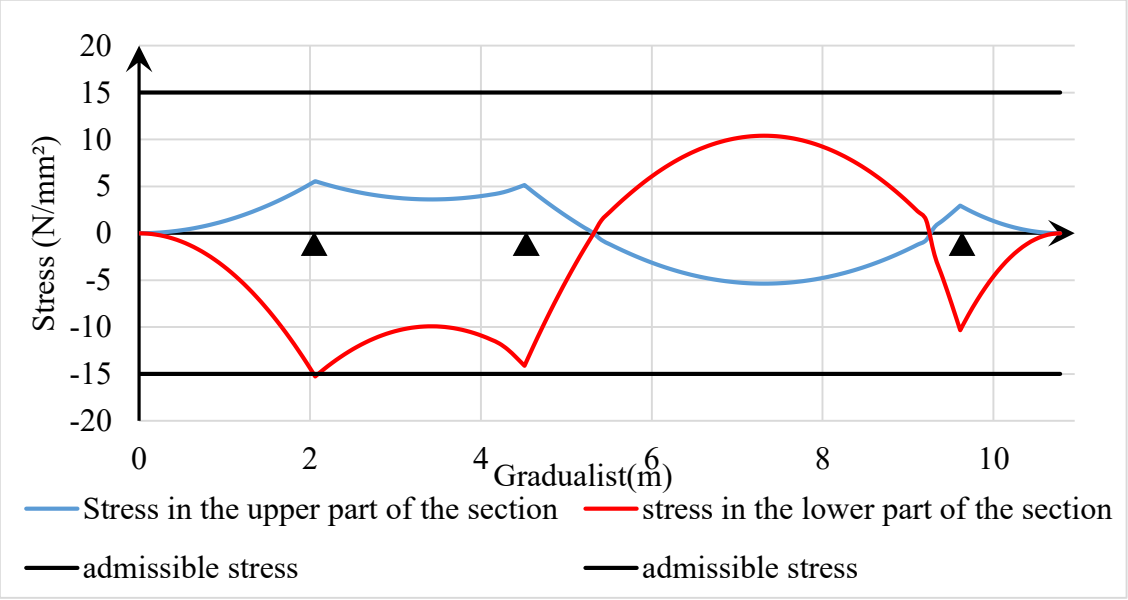

(a)

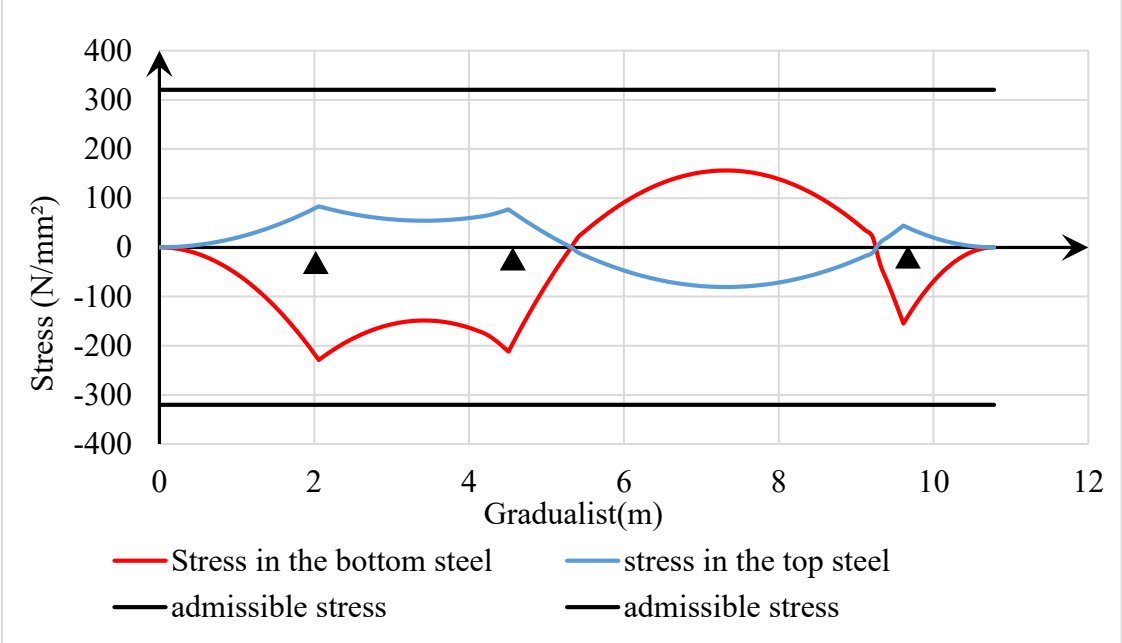

(b)

Figure 3.16. Recapitulative curve of stress verification of the beam: (a) in the concrete ;(b) in the steel

The structural detailing of the beam is presented in figure 3.17**.**

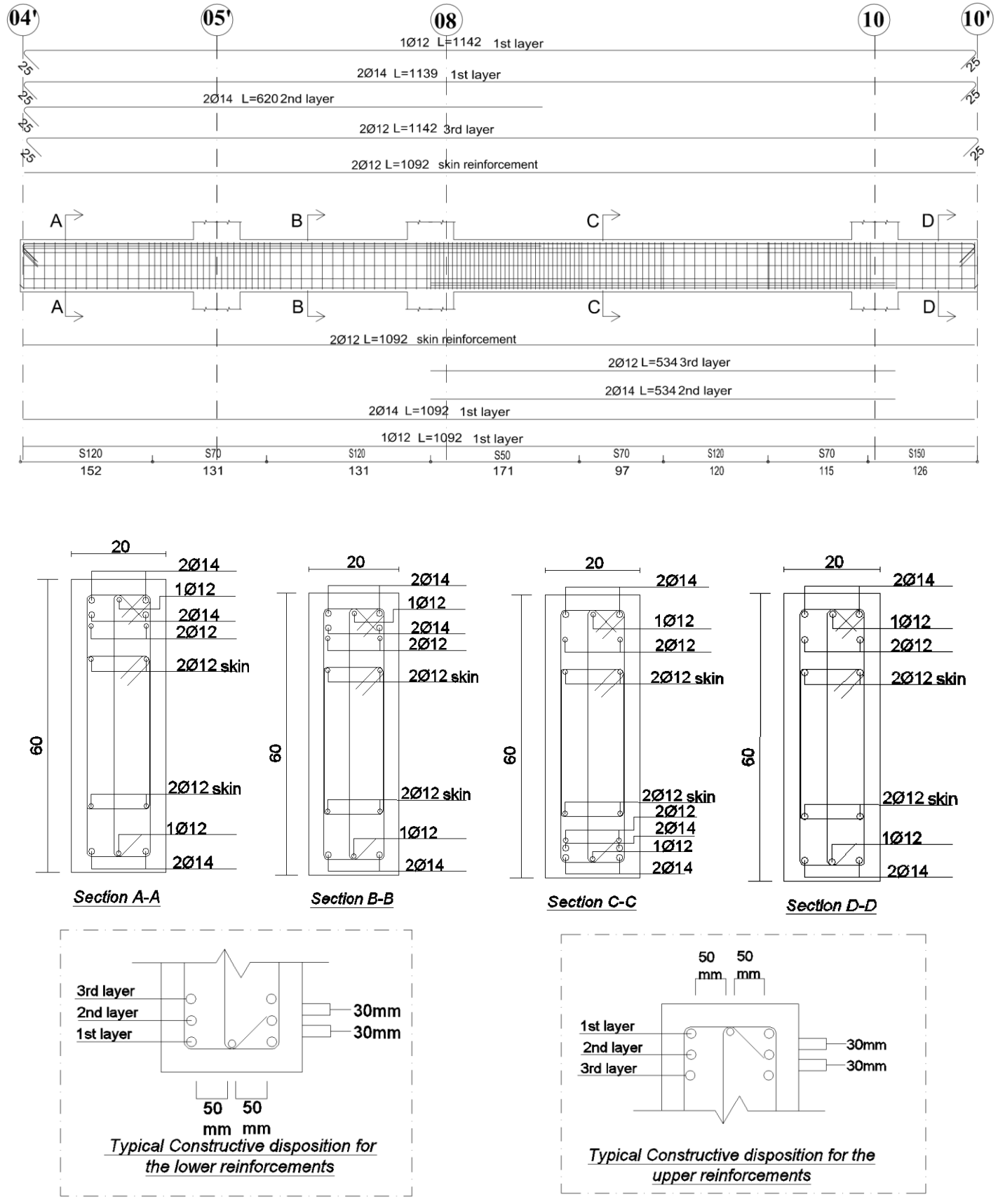

Figure 3.17. Structural detailing of the chosen beam

3.4.3. Design of columns row

The preliminary design, the M-N verification, the shear verification and slenderness are presented.

3.4.3.1. Preliminary design

The column chosen for the design is the column B8 presented in the figure 3.18.The vertical elements as well as the horizontal elements are modelled as frame elements.

.

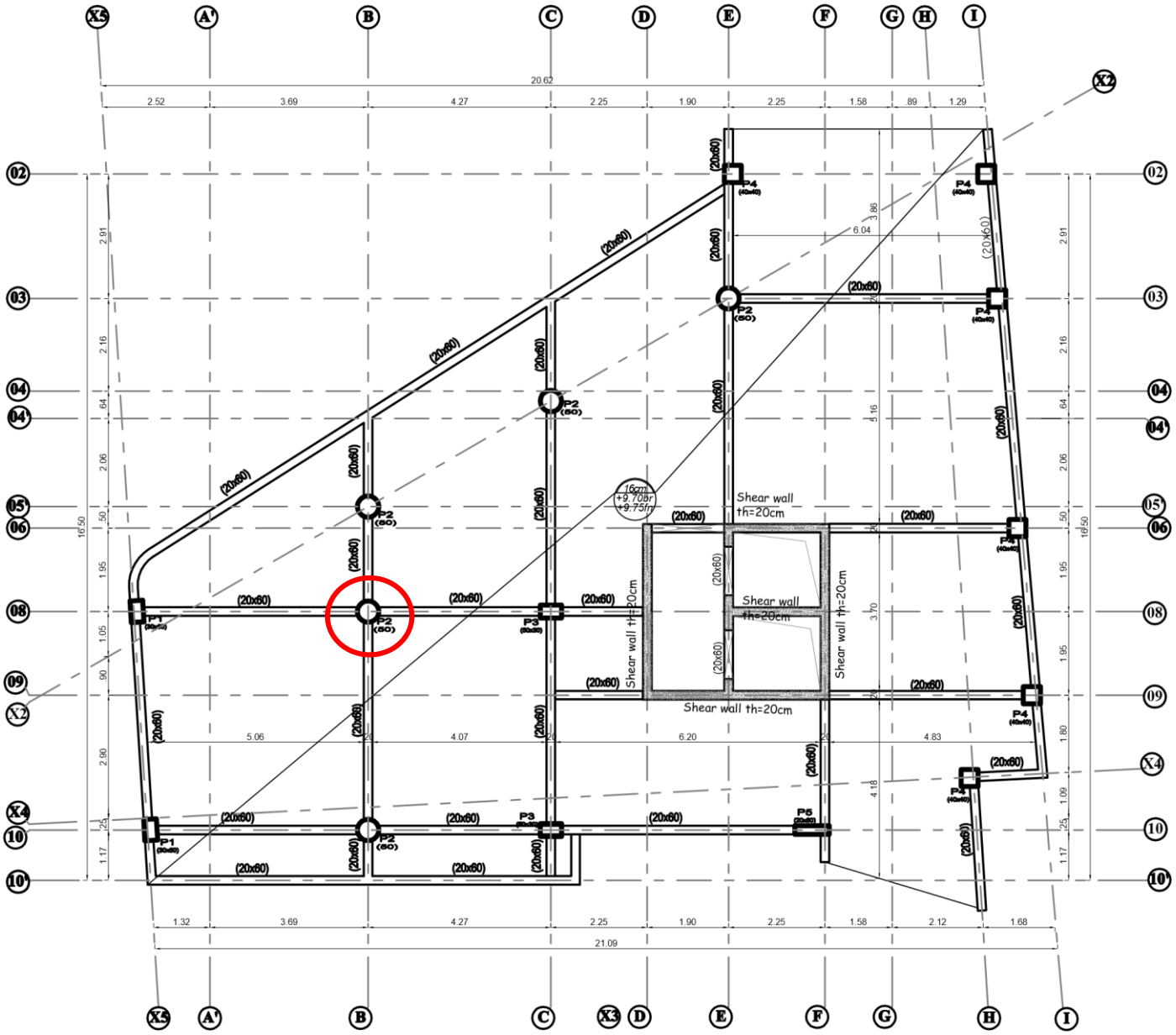

Figure 3.18. Choice of the studied column.

The columns are designed by modelling the structure in 3D with fixed supports at the base. The 3D model is presented in figure 3.19. The procedure is similar to that of horizontal structural element.

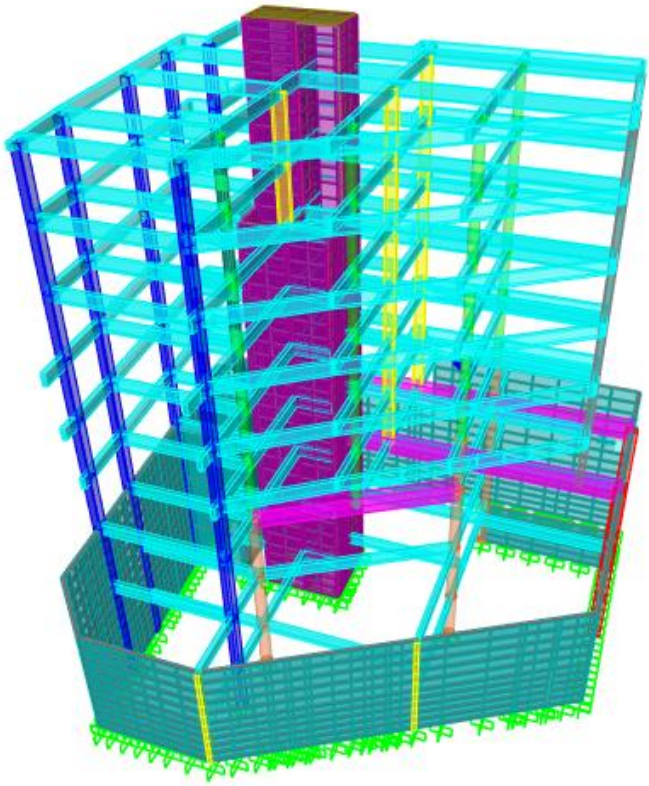

Figure 3.19.3D model with fixed base

We can thus compute the minimum area section of the column by using the equation 3.1.

$$N_{Rd} = 0{,}6 f_{cd} \times A_c \geq N_{Sd} \quad (3.1)$$

Where:

A_c is the area of concrete section;

N_{Sd} is the axial load computed using the recovery area of the column as shown in formula (3.2).

$$N_{Sd} = q \times S_r \times n \quad (3.2)$$

Where:

q is the uniform distributed load on each floor computed at ULS;

S_r is the recovery area of the column;

n is the Number of floor of the building.

We obtain for the level 1 up to the roof $Ac \geq \frac{qxSrxn}{0,6xfcd}$ =69000mm² using the same principle for the basement 2 up to the ground level we obtain Ac ≥107215,35mm².

Assuming a circular section, we can take a diameter of 50cm for the level 1 up to the roof, and 60cm diameter for the basement 2 up to the ground floor. The beams have the same geometric characteristics previously mentioned.

3.4.3.2. Bending moment and axial force verification in the columns

Columns are designed for the six previous loads combinations. This permit to obtain different solicitation envelope curves for the axial loads and bending moment presented in figure 3.20, figure 3.21 and figure 3.22 respectively.

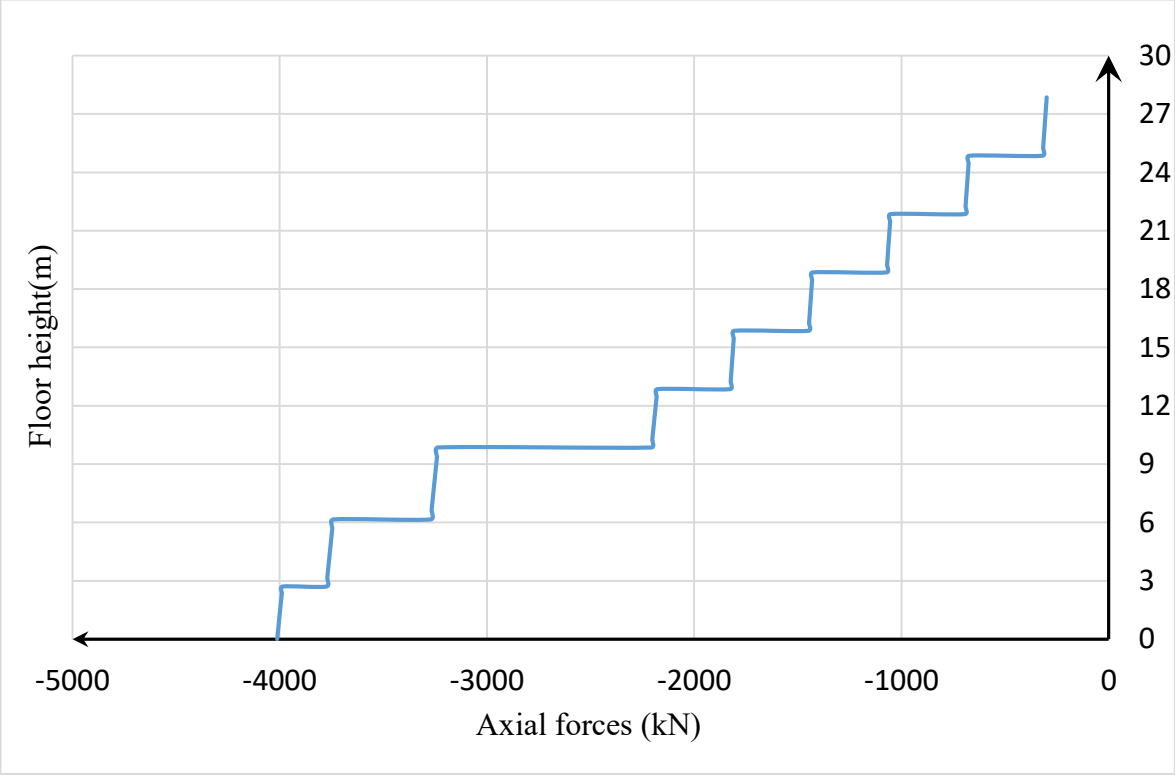

Figure 3.20. Axial load envelope curve.

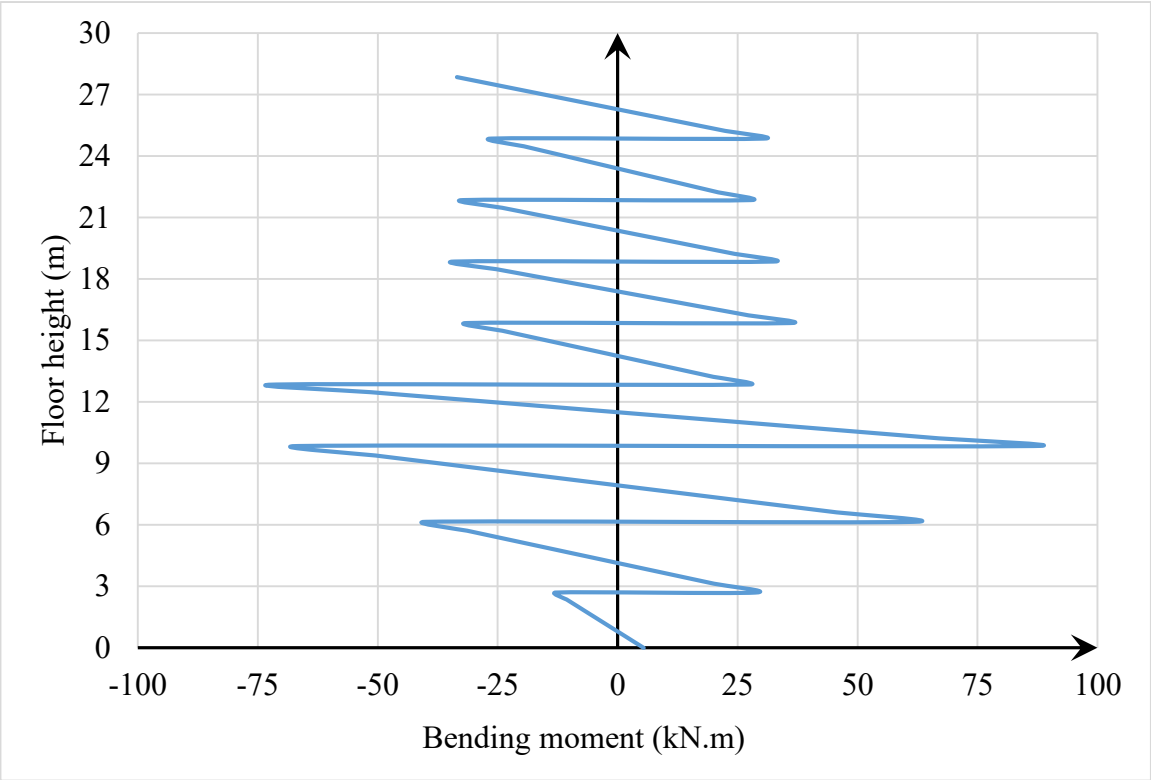

Figure 3.21. Bending moment curve around the x-axis in the column.

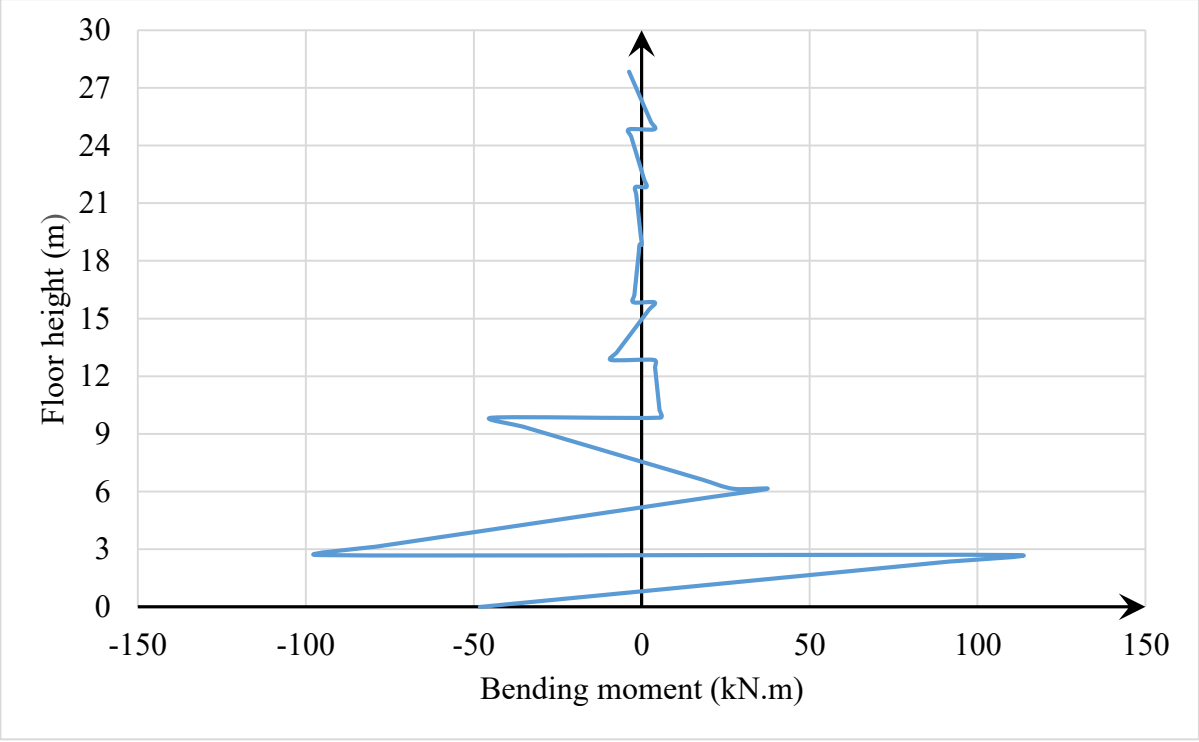

Figure 3.22. Bending moment curve around the y-axis in the column.

The verification of the axial loads and the bending moments is done through the interaction diagram.

Table 3.6. Columns reinforcement

	Section (diameter cm)	As,min (mm^2)	As,max (mm^2)	Reinforcement	As, provided (mm^2)
Ground floor, basement 1&2	60	1117	11309,73	8Ø14	1231,50
Level 1 to the roof	50	889	7853,98	8Ø12	904,78

The two typical cut sections of the column with their longitudinal reinforcements are presented in figure3.23.

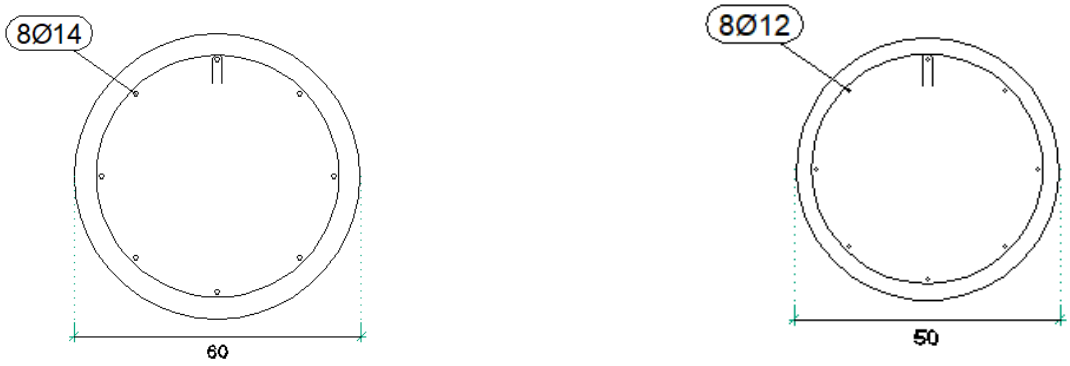

(a) (b)

Figure 3.23. (a) Typical cut section of the column with 60 cm diameter ;(b) Typical cut section of the column with 50 cm diameter

By using previous curve plotted in figure 3.20, 3.21 and 3.22, the table 3.7 is obtained.

Table 3.7. Recapitulative of axial forces and bending moments in the column.

Level	Axial forces (kN)	Bending moment around the x-axis (kN.m)	Bending moment around the y-axis (kN.m)
Basement 2	-4011,84	5,42	-48,17
Basement 1	-3774,50	28,65	-95,97
Ground floor	-3271,44	61,67	27,23
Level 1	-2205,85	86,67	5,56
Level 2	-1826,24	27,27	-9,12
Level 3	-1448,096	36,02	-2,40
Level 4	-1071,63	32,45	0,00
Level 5	-693,00	27,74	1,42
Level 6	-318,75	30,41	3,74

The interaction diagram of the columns in the two directions are presented in the figure 3.24 and the figure 3.25 for the two directions.

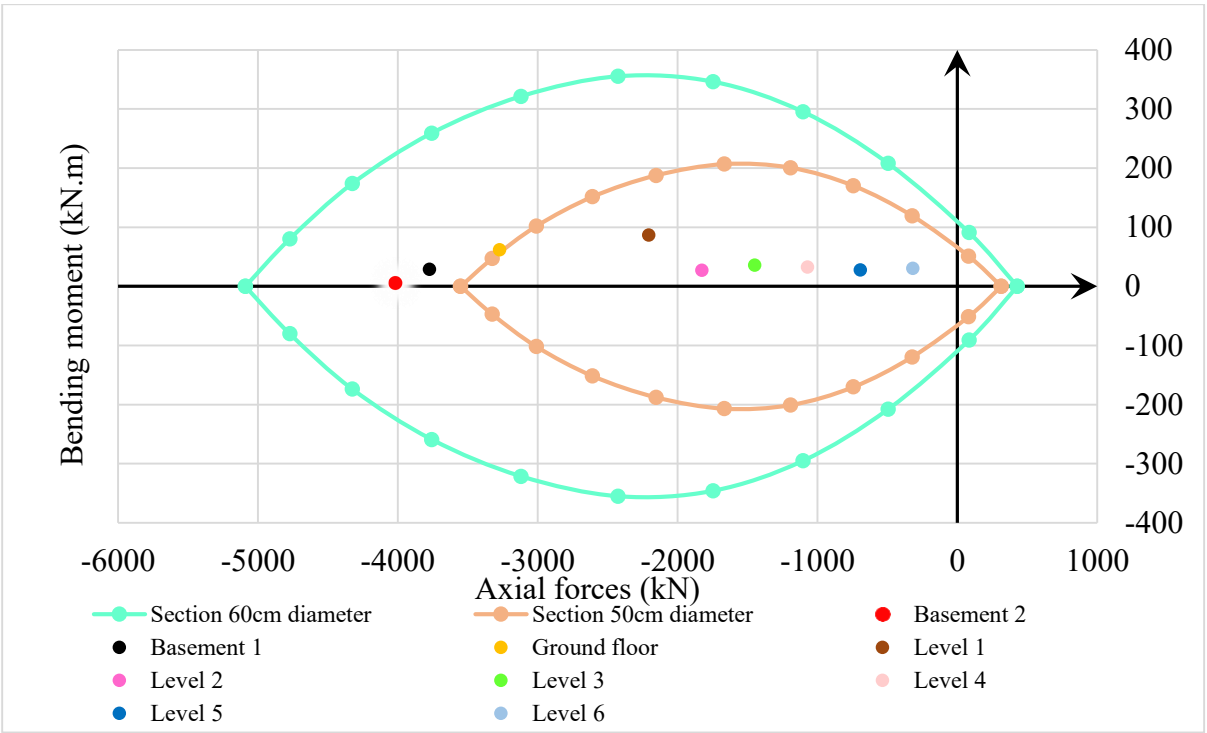

Figure 3.24. Interaction diagram of column B8 around the x direction

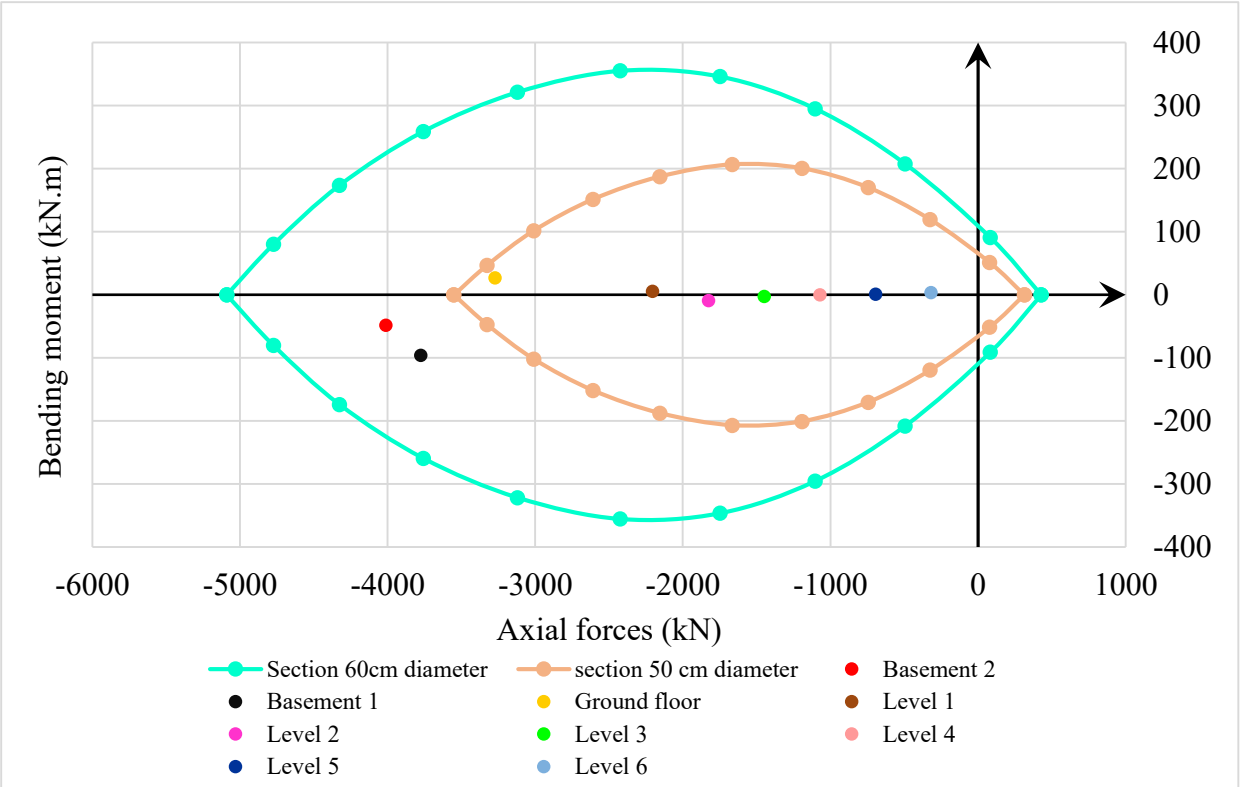

Figure 3.25. Interaction diagram of column B8 around the y direction.

Figure 3.24 and figure 3.25 show that the bending moment and the axial force solicitations of the column is inside the diagram so the section is correct.

3.4.3.3. Shear verification

By using the same previous loads combination, this permit to obtain different solicitation curves. The Shear forces in x direction and in y direction as well, are presented in figure 3.26 and figure 3.27 respectively.

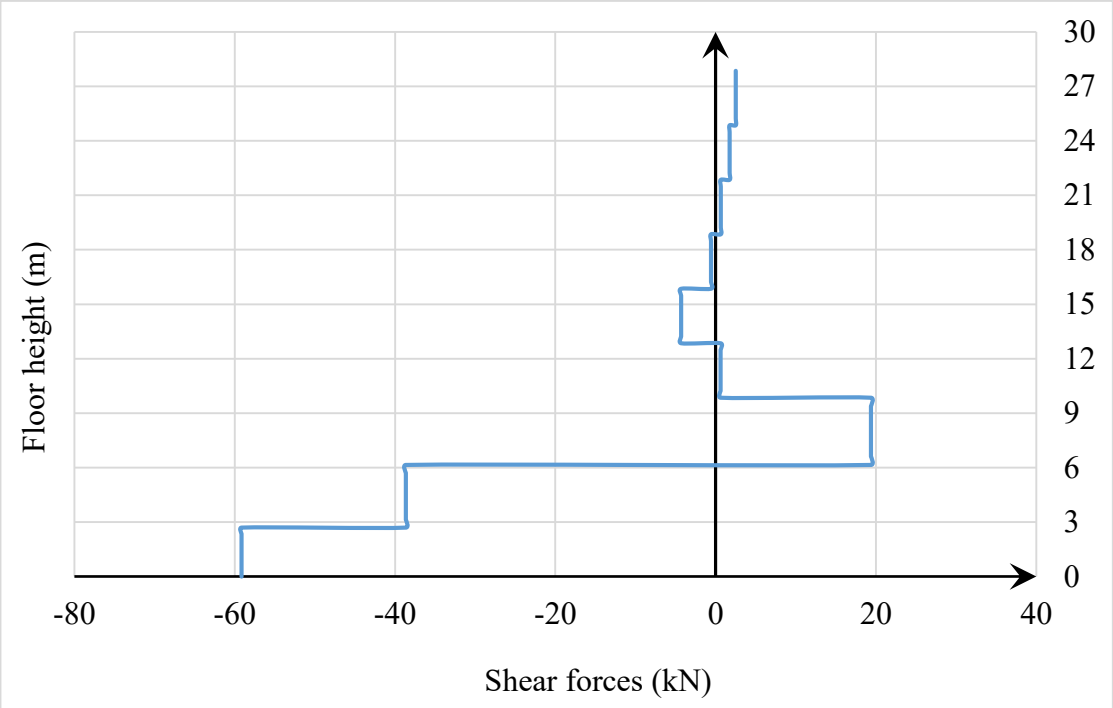

Figure 3.26. Shear force in the x direction

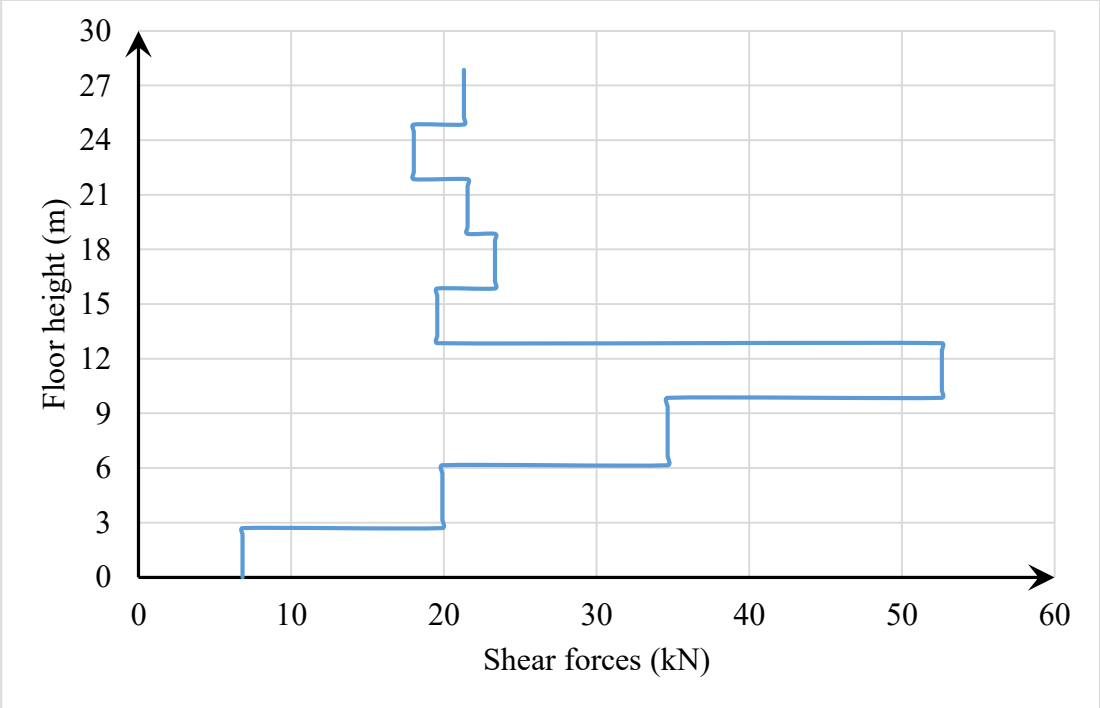

Figure 3.27. Shear force in the Y direction.

Applying the procedure presented in the section 2.6.2.1.b, the shear resistance of the section without shear reinforcement is greater than the maximum shear solicitation on the column with

Vrd=254,46kN.So the detailing of members has to be applied to have the spacing. In our case, we consider a diameter of $6mm$ and the maximum spacing of the transverse reinforcement is given by equation 2.44.

$$S_{cl,\max} = \min(240,600,400) = 240mm$$

Finally a spacing of 150mm is adopted.

3.4.3.4. Slenderness verification

Following the procedure presented on the section 2.4.3.3, the different parameters are evaluated and presented in table 3.8.

Table 3.8. Parameter for slenderness verification.

Level	λx	λy	$\lambda limx$	λlim y
Basement 2	18	18	30,42	38,83
Basement 1	23	23	42,78	35,09
Ground level	24,67	24,67	40,80	40,80
Level 1	20	20	43,91	53,38
Level 2	24	24	43,71	44,45
Level 3	24	24	55,55	54,59
Level 4	24	24	69,49	65,94
Level 5	24	24	85,21	86,21
Level 6	24	24	124,43	123,95

The table 3.8 shows that $\lambda < \lambda_{lim}$, so the slenderness of the column is verified.

The detailing of the column is presented in figure 3.28.

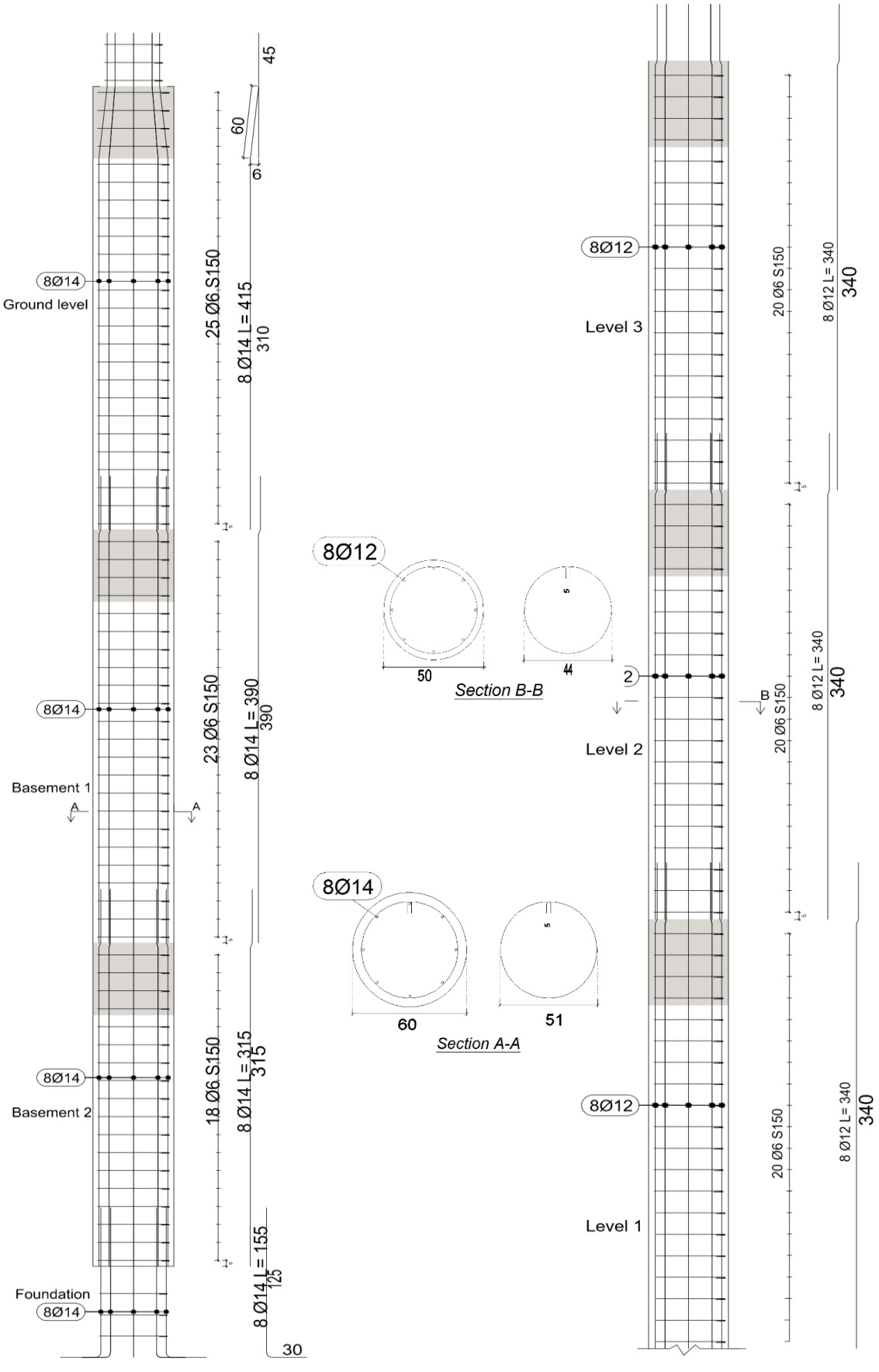
8Ø14
Ground level
25 Ø6 S150
8 Ø14 L= 415
310
45
60
6
8Ø14
Basement 1
A
A
23 Ø6 S150
8 Ø14 L= 390
390
8Ø14
Basement 2
18 Ø6 S150
8 Ø14 L= 315
315
Foundation
8Ø14
8 Ø14 L= 155
125
30
8Ø12
50
Section B-B
44
8Ø14
60
51
Section A-A
8Ø12
Level 3
20 Ø6 S150
8 Ø12 L= 340
340
2
B
Level 2
20 Ø6 S150
8 Ø12 L= 340
340
8Ø12
Level 1
20 Ø6 S150
8 Ø12 L= 340
340

(a) (b)

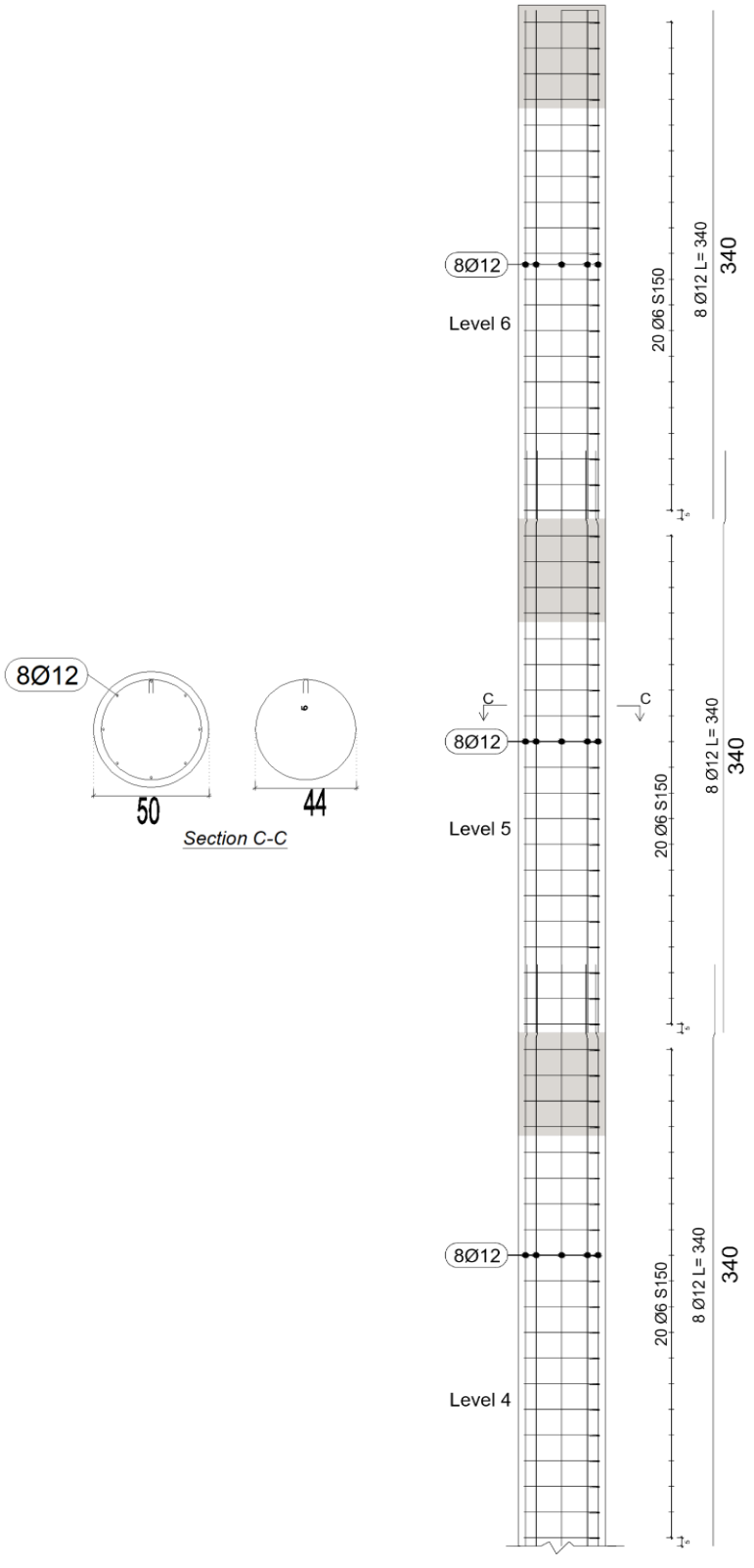

(c)

Figure 3.28. Detailing of the chosen column (a) Basement1 to ground level (b) level1 to level 3(c) level4 to level6

3.4.4. Retaining wall design

This part concern the study of the retaining wall at the basement levels of the structure. A preliminary design and structural analysis will be presented. The sliding and overturning verifications are not necessary, due to the fact that the wall is directly linked to the whole structure.

3.4.4.1. Preliminary design

The plan view and the typical cut section of the chosen retaining wall for the design are highlighted in the figure 3.29 and 3.30 respectively.

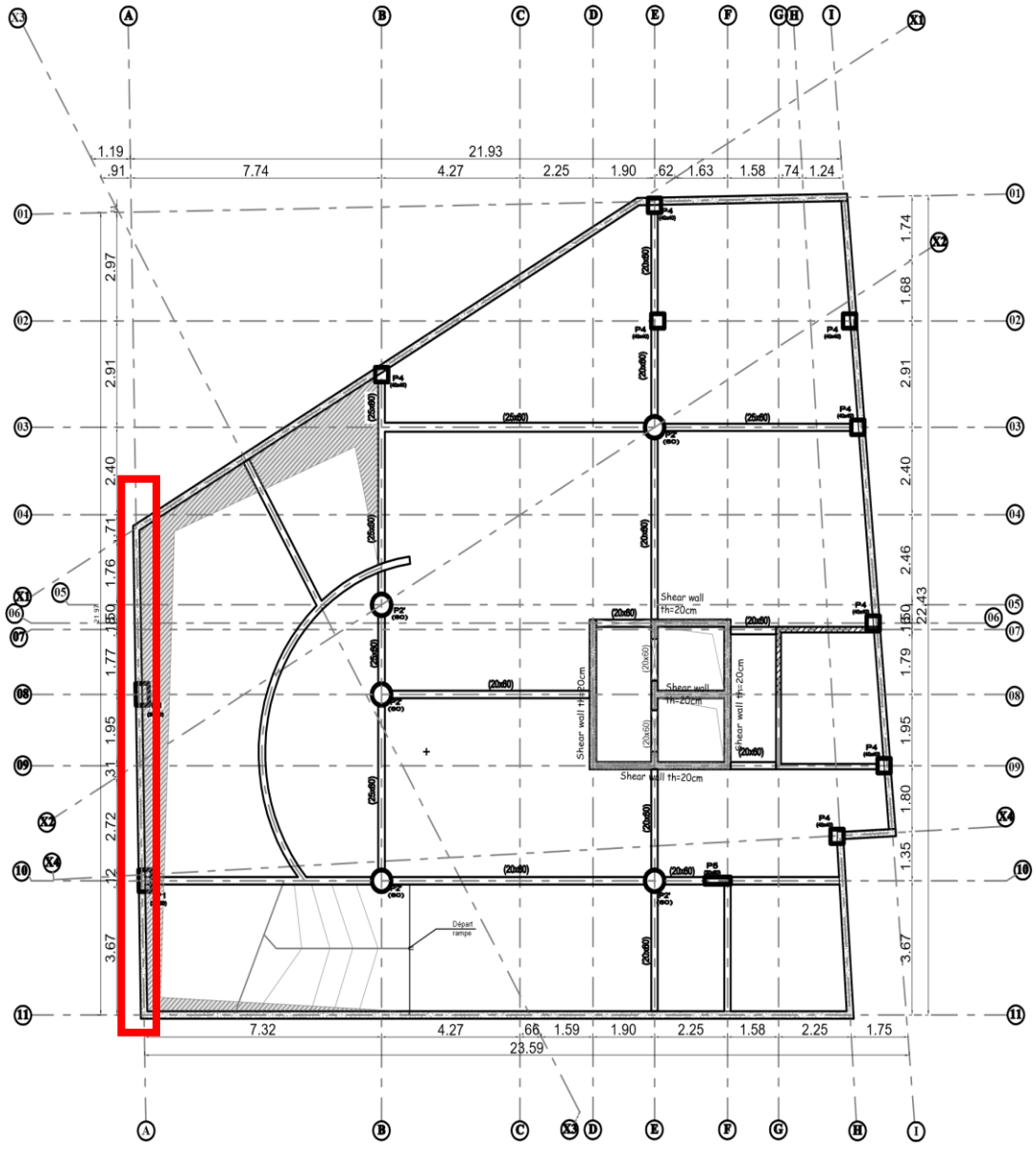

Figure 3.29. Chosen part of the retaining wall

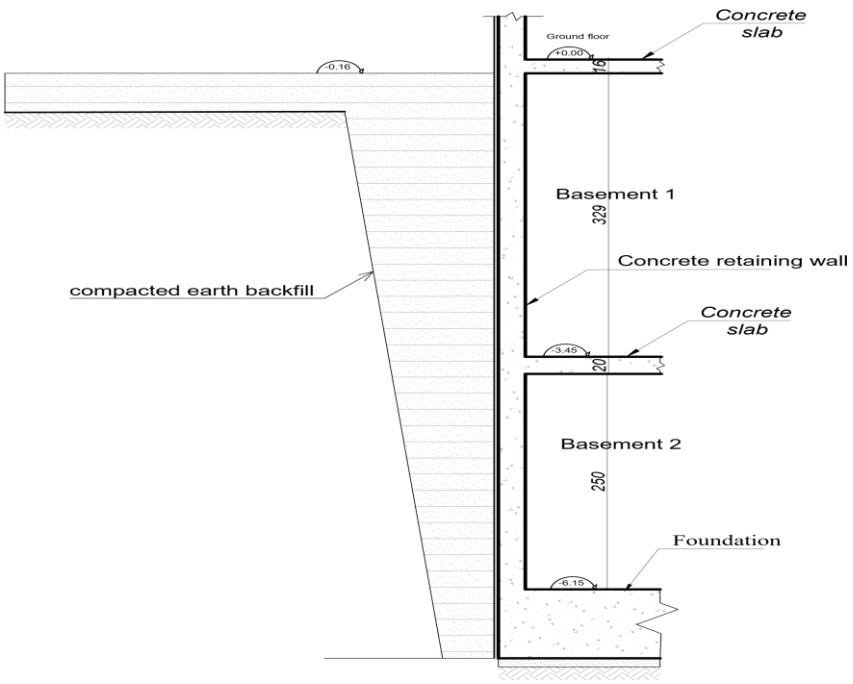

Figure 3.30. Typical cut section of the chosen retaining wall.

The retaining wall thickness is determined using certain criterion.

$$\begin{cases} t \geq 15cm \\ t \geq \frac{h}{200} = 16{,}45cm \end{cases} \qquad \text{Choose } t = 25\ cm$$

3.4.4.2. Loads and loads combination

The different type of loads which are acting on the wall are summarize in figure 3.31.

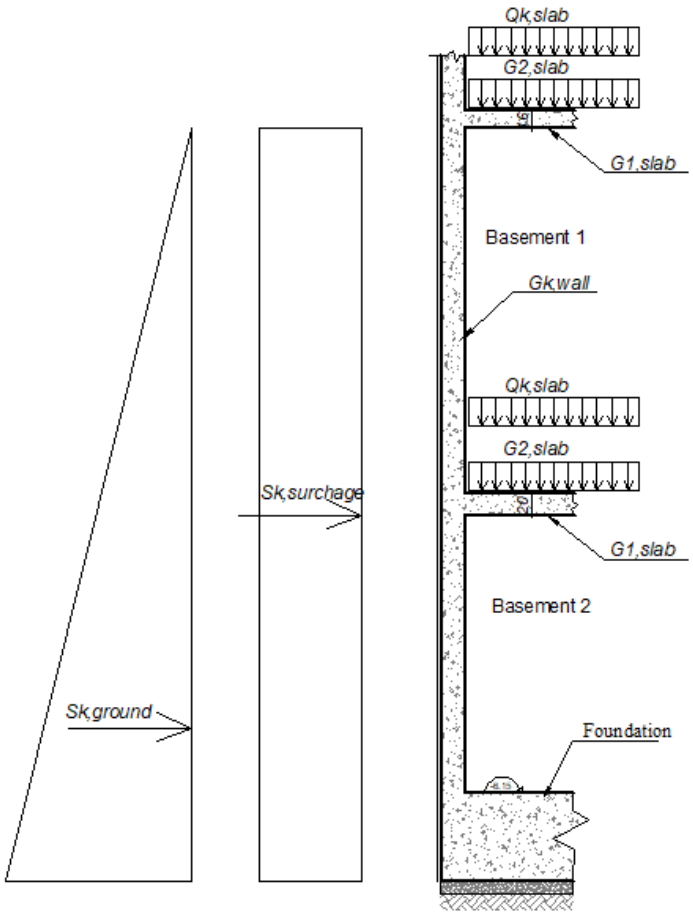

Figure 3.31. Different type of loads acting on the retaining wall.

Where:

Sk,ground is Ground horizontal force;

Sk,surcharge is Surcharge horizontal force provided by the surcharge on the embankment;

Gk,wall is the self-weight of wall;

Qk,slab is the imposed load acting on the slab;

G1,slab is the self-weight of the slab;

G2,slab is the surcharge load acting on the slab.

Based on the geotechnical data which are presented in table 3.9, Sk,ground and the load Sk,surcharge can be computed.

Table 3.9. Geotechnical data.

Geotechnical data	Symbols	Values
Soil weight density	γ	18kN/m³
Angle of shearing resistance	Φ	33,3°
Factor of horizontal active earth pressure	Ka	0,29
Wall-ground interface friction angle	δ	0°

Based on the equation 2.48 and 2.49 the value of Sk,ground and Sk,surcharge are obtained. So Sk,surcharge =19.72kN/m and Sk,ground=120.69kN/m.

The wall will be designed under the load combination presented in equation 3.3.

ULS,wall=1.35 x Sk,ground+1.5 x Sk,surcharge+1.35x Gk,wall+1.35x G1,slab+1.35x G2,slab+1.5xQk,slab (3.3)

3.4.4.3. Bending moment design

The 3D modelling of the building in SAP 2000 with a fixed base is used to extract the required solicitations. The 3D view of the retaining wall is presented in figure 3.32.

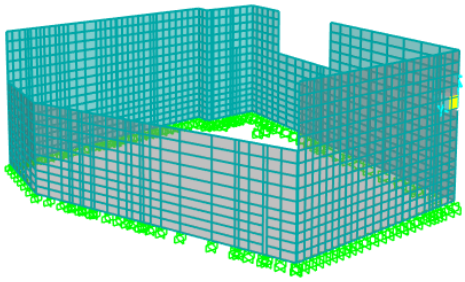

Figure 3.32. 3D view of the retaining wall in the numerical model.

The bending moment along the y-axis and the z-axis are cartography in figure 3.33.

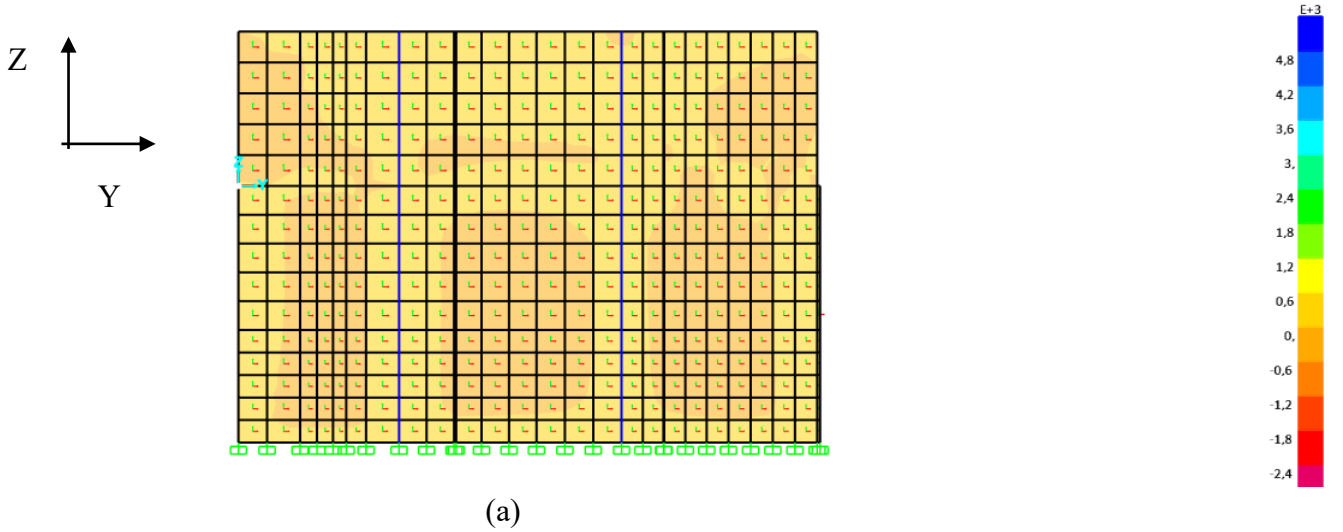

(a)

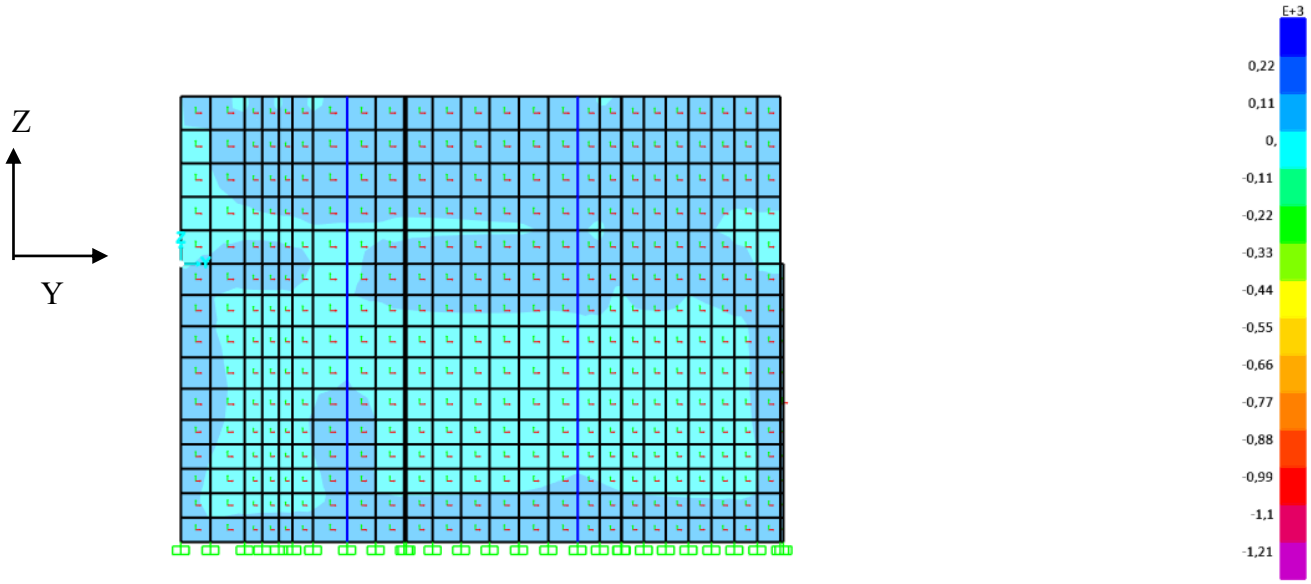

(b)

Figure 3.33. Moment distribution (a) along Y ;(b) along Z.

The designed moments are presented in table 3.10.

Table 3.10. Moment values inside the chosen panel.

	Y direction	Z direction	Units
Positive moment	34,55	48,59	kN.m
Negative moment	-93,67	-116,94	kN.m

Notice that the lower fibre is the face of the wall inside the building.

Assuming a 14 mm diameter bars to be used and a concrete cover of 50 mm. the effective depth of the outer layer to be used in the design for moments in the both direction is:

$$d=250-50-\frac{14}{2}=193mm$$

From this, the reinforcement for each face of the wall is computed and presented in table 3.11 and table 3.12 respectively.

Table 3.11. Reinforcement for the face of the wall inside the building.

	Theoretical reinforcement (mm² /m)	Provided reinforcement per meter	Spacing (mm)
Y direction	571,85	8Φ10	125
Z direction	804,42	10Φ12	100

Table 3.12. Reinforcement for the face of the wall outside the building.

	Theoretical reinforcement (mm² /m)	Provided reinforcement per meter	Spacing (mm)
Y direction	1550,38	8Φ16	125
Z direction	1935,53	10Φ16	100

3.4.4.4. Axial forces verification

The axial force solicitation through the retaining wall under the ULS,wall combination is represented in figure 3.34.

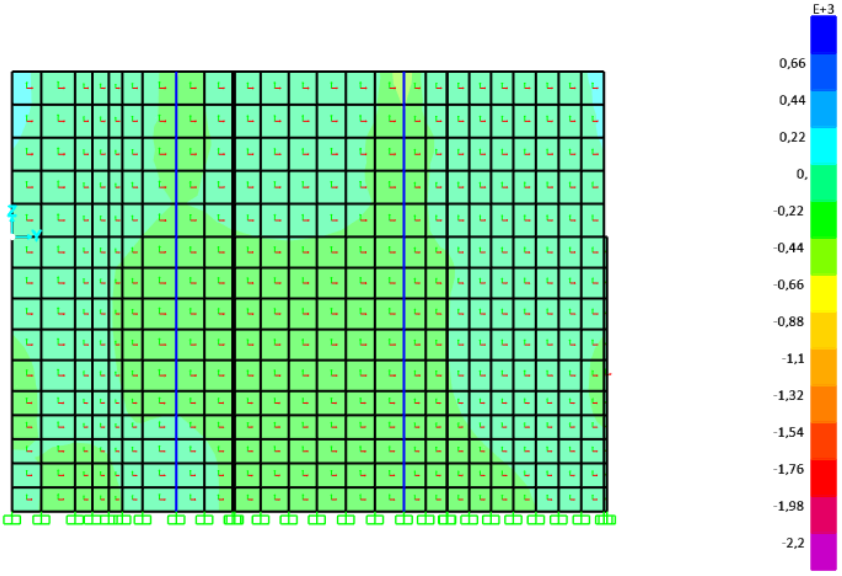

Figure 3.34. Axial forces distribution inside the wall

So the design axial force will be Ned=-687,81kN.

The resisting axial force provided by one meter length of the concrete part of the wall is given in equation 3.4.

$$Nrd=\frac{\alpha \text{ x } Br \text{ x} fcd}{0.9} \qquad (3.4)$$

Where:

$\alpha=\frac{0.65}{1+\frac{0.2 \text{ x}\lambda}{30}}$ with λ the slenderness ratio of the wall.

Br is the reduction section of the wall.

By using equation 3.2 Nrd=2419,44 kN > Ned.

So the wall can resist to the axial force only using its concrete resistance.

The detailing of the retaining wall is shown in figure 3.35.

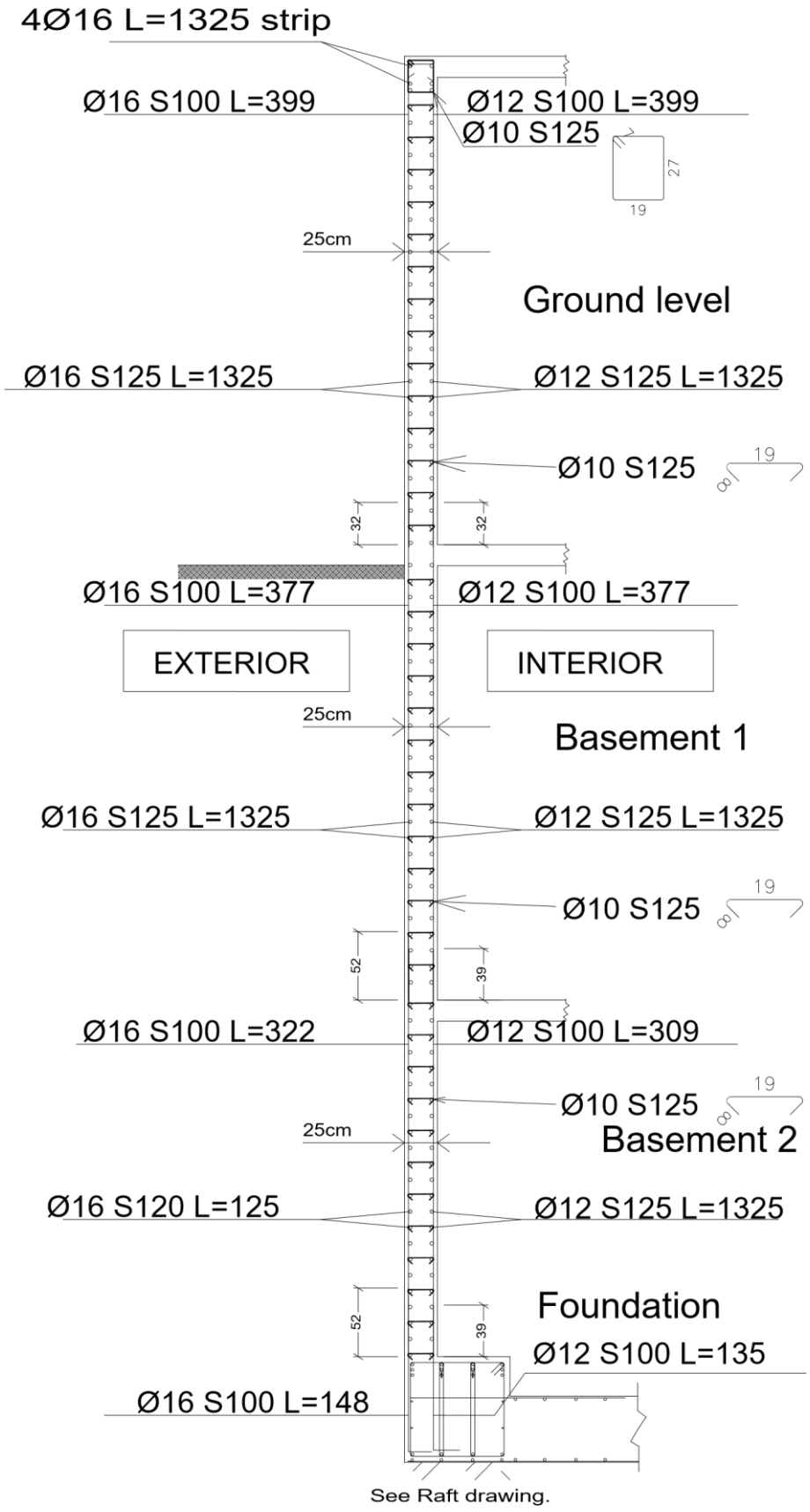

Figure 3.35. Detailing of the study part of the retaining wall.

3.4.5. Foundation design

The foundation is made by a raft.

3.4.5.1. Description of the foundation system

The raft is composed by a slab and the strengthening beams as shown in figure 3.36 and figure 3.37 .At first approximation the depth of the slab is taken to be 40cm and for strengthening beams, it is considered a section of 80cmx80cm.

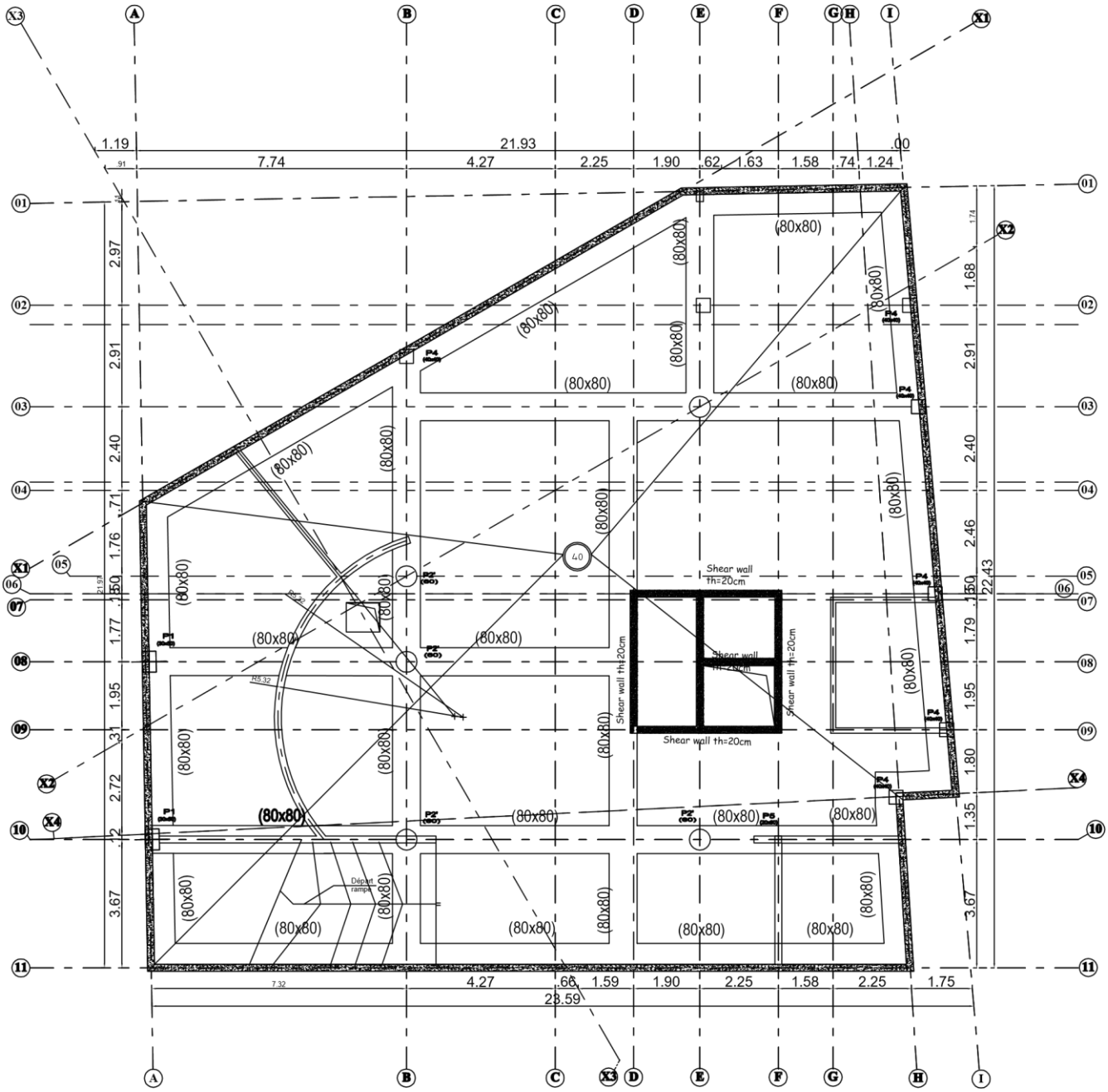

Figure 3.36. Foundation plan

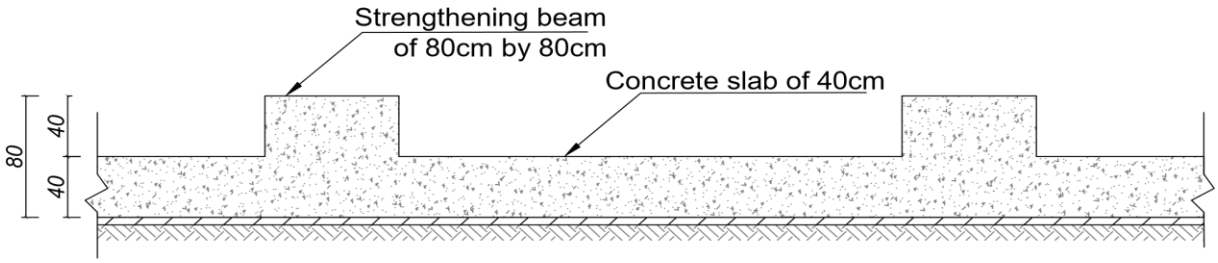

Figure 3.37. Typical cut section of the raft

The load combination presented in equation 3.5 will be used at the SLS.

$$SLS,raft=1.00 \times Sk,ground+1.00 \times Sk,surcharge+1.00x\ Gk,wall+1.0x\ G1,slab+1.0x\ G2,slab+1.0xQk,slab \quad (3.5)$$

For the ULS, the load combination presented in equation 3.1 will be applied.

To carry out this study a 3D numerical model of the building with the raft foundation have been realised using SAP 2000 as shown in figure 3.38.The raft have been modelled by using shell thick element and in the other hand strengthening beams have been modelled as a frame element. The subgrade modulus of the soil Ks=8317 kN/m² /m which is given by the geotechnical report of the site of the project, have been used to implement the raft like a linear area spring object.

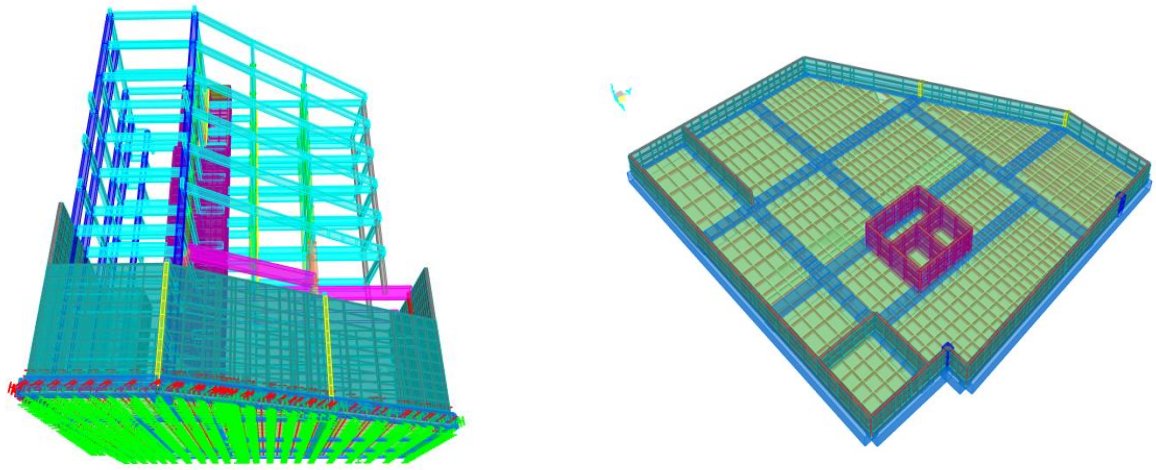

(a) (b)

Figure 3.38. Numerical model (a) 3D view (b) view on the raft

3.4.5.2. Admissible soil stress verification

Using the numerical model the soil pressure under the raft can be obtained for the load combination SLS, raft as shown in figure 3.39.

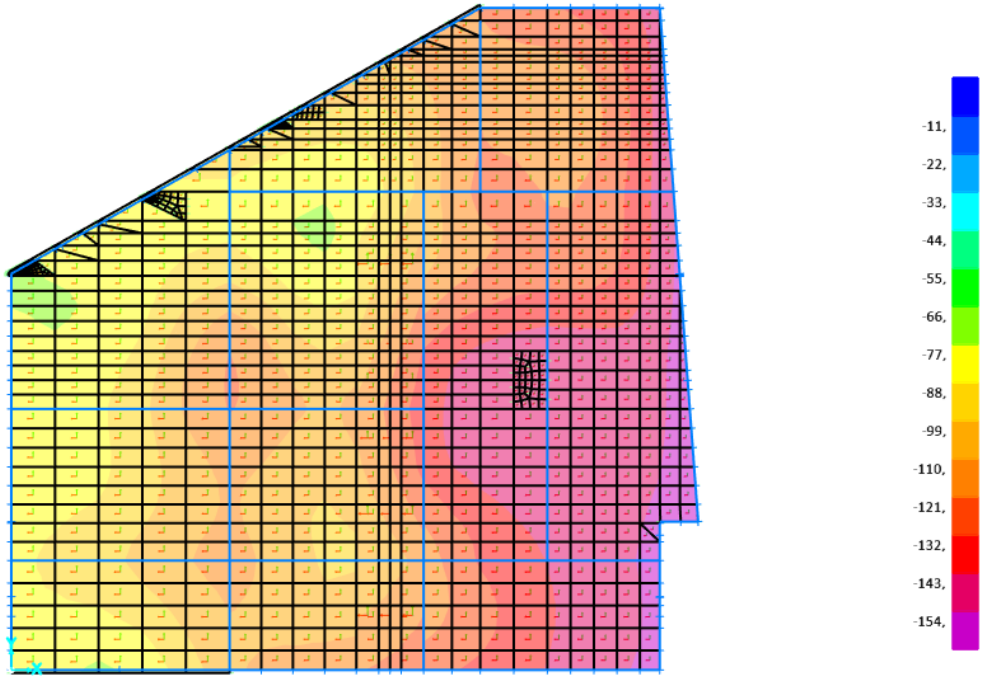

Figure 3.39. Soil pressure distribution under the raft

The admissible soil stress provided by the geotechnical study of the site is 0.165MPa.

The maximum soil pressure is 0,163 MPa $< \sigma_{adm} =$ 0,165 MPa. The admissible soil stress condition is satisfied.

3.4.5.3. Slab design

The slab will be design in flexion. The moment distribution along x and y for the chosen ULS combination are presented in the figure 3.40.

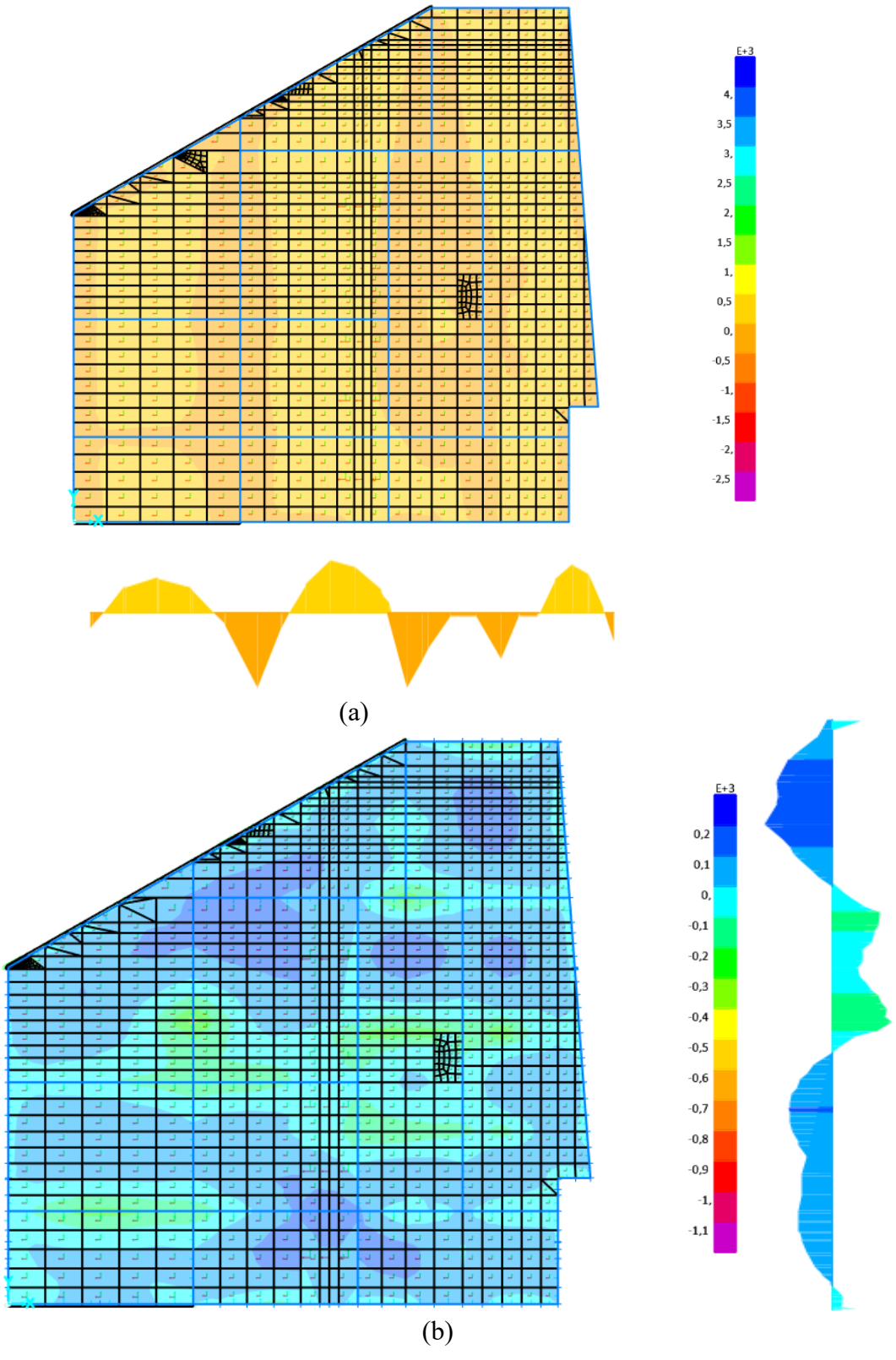

Figure 3.40. Moment distribution in the foundation mesh (a) along X; (b) along Y.

The designed moments are presented in table 3.13.

Table 3.13. Moment values inside the chosen panel.

	X direction	Y direction	Units
Maximum positive moment	577,75	438,33	kN.m
Maximum negative moment	-309,32	-265,97	kN.m

The minimum required steel reinforcement for 1m length is computed Asmin=1147mm²/m.

The recapitulative of the flexural design is presented in table 3.14 and 3.15.

Table 3.14. Reinforcement at the bottom of the raft.

	Theoretical reinforcement (mm² /m)	Provided reinforcement per meter	Spacing (mm)
X direction	1790	6Φ20	160
Y direction	1350	7Φ14	140

Table 3.15. Reinforcement at the top of the raft.

	Theoretical reinforcement (mm² /m)	Provided reinforcement per meter	Spacing (mm)
X direction	1147	8Φ14	125
Y direction	1147	8Φ14	125

3.4.5.4. Strengthening beam design

The chosen strengthening beam is highlighted in figure 3.41.

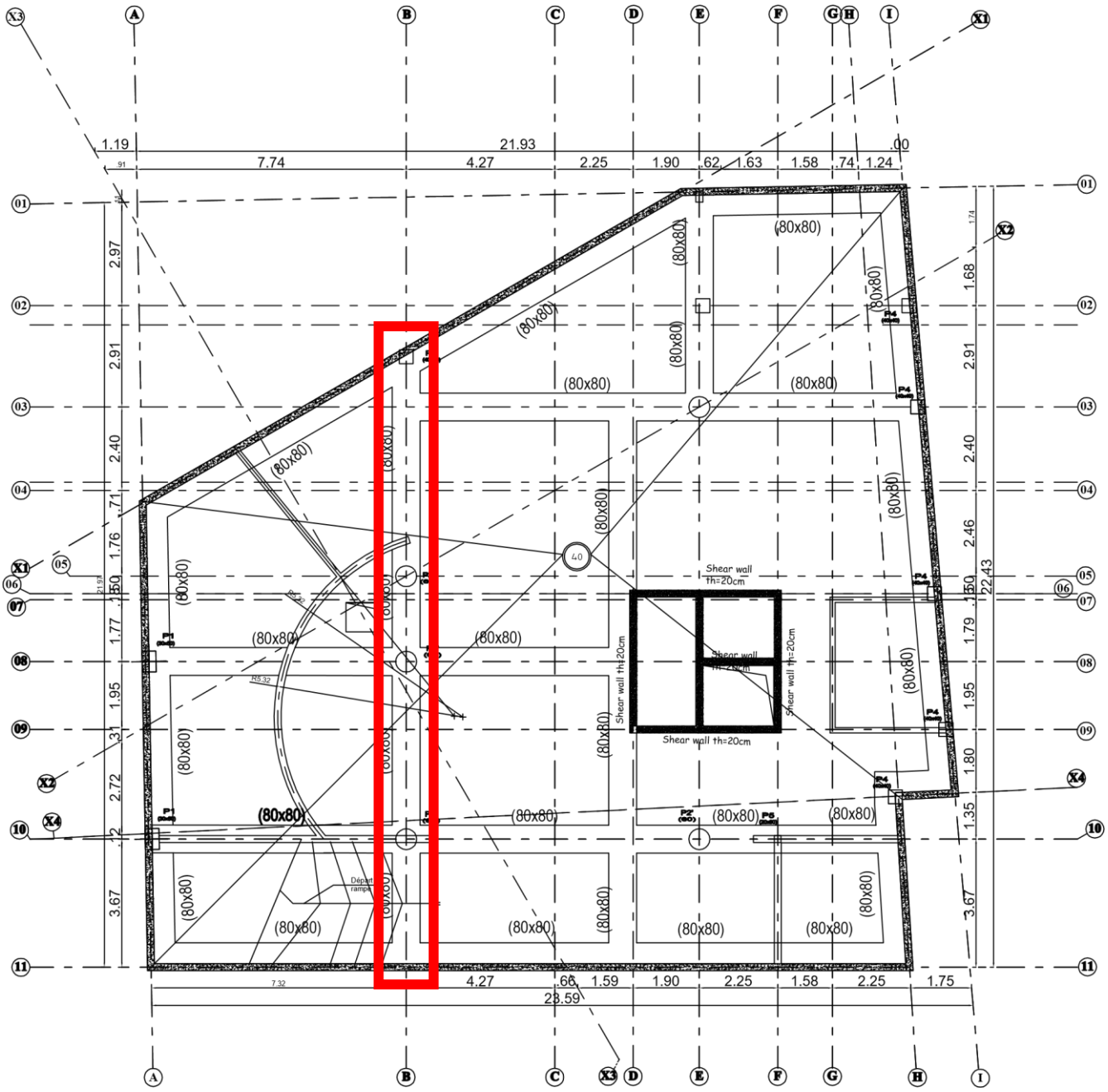

Figure 3.41. Chosen strengthening beam.

The strengthening beam will be designed in flexion and for the shear forces. Flexural reinforcements are design using equation 2.11 and the required shear reinforcement is provided by the procedure described in section 2.4.2.1.b .The recapitulative of the flexural design and

the shear design are presented in figure 3.42 and 3.43 respectively. Notice that the stirrups are made by a reinforcement of 10mm diameter and the concrete cover is 50mm.

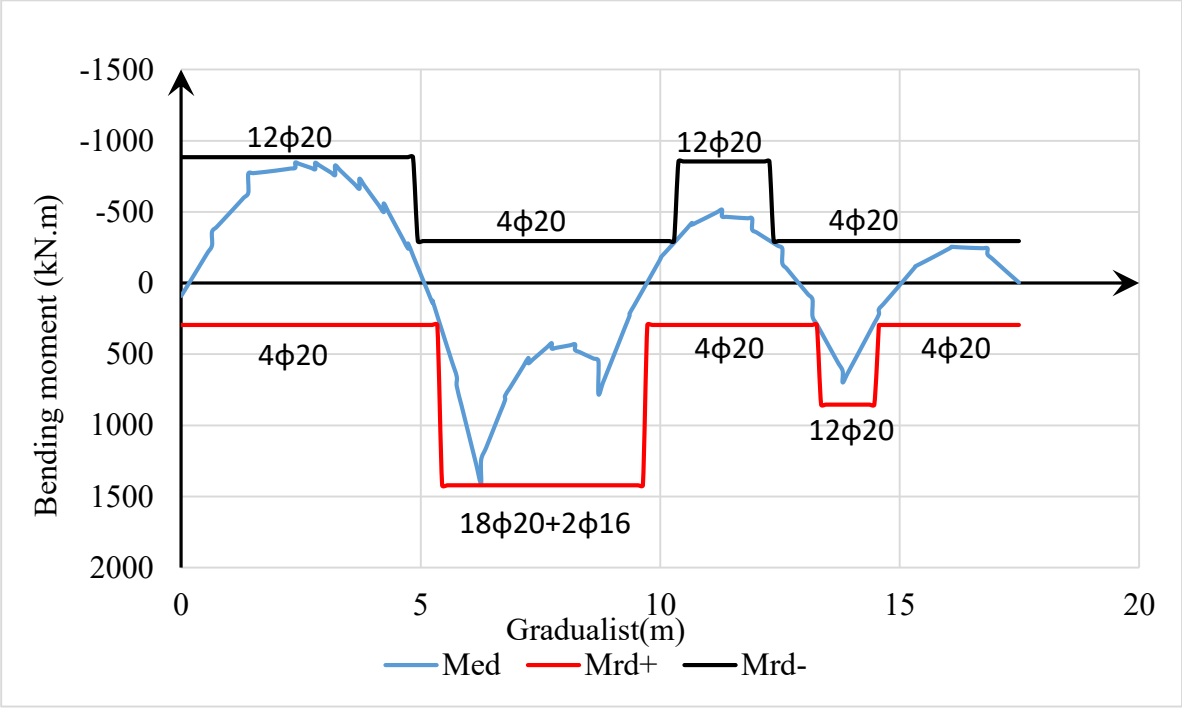

Figure 3.42. Recapitulative curve of the bending moment verification of the strengthening beam

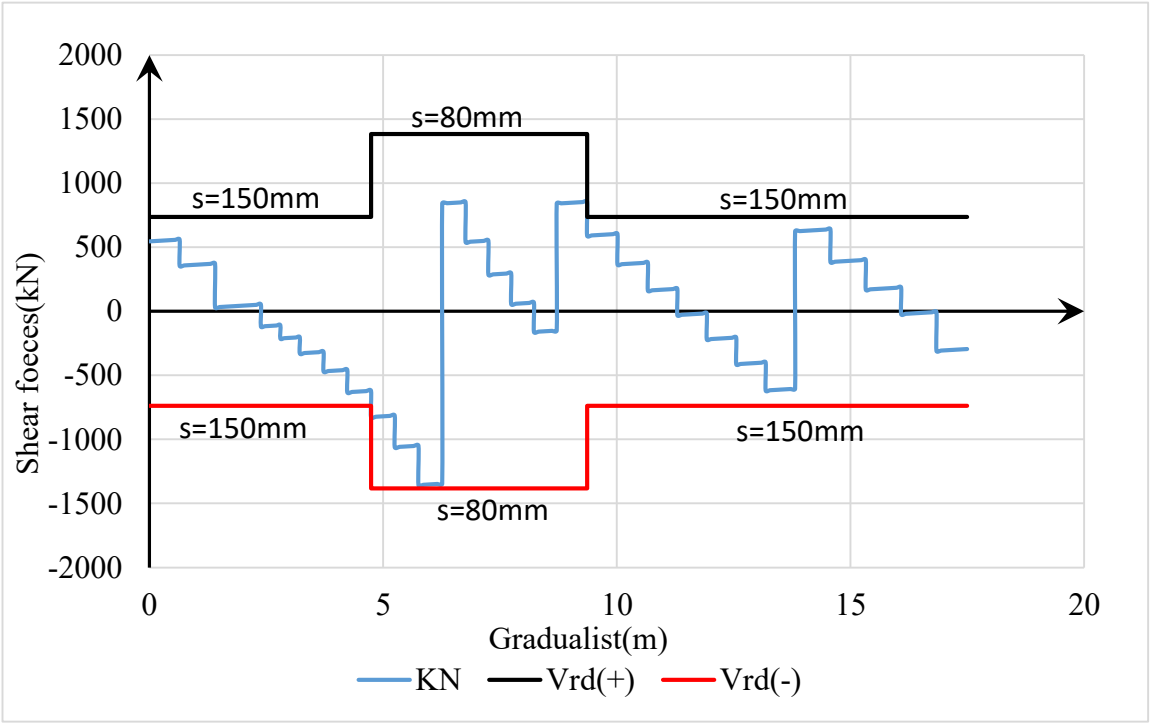

Figure 3.43. Recapitulative curve of the shear verification of the strengthening beam

Detailing of the raft foundation is represented in figure 3.44 and figure 3.45.

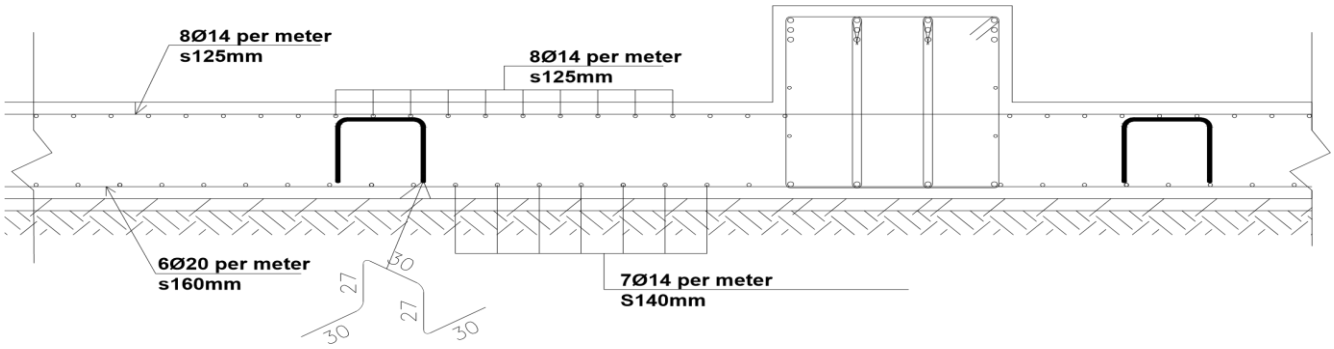

Figure 3.44. Typical Detailing of the raft in the x-direction.

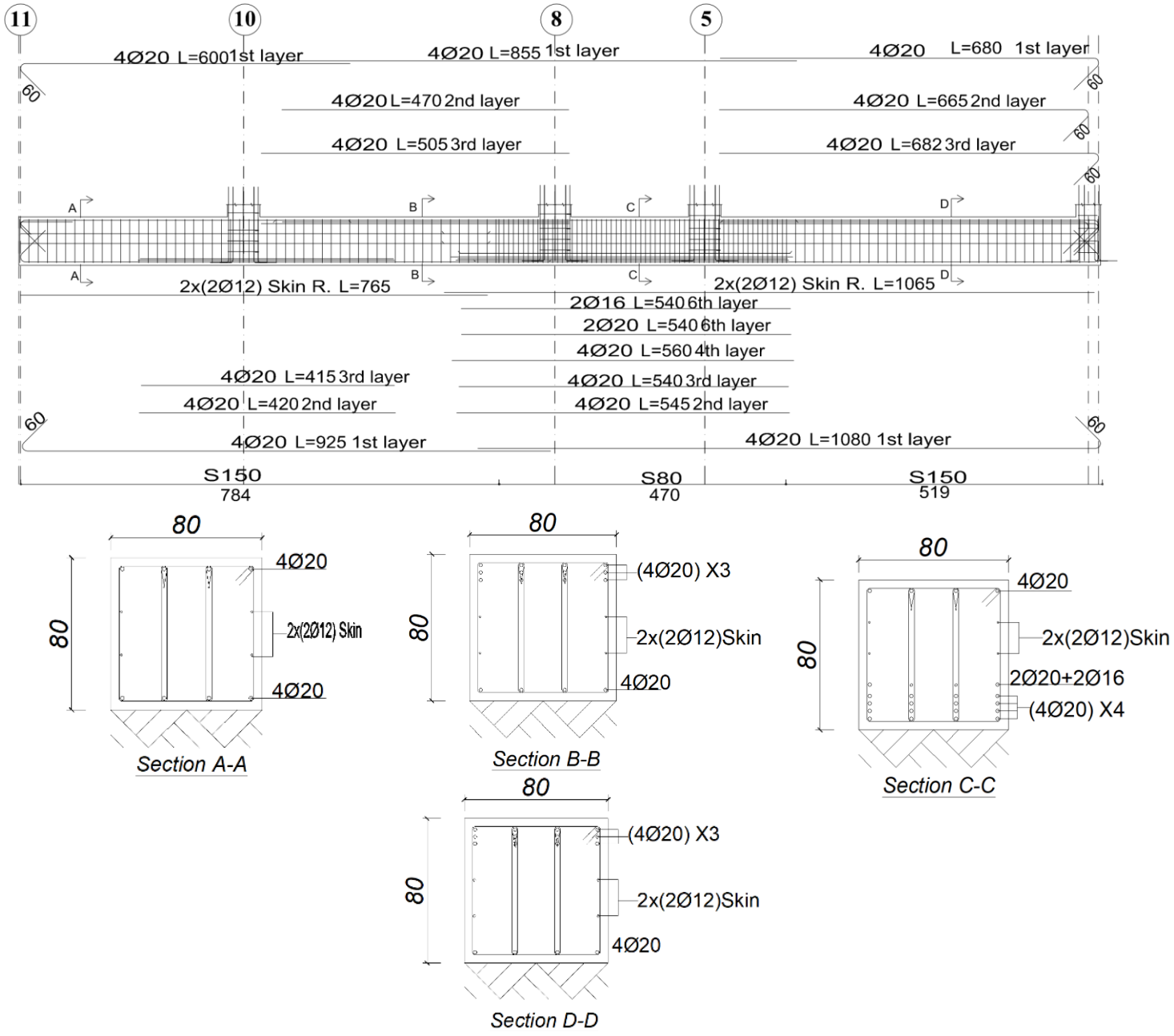

Figure 3.45. Detailing of the chosen strengthening beam.

3.5. Response analysis

The static analysis performed on the structure permit to define the base for the design of the Structural system. This part study the effect of soil-structure interaction on the case study by considering different types of soil. We are analysing response and behaviour of the structure using response spectrum analysis in SAP 2000 v22 software package.

3.5.1. Development of soil springs

The present study involves three major categories of soil, hard soil, medium soil and soft soil as well. The hard soil is represent by shale, the medium soil is a dense sand and finally the soft soil is approach with a soft clay. All the soil considering parameters are presented in table 3.16. Properties are taken from Bowles ‘‘foundation analysis and design’’ as most of the researchers consider this as standard.

Table 3.16. Soils parameters

Soil types	Modulus of elasticity(kN/m²)	Poisson’s ratio	Shear modulus (kN/m²)	Shear wave velocity Vs (m/s)
Shale	5000000	0,1	2272727,3	500
Dense sand	150000	0,3	57692,3	250
Soft clay	20000	0,4	7142,8	120

Using above soil parameter and the dimension of the raft foundation, the soil spring stiffness are calculated for vertical and horizontal directions. The calculated soil springs values are applied to the raft foundation for each respective models by defining soil spring in SAP 2000 software. Table 3.17 presented the obtained soil spring stiffness.

Table 3.17. Springs values.

Soil type	Vertical springs (Z-direction) (kN/m/m²)	Horizontal springs along x-direction (kN/m/m)	Horizontal springs along y directions (kN/m/m)
Shale	367697.61	6557377,05	7463952,50
Dense sand	12011.97	185928,96	212892,28
Soft clay	4858.84	68306	78368

3.5.2. Earthquake loading

For dynamic analysis strong ground motion of Loma Prieta earthquake of USA in 1989 ground motion with a peak ground acceleration of 0.367g is used.

3.5.2.1. Design response spectrum

The building is classified as importance class II and the corresponding importance factor amounts to $\gamma_I = 1.0$. The design ground acceleration a_g is defined as $ag = \gamma I * a_{gR} = 1.0 \times 0.367g = 0.367g$. Table 3.18 presents the different parameters used to response spectrum curve for each type of soil.

Table 3.18. Seismic action characteristics.

Ground type	Damping %	Soil factor	$a_g(g)$	$T_B(s)$	$T_C(s)$	$T_D(s)$	Behaviour factor q
Shale (type A soil)	5	1,00	0,367	0,15	0,40	2,00	1
Dense sand (type C soil)	5	1,15	0,367	0,2	0,60	2,00	1
Soft clay (type D soil)	5	1,35	0,367	0,2	0,80	2,00	1

The elastic spectrum are plotted in the software Excel for each type of soil as presented in the figure 3.46.

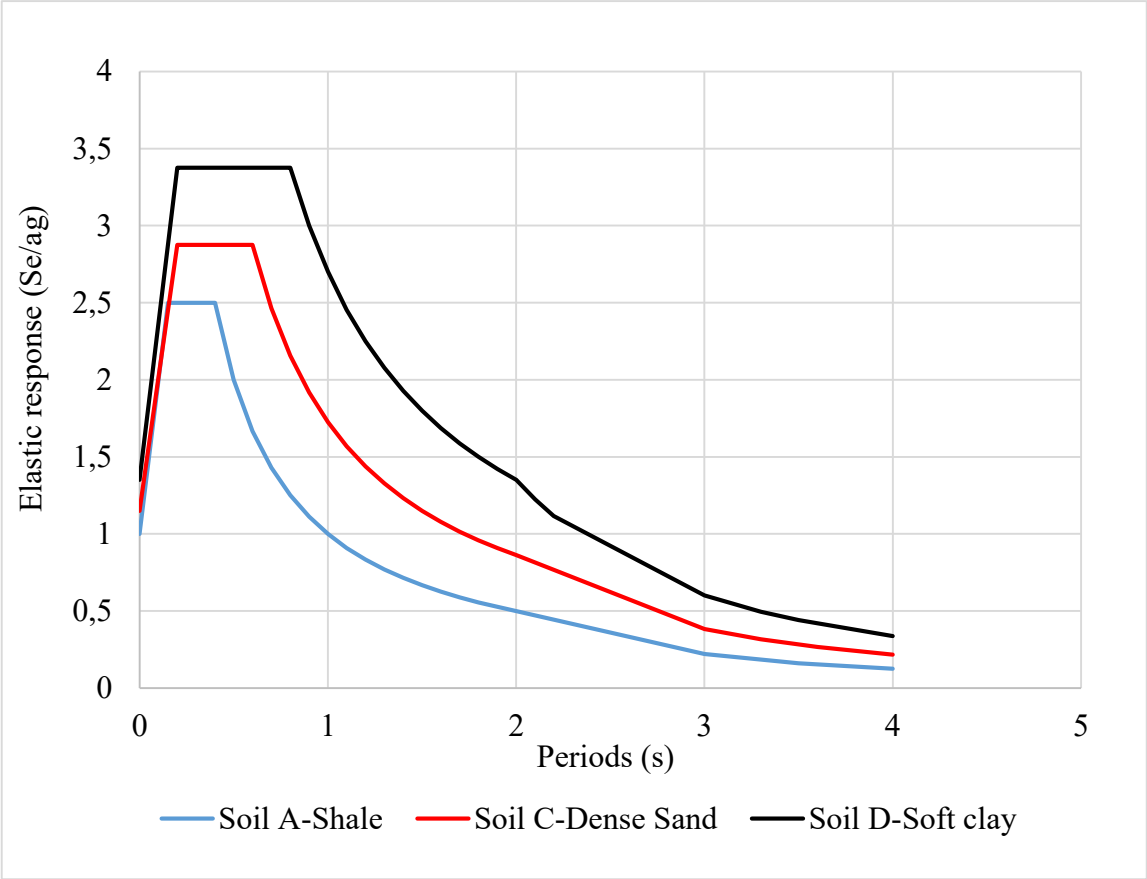

Figure 3.46. Response spectrum design curve for each type of soil.

3.5.2.2. Foundation input motion

When soil-structure interaction is considered, the seismic input motion for buildings with large base areas are reduced due to incoherence of ground motion that occur over the base area, This base slab averaging is a one of the kinematic effect of soil structure interaction which is more presented in section1.3.2.1 . The superstructure will experience foundation input motions (FIM) that will be filtered through the presence of the raft foundation in the horizontal mode. For the structural period T, the transfer function Hu expose in figure 1.5 can be applied to calculate FIM horizontal spectrum Sa,FIM using equation 3.6.

$$Sa,FIM = Sa,design \times Hu \qquad (3.6)$$

To plot the response spectrum curve for the foundation input motion for each type of soil, we developed an Excel as shown in tables 3.19, 3.20 and 3.21.

Table 3.19. Parameters for the response spectrum for FIM in the case of shale.

SHALE-SOIL TYPE A		
Time(s)	Hu(T)	Elastic Spectrum(Se/ag)
0,00	0,870	0,870
0,15	0,870	2,176
0,40	0,981	2,454
0,50	0,988	1,976
0,60	0,992	1,653
0,70	0,994	1,420
0,80	0,995	1,244
0,90	0,996	1,107
1,00	0,997	0,997
1,10	0,998	0,907
1,20	0,998	0,832
1,30	0,998	0,768
1,40	0,998	0,713
1,50	0,999	0,666
1,60	0,999	0,624
1,70	0,999	0,588
1,80	0,999	0,555
2,00	0,999	0,500
3,00	1,000	0,220
3,50	1,000	0,160
4,00	1,000	0,125

Table 3.20. Parameters for the response spectrum for FIM in the case of dense Sand.

DENSE SAND-SOIL TYPE C		
Time(s)	Hu(T)	Elastic Spectrum (Se/ag)
0,00	0,720	0,828
0,20	0,716	2,059
0,60	0,967	2,780
0,70	0,976	2,405
0,80	0,981	2,116
0,90	0,985	1,888
1,00	0,988	1,704
1,10	0,990	1,553
1,20	0,992	1,426
1,30	0,993	1,318
1,40	0,994	1,225
1,50	0,995	1,144
1,60	0,995	1,073
1,70	0,996	1,011
1,80	0,996	0,955
1,90	0,997	0,905
2,00	0,997	0,860
3,00	0,999	0,383
3,30	0,999	0,316
3,60	0,999	0,266
4,00	0,999	0,215

Table 3.21. Parameters for the response spectrum for FIM in the case of soft clay.

SOFT CLAY-SOIL TYPE D		
Time(s)	Hu(T)	Elastic Spectrum(Se/ag)
0,00	0,270	0,365
0,20	0,280	0,944
0,80	0,949	3,202
0,90	0,959	2,878
1,00	0,967	2,611
1,10	0,973	2,388
1,20	0,977	2,198
1,30	0,980	2,036
1,40	0,983	1,896
1,50	0,985	1,774
1,60	0,987	1,666
1,70	0,989	1,570
1,80	0,990	1,485
1,90	0,991	1,408
2,00	0,992	1,339
2,10	0,992	1,215
2,20	0,993	1,108
3,30	0,997	0,494
3,50	0,997	0,440
4,00	0,998	0,337

The modified elastic spectrum are plotted in the software Excel for each type of soil as presented in the figure 3.47.

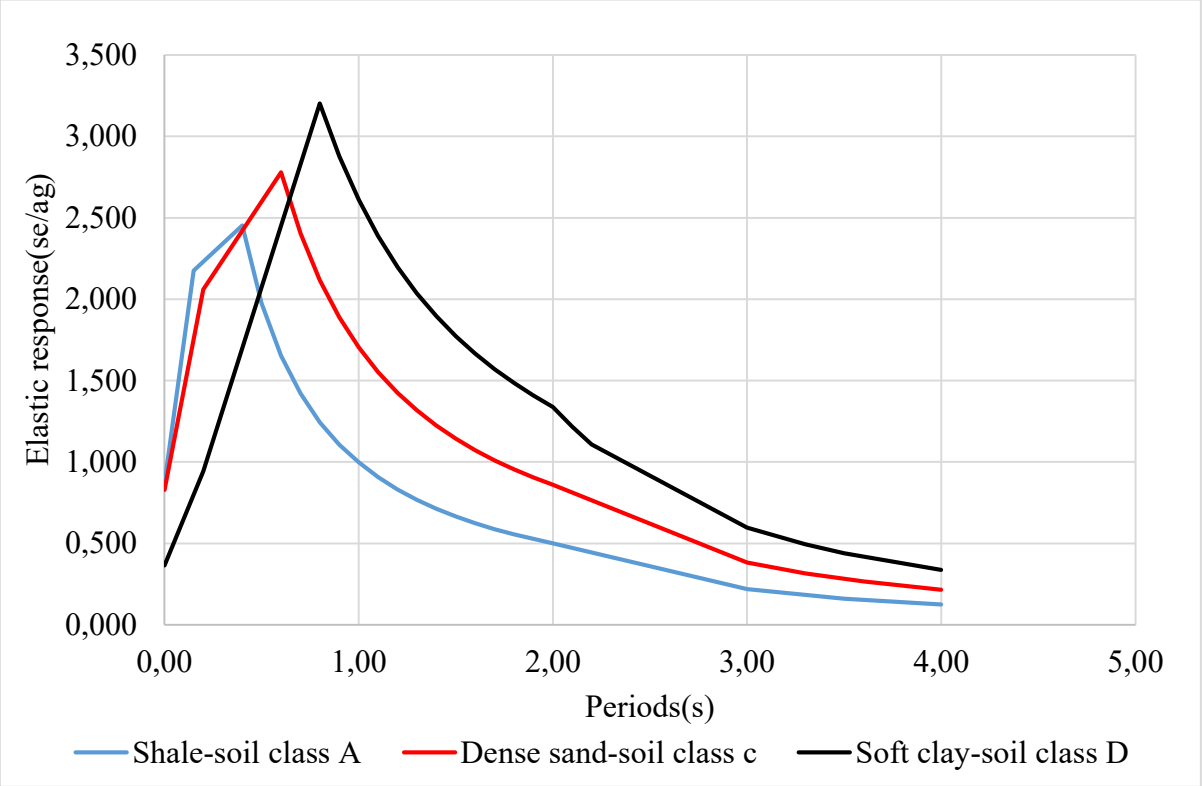

Figure 3.47. Modified response spectrum curves

Seven combinations of actions were considered for seismic response of the building, and are presented in equation 3.5 up to 3.11.

Seismic 1: $\sum_k G_k + 0.3 \sum_k Q_k + E_x + 0.3E_y$ (3.5)

Seismic 2: $\sum_k G_k + 0.3 \sum_k Q_k + E_x - 0.3E_y$ (3.6)

Seismic 3: $\sum_k G_k + 0.3 \sum_k Q_k - E_x - 0.3E_y$ (3.7)

Seismic 4: $\sum_k G_k + 0.3 \sum_k Q_k - E_x + 0.3E_y$ (3.8)

Seismic 5: $\sum_k G_k + 0.3 \sum_k Q_k + 0.3E_x + E_y$ (3.9)

Seismic 6: $\sum_k G_k + 0.3 \sum_k Q_k - 0.3E_x + E_y$ (3.10)

Seismic 7: $\sum_k G_k + 0.3 \sum_k Q_k + 0.3E_x - E_y$ (3.11)

3.5.3. Description of the models

For this study, four models that differ by the type of the support condition have been developed. In the first model the building rests on fixed base, in the three other models the building rests on raft foundation on flexible support with a stiffness correspond to the type of soil. This

parametric study carries out the response of these four models in terms of the period, the lateral deformation of the building, the inter-storey drift, the base shear and the storey shear.

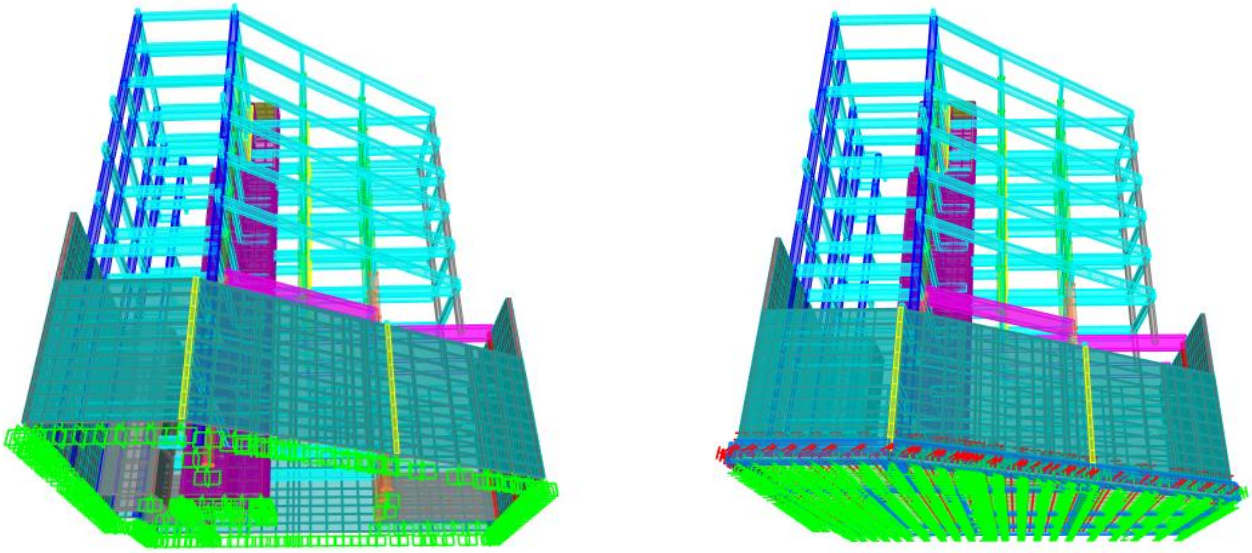

(a) (b)

Figure 3.48. Structure models: (a) model with fixed base, (b) model with raft foundation with flexible base.

3.5.4. Natural time periods

This part consist to study the natural time period at different soil condition. The vibration period is an important parameter of a structure to estimate its seismic demand. Modern building codes generally use the period ratio (flexible base period, $\tilde{T}$, to the fixed-base period, T) of buildings to assess their response to seismic loadings. Table 3.22 provides the vibration periods of the building models with different base conditions.

Table 3.22. Vibration periods for the models with different base conditions.

Modes	Fixed base	shale	Dense sand	Soft clay	Units
Mode 1	0,58	0,79	1,08	1,41	s
Mode 2	0,53	0,74	0,99	1,23	s
Mode 3	0,41	0,55	0,59	0,62	s

To show explicitly the change in term of natural time periods figure 3.49 is plotted.

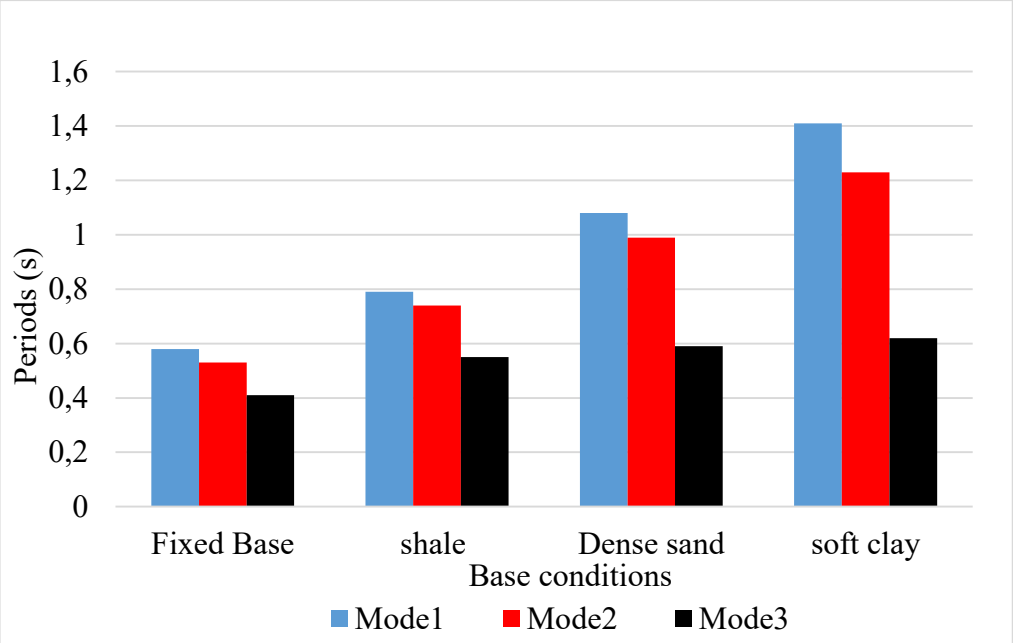

Figure 3.49. Natural time periods at different base conditions

From results of modal analysis, increase in the value of natural time period of all the flexible base models is observed compared to their respective fixed base model.

This is due to the fact that flexible base considers the deformability of the foundation system and the soil, and it leads to an increase of the system period.

3.5.5. Lateral deformation

Storey displacement is very essential parameter for nearby building collision effect in seismic event for making enough separation between nearby element. The deflection profile in x-direction and y-direction for each type of soil are presented in figure 3.50 and figure 3.51 respectively. Each flexible model is associated with a fixed model where the elastic spectrum acceleration correspond to the appropriate type of soil is applied.

Table 3.23. Relative displacement of the structure in x-direction.

Lateral deformation in x-direction (mm)						
Floor height	Shale-Fixed	Dense sand-fixed	Soft clay-fixed	Shale-flexible	Dense sand-flexible	Soft clay-flexible
-6,15	0	0	0	0,05	2,68	14,58
-3,45	0,18	0,23	0,26	0,84	9,4	34,02
0	0,76	1,05	1,24	2,42	18,41	61,69
3,7	3,65	5,19	6,07	7,33	32,95	99,92
6,7	10,06	14,34	16,74	15,86	49,19	137,57
9,7	17,47	24,92	29,01	25,58	66,41	176,6
12,7	24,9	35,48	41,38	35,21	83,48	215,6
15,7	32,35	46,03	53,66	44,77	100,41	254,52
18,7	41,33	58,8	68,54	56,23	119,32	296,16
21,7	48,63	69,05	80,46	65,68	135,81	334,45
23,95	43,81	60,57	69,32	58,44	131,2	340,58

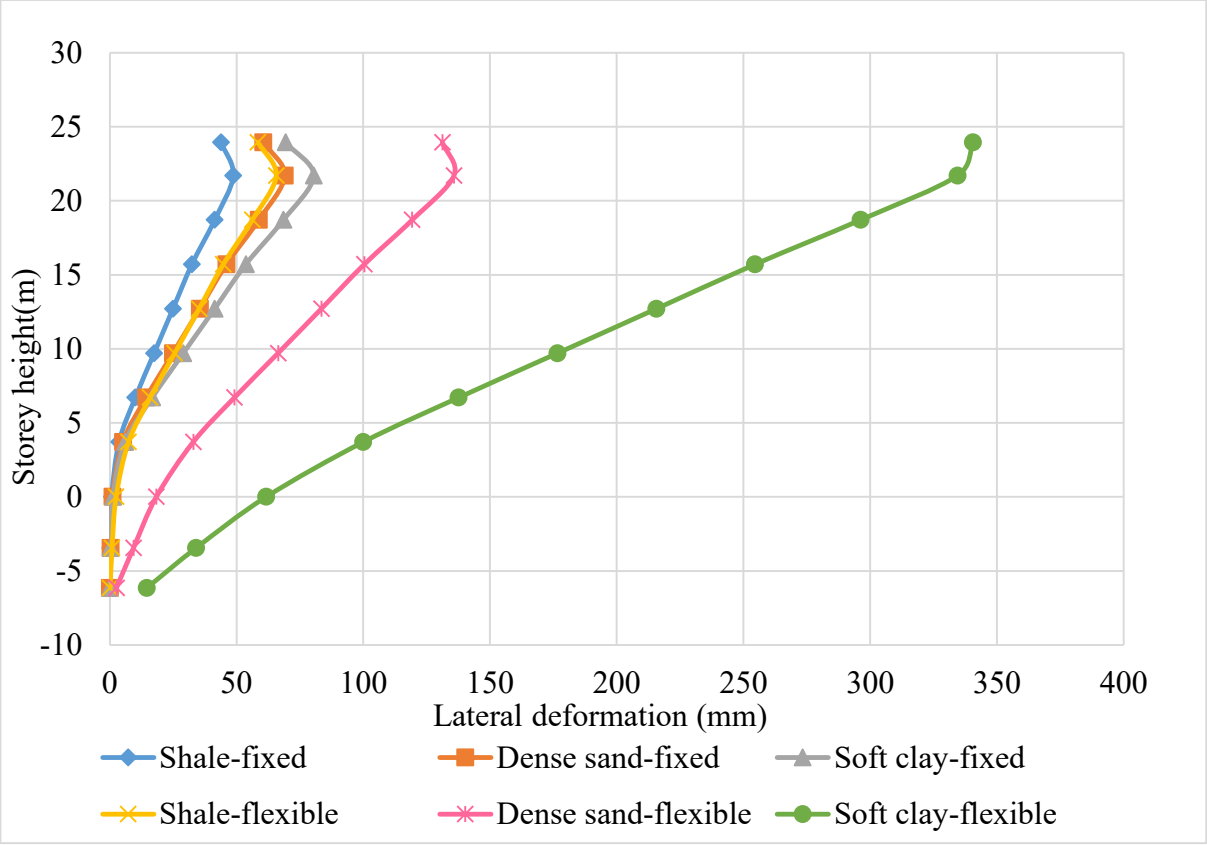

Figure 3.50. Maximum lateral deformation of the structure for the different types of soil in x-direction.

Table 3.24. Relative displacement of the structure in y-direction.

Lateral deformation in y-direction (mm)						
Floor height	Shale-Fixed	Dense sand-fixed	Soft clay-fixed	Shale-flexible	Dense sand-flexible	Soft clay-flexible
-6,15	0	0	0	0,29	2,87	13,21
-3,45	0,21	0,3	0,35	0,99	8,68	31,87
0	0,55	0,79	0,93	2,08	16,66	58,43
3,7	1,02	1,46	1,71	3,4	25,42	87,66
6,7	5,5	7,32	8,56	9,78	38,85	121,72
9,7	9,68	12,75	14,89	15,48	51,19	154,08
12,7	14,16	18,78	21,97	21,64	64,45	187,99
15,7	18,83	25,19	29,49	28	78,21	22,71
18,7	24,23	35,52	38,09	35,27	92,99	258,99
21,7	29,41	39,78	46,62	42,57	107,91	295,41
23,95	35,3	51,44	60,28	51,06	126,19	333,26

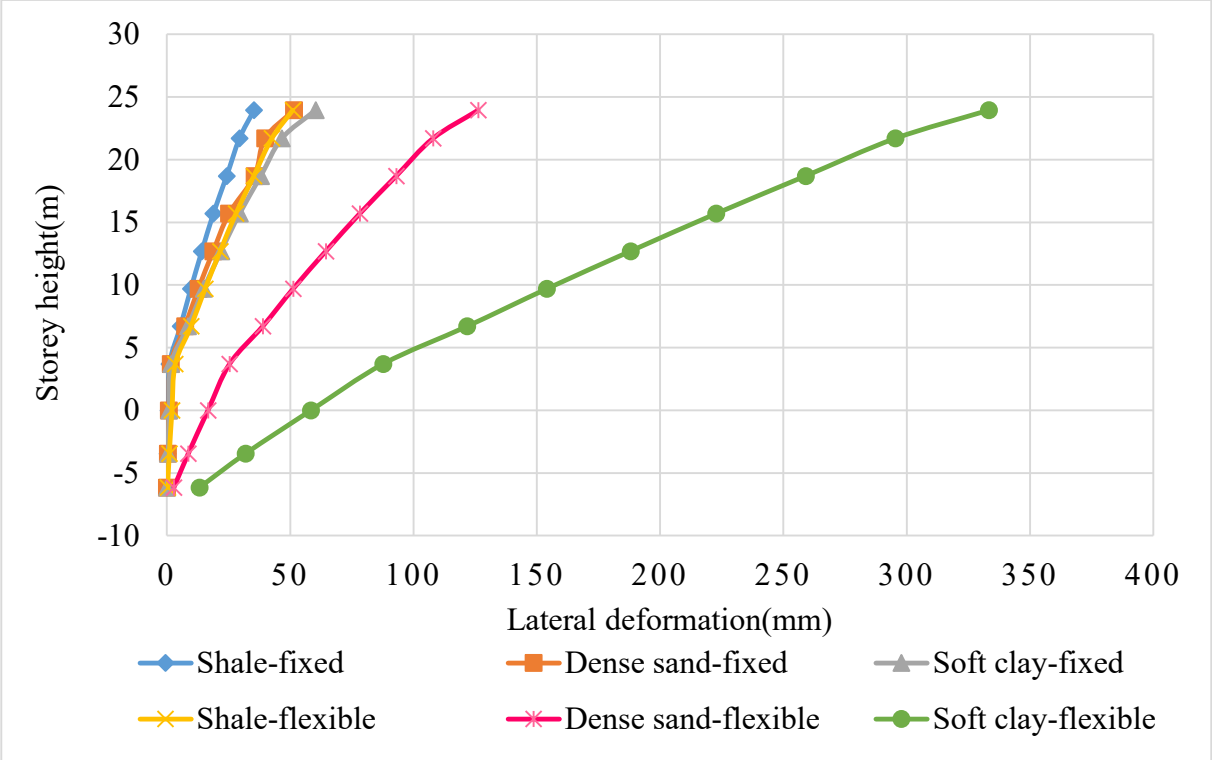

Figure 3.51. Maximum lateral deformation of the structure for the different types of soil in y-direction.

Increase in top storey displacement is observed in all flexible base building models with soil structure interaction when is compared to their respective fixed base models. The increase of flexibility of soil induced more displacement in the building .For example, in the case of dense sand is observed an increasing of 122, 6% of the lateral deformation in y –direction in the

flexible model compared to its respective fixed model when in the other hand for soft clay it is shown an increasing of 276, 42%.

3.5.6. Inter-storey drift

Storey drift is one of the parameter for lateral load effect on vertical members in stability analysis. The inter-storey drifts are defined as the difference between the lateral deflections of two adjacent stories divided by the height of that storey. For this class of building with brittle materials and a reduction factor $\nu = 0.4$, the limit computed following Eurocodes is 1.25%. Table 3.25 and table 3.26 presents the corresponding maximum inter-storey drift for the different types of soil along x and y respectively. Using these tables the inter-storey diagrams are plotted for both directions as shown in figure 3.52 and 3.53.

Table 3.25. Inter-storey drift in x-direction.

Inter-storey drift in x-direction (%)						
Floor height	Shale-Fixed	Dense sand-fixed	Soft clay-fixed	Shale-flexible	Dense sand-flexible	Soft clay-flexible
-6,15	0,0067	0,009	0,010	0,029	0,249	0,720
-3,45	0,0168	0,024	0,028	0,046	0,261	0,802
0	0,0781	0,112	0,131	0,133	0,393	1,033
3,7	0,2137	0,305	0,356	0,284	0,541	1,255
6,7	0,2470	0,353	0,409	0,324	0,574	1,301
9,7	0,2477	0,352	0,412	0,321	0,569	1,300
12,7	0,2483	0,352	0,409	0,319	0,564	1,297
15,7	0,2993	0,426	0,496	0,382	0,630	1,388
18,7	0,2433	0,342	0,397	0,315	0,550	1,276
21,7	-0,2142	-0,377	-0,495	-0,322	-0,205	0,272

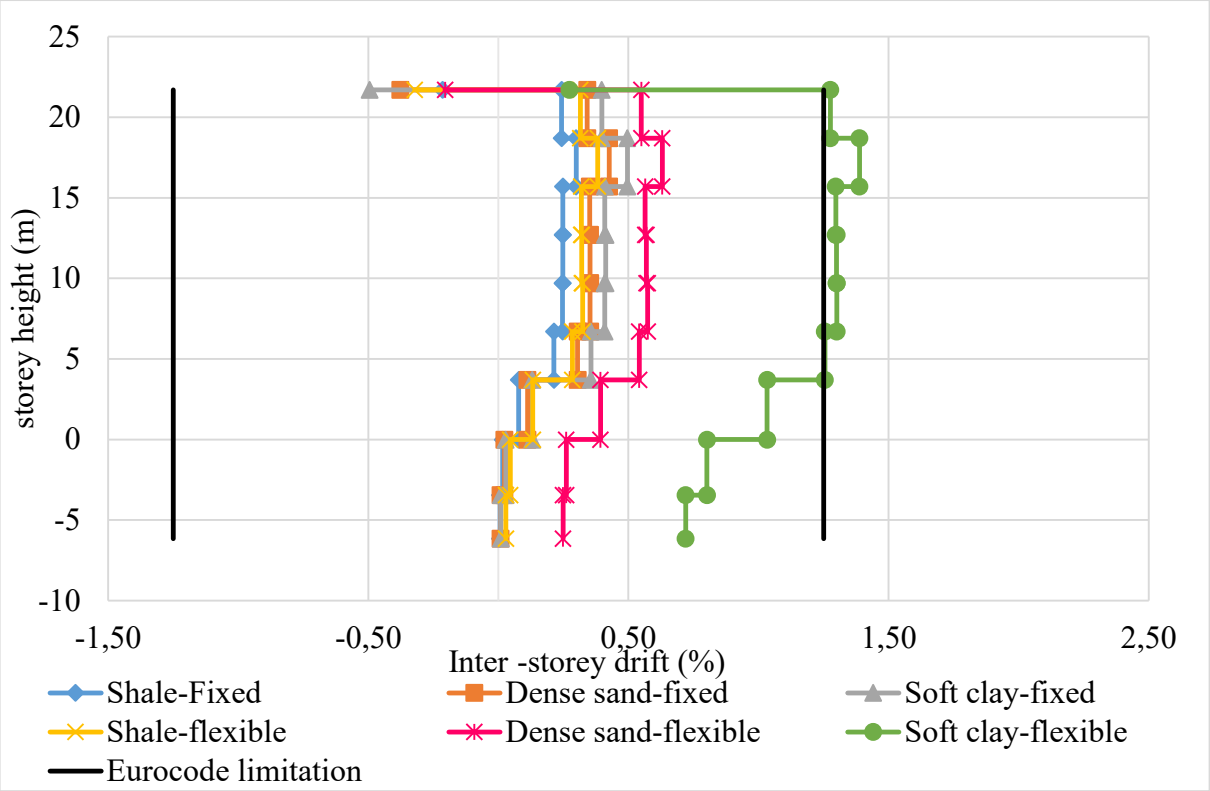

Figure 3.52. Inter-storey drift in x-direction.

Table 3.26. Inter-storey drift in y-direction.

Inter-storey drift in y-direction (%)						
Floor height	Shale-Fixed	Dense sand-fixed	Soft clay-fixed	Shale-flexible	Dense sand-flexible	Soft clay-flexible
-6,15	0,0078	0,011	0,013	0,026	0,215	0,691
-3,45	0,0078	0,011	0,013	0,026	0,215	0,691
-3,45	0,0099	0,014	0,017	0,032	0,231	0,770
0	0,0099	0,014	0,017	0,032	0,231	0,770
3,7	0,0127	0,018	0,021	0,036	0,237	0,790
6,7	0,1493	0,195	0,228	0,213	0,448	1,135
9,7	0,1393	0,181	0,211	0,190	0,411	1,079
12,7	0,1493	0,201	0,236	0,205	0,442	1,130
15,7	0,1557	0,214	0,251	0,212	0,459	-5,509
18,7	0,1800	0,344	0,287	0,242	0,493	7,876
21,7	0,1727	0,142	0,284	0,243	0,497	1,214

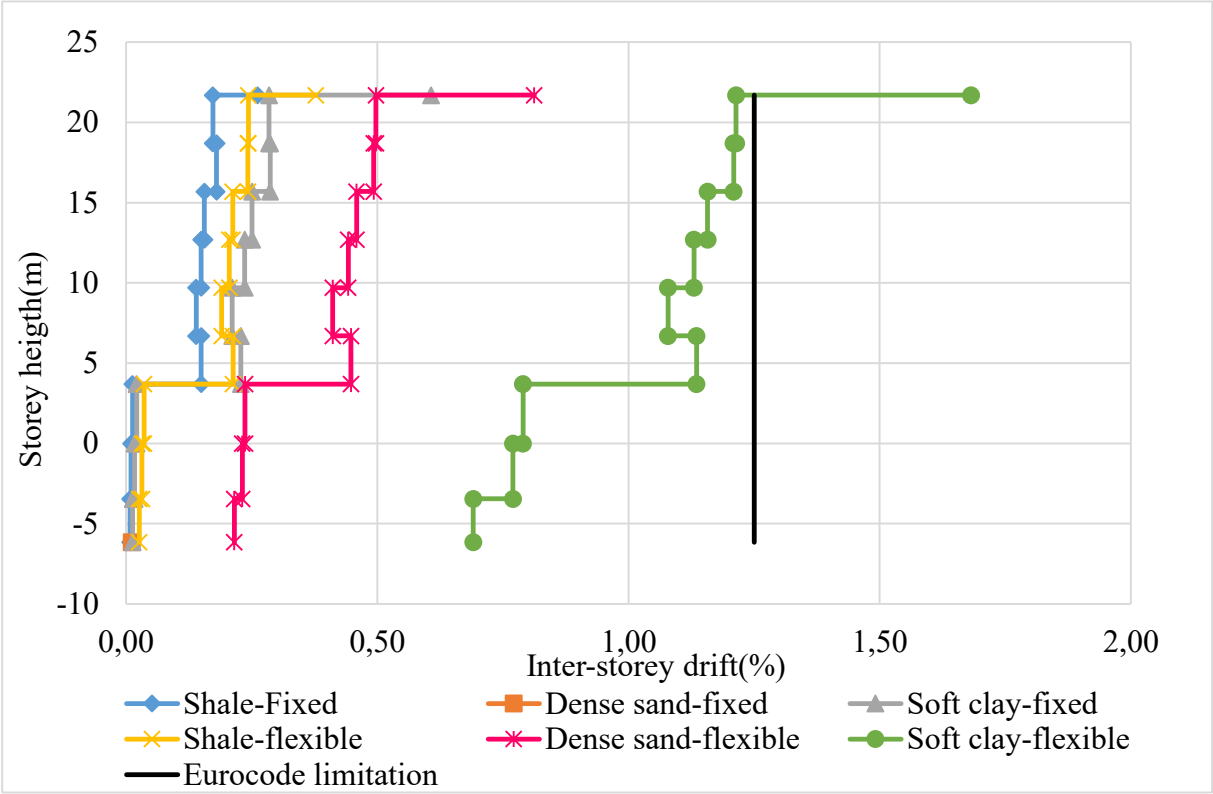

Figure 3.53. Inter-storey drift in y-direction.

Models with fixed base show a reduction of inter-storey drift in comparison to their respective soil-structure interaction models. This prove that SSI tends to increase inter-storey drifts of the superstructure. In the case of soft soil we have an increase of 213.73% of the inter-storey drift in both directions for the flexible model compared to the fixed models. The limitation provided by the Eurocode is also overwhelmed by the soft clay flexible model which provided the greatest value of inter-storey drift. This demonstrate that an increase of the soil flexibility tends to increase inter-storey drift.

We will able to conclude that a non-consideration of SSI underestimate the effect of lateral load on vertical members in stability analysis especially in the case of medium and soft soil.

3.5.7. Storey shear

Storey forces for x-direction and y-direction are reported in table 3.27 and 3.28 respectively. Using these forces the resulting storey shear force is plotted. Figure 3.54 and 3.55 represent the storey shear flexible base compared with fixed base for both direction.

Table 3.27. Storey force in the x-direction.

Storey force in the X-direction							
Storey	Shale-fixed	Fixed-sand	Fixed-soft	Shale-flexible	Dense sand - flexible	Soft clay-flexible	Units
Roof	26,66	33,58	40,59	46,67	50,74	82,83	kN
Level 6	2419,97	2531,56	3033,87	2757,99	3172,52	5149,19	kN
Level 5	1674,84	2235,56	2756,57	2095,19	2614,48	4239,1	kN
Level 4	1393,92	1874,38	2250,78	1762,5	2098,52	3342,17	kN
Level 3	1276,31	1606,29	1935,1	1880,78	2031,6	3150,39	kN
Level 2	1107,73	1273,25	1567,62	1896,34	2031,59	3192,68	kN
Level 1	832,53	851,54	1112,45	1670,47	1953,6	3312,83	kN
Ground level	461,51	384,92	589,7	1257,37	1969,47	3860	kN
Basement 1	669,11	194,45	259,72	808,51	2027,65	5067,75	kN
Basement 2	38,96	36,6	47,67	238,45	1044,85	8370,83	kN
Foundation	0	0	0	122,84	2468,96	18251,37	kN

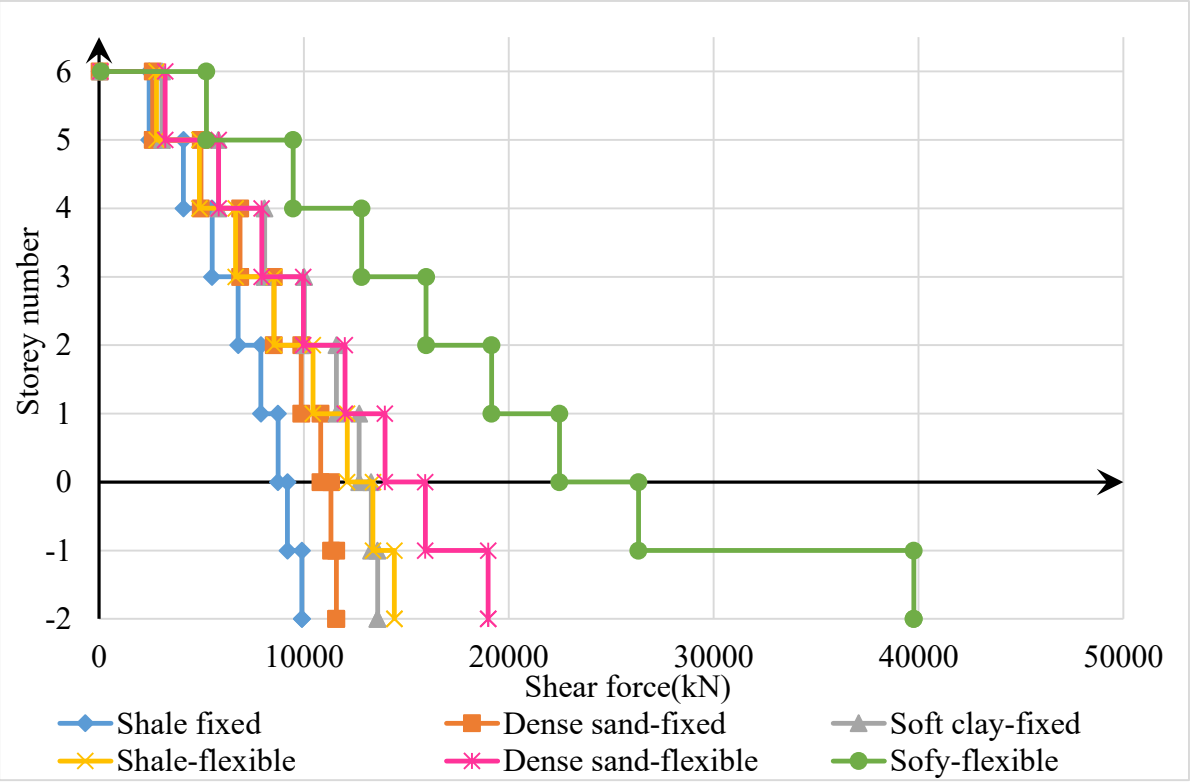

Figure 3.54. Storey shear in x-direction.

Table 3.28. Storey force in the y-direction.

Storey force in the Y-direction							
Storey	Shale-fixed	Fixed-sand	Fixed-soft	Shale-flexible	Dense sand - flexible	Soft clay-flexible	Units
Roof	26,66	33,58	39,43	49,11	55,39	92,93	kN
Level 6	2332,51	2531,56	2971,83	2766,64	3362,74	5478,15	kN
Level 5	1536,51	2235,56	2624,5	1962,06	2634,25	4274,97	kN
Level 4	1347,99	1874,38	2200,35	1826,05	2139,32	3415,62	kN
Level 3	1229,67	1606,29	1885,65	1893,64	2094,72	3267,91	kN
Level 2	1035,29	1273,25	1494,69	1792,52	2056,29	3215,13	kN
Level 1	733,63	851,54	999,63	1467,23	1887,08	3197,18	kN
Ground level	350,65	384,92	451,93	996,68	1783,42	3862,71	kN
Basement 1	533,45	194,45	228,27	738,56	1783,71	4404,84	kN
Basement 2	32,54	36,6	42,96	220,37	779,08	7051,14	kN
Foundation	0	0	0	78,6	1237,97	14725,89	kN

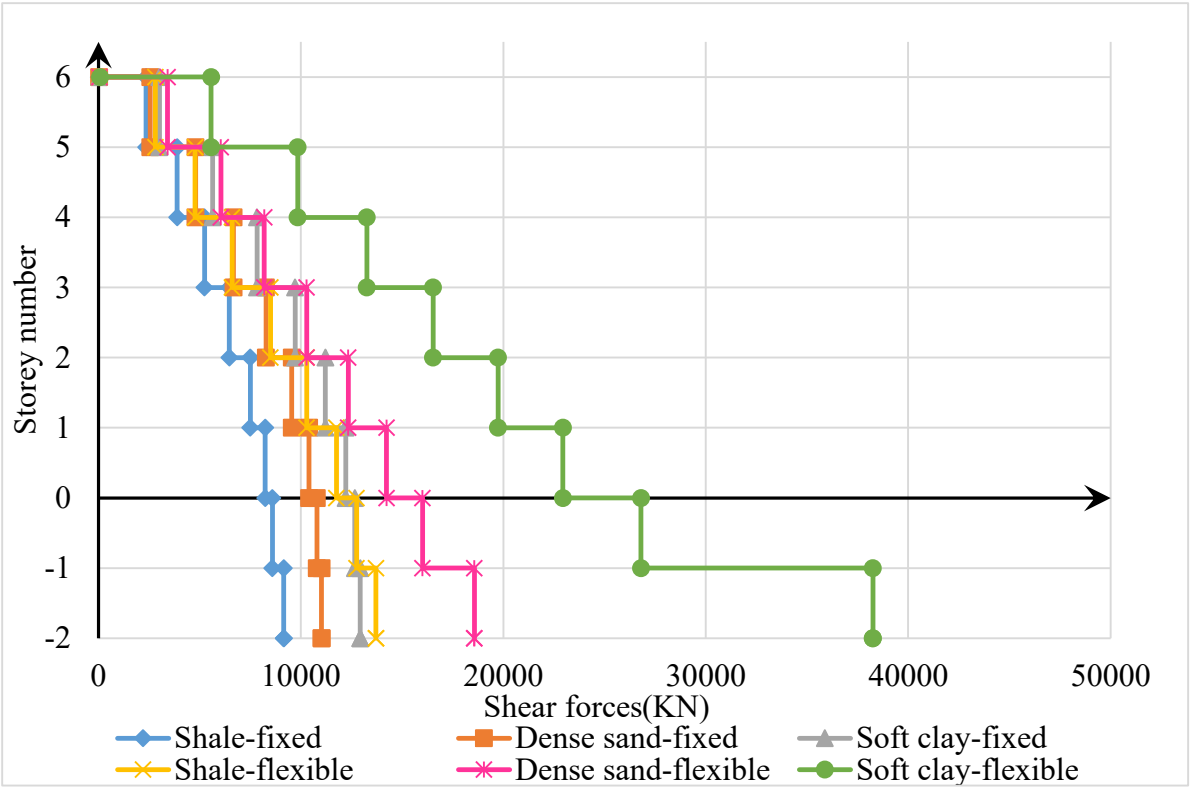

Figure 3.55. Storey shear in y-direction

From results of this analysis, increase in the storey shear of all the flexible base models is observed compared to their respective fixed base model.

3.5.8. Base shear

The base shear which represent the total lateral seismic force, is given for different base condition for the both axis in table 3.29.To carry out the difference between the base shear of each model, the figures 3.56 and 3.57 are plotted.

Table 3.29. Base shear in x and y direction

Shale-fixed	Shale-flexible	Dense sand - fixed	Dense sand - flexible	Soft clay-fixed	Soft clay-flexible	units
9901,54	11580,12	11022,13	18995,02	13594,07	39767,77	kN
9158,9	13712,86	11022,13	18576	12939,24	38260,58	kN

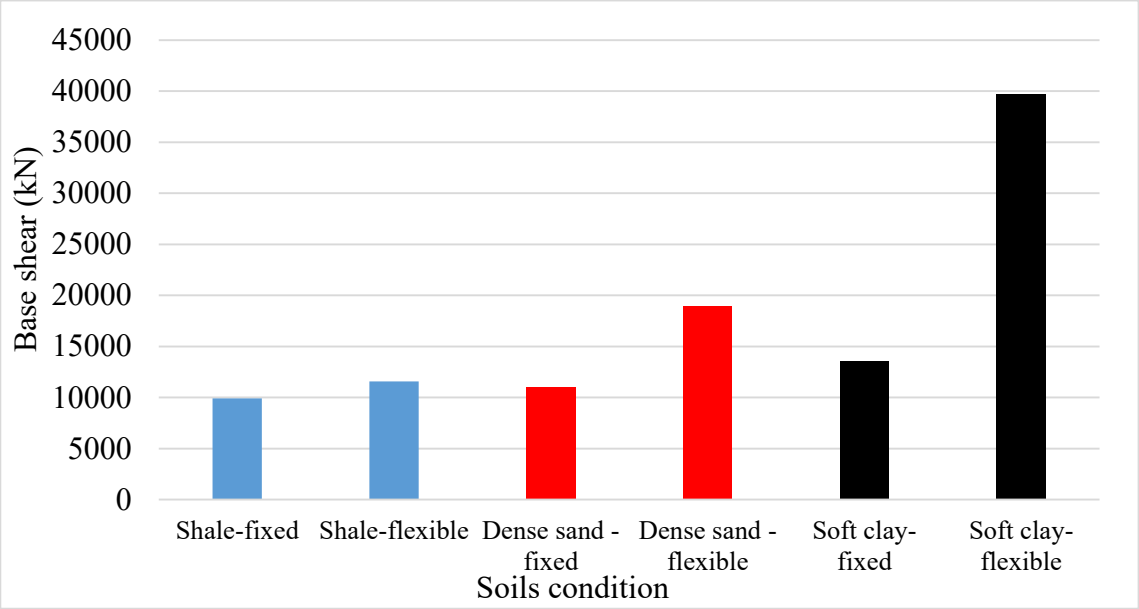

Figure 3.56. Base shear in x-direction

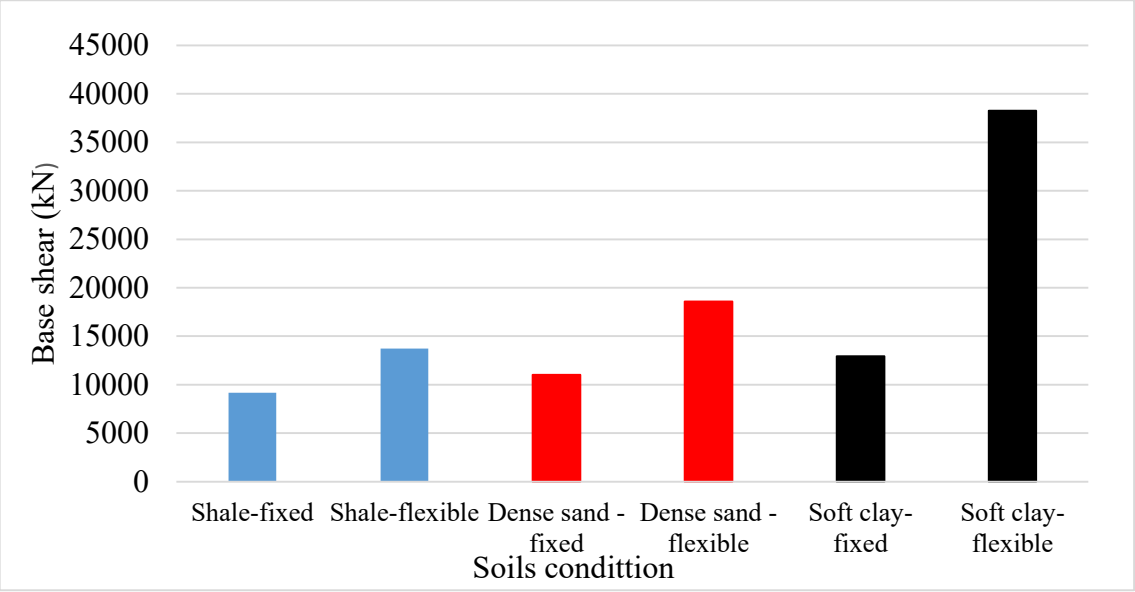

Figure 3.57. Base shear in y-direction.

According to the performed comparison study, it is been observed that the ratio of differences between SSI numerical cases and fixed base cases for base shear were about 16%, 72%,192,54 %for the structures that embedded by shale ,dense sand and soft clays respectively. Thus according to the results of the current study, it can be concluded that fixed base concept underestimates the response of structures rested on these type of soil profiles under dynamic loading .When the dynamic responses of the fixed base models compared to the SSI cases, maximum responses values occurred in soft soil profile and these values decrease towards rock soil condition. It is because of the fact that soft soils has less stiffness when compared to the medium and rock soil, on the other hand soft soil are highly compressible because of the large percentage of voids ratios in it .Since total base shear are increased especially in the soft soil, this leads to overstress and subsequently failure in the structural elements. For avoiding situations like that, a selection of appropriate structural systems to accommodate anticipated forces is required.

Conclusion

The aim of this chapter was to present the case study, to perform the analysis and the design of the structural elements and to compare its seismic behaviour considering different types of soil conditions. At the end a section of 60 cm height and 20 cm width is obtained for beams and a circular section of 60 cm diameter for the most solicited column at the basement level. The design retaining wall which carries the lateral earth forces has a thickness of 25 cm. concerning the substructure, foundation was designed which is a raft foundation with strengthening beams. The analysis of building is done with fixed base and raft foundation where different soil springs are implemented to represent the corresponding elastic soil behaviour. At the end, we found that the fixed base approach underestimates the building periods, the lateral deformation, the inter-storey drift, storey shear and base shear compared to the SSI approach. It is also noticed that the increase in soil flexibility increases the response of the building and this is why the soil-structure interaction model of the soft clay soil gives the largest values for the building periods, the lateral deformation, inter-storey drift, the storey shear and the base shear.

GENERAL CONCLUSION

The purpose of this work was to carry out the effects of the soil-structure interaction on the seismic response of an irregular concrete building for different types of soil conditions.

This study has been done firstly through a literature review on soil-structure interaction. Secondly, the methodology of the analysis and design of structural elements and foundation elements was presented. Then following this methodology, an irregular six storey building with two basements were designed. Three types of soils were study for that building in order to make a comparative study. The analysis was performed through the software SAP 2000 (version 22).

The results obtained from the analysis revealed that :**(1)** The consideration of soil flexibility increases the vibration periods of the building compare to the fixed base assumption. Moreover, soft clay soil gives higher values compared to the rest of soil types. **(2)** SSI amplifies lateral deflection of the building and this amplification is inversely proportional to the soil stiffness in the sense that soft clay soil gives the largest value.**(3)** The inter-storey drift follows the same pattern as the lateral deformation with the largest value given by the soft clay soil. **(4)** Increase in soil flexibility increases the response of the structure. Storey shear and base shear are found to be increasing as soil flexibility increases. **(5)** It is necessary to consider soil-structure interaction effect when structure rest on soft soils.

This research has short comings related to the non-consideration of the springs damping coefficient and the assumption of linear behaviour of soil and the superstructure.

To assure continuity in the research it is suggested to adopt a direct method of analysis, where the soil is modelled as solid finite element. This approach allows to capture effects such as non-linearity in the behaviour of soil and superstructure, material and radiation damping, and permit to have results closer to the reality.

BIBLIOGRAPHY

BOOKS AND ARTICLES

Bowles, J. E. (1996). Foundation analysis and design. *The McGraw-Hill Companies, Inc. 16-127.*

NIST. (2012). Soil-Structure Interaction for building structures. *USA: NEHRP Consultants Joint-Venture, 10-12.*

Lysmer.J, & Kuhlemeyer, R. L. (1969*).* Finite dynamic model for infinite media. *Journal of Engineering Mechanics Division*, 859-877.

Kutanis, M., & Elmas, M. (2001*).* Non-linear seismic soil-structure interaction analysis based on the substructure method in the time domain. *Turkish Journal of Engineering and Environmental Science*, 617-626.

Carbonari, S., Dezi, F., & Leoni, G. (2011). Linear soil-structure interaction of coupled wall-frame structures on pile foundations. *Soil Dynamics and Earthquake Engineering, 31*, 1296-1309.

Allotey, N., & El Naggar, M. H. (2008). Generalized dynamic Winkler model for nonlinear soil-structure interaction analysis. *Canadian Geotechnics Journal, 45*(4), 560-573.

Liu, Y., Wang, X., & Zhang, M. (2015). Lateral vibration of pile groups partially embedded in layered saturated soils. *International Journal of Geomechanics*,246-257.

Wolf, J. P. (1985). Dynamic Soil-Structure Interaction. *(U. S. River, Ed.) New Jersey: PrenticeHall*, 144-159.

Wolf, J. (1998). Soil-structure interaction analysis in time domain. *(U. S. River, Ed.) New Jersey: Prentice Hall, 105-125.*

Bielak, J. (1976). Modal analysis for building-soil interaction. *Journal of Engineering Mechanics, 102*, 771-786.

Veletsos, A., & Nair, V. (n.d.). Seismic interaction of structures on hysteric foundations. *Journal of Structural Engineering, 101*, 109-129.

Veletsos, A., & Prasad, A. M. (1989). Seismic interaction of structures and soils:Stochastic approach. *Journal of Structural Engineering, 115*(4), 935-956.

Veletsos, A., Prasad, A., & Wu, W. (1997). Transfer functions for rigid rectangular foundations. *Earthquake Engineering and Structural Dynamics, 26*(1), 5-17.

Mylonakis, G., Nikolaou, S., & Gazetas, G. (2006). Footings under seismic loading: Analysis and design issues with emphasis on bridge foundations. *Soil Dynamics and Earthquake Engineering, 26*, 824-853.

Kramer, S. L. (1996). Geotechnical Earthquake Engineering. *New Jersey, USA: Prentice Hall.*

Kramer, S. L., & Stewart, J. P. (2004). Geotechnical aspects of seismic hazards. (Y. Bozorgnia, & V. V. Bertero, Eds.) *Earthquake Engineering from Engineering Seismology to Performance-Based Engineering* (941), 47-65.

Kim, S., & Stewart, J. (2003). Kinematic soil-structure interaction from strong motion recordings. *Journal Geotechnical and Geoenvironmental Engineering, 129*, 323-335.

Hokmabadi, A. S., & Fatahi, B. (2015). Influence of foundation type on seismic performance of buildings considering soil-structure interaction. *International Journal of Structural Stability and Dynamics, 16*, 29. doi: 10.1142/S0219455415500431,3-4.

Hokmabadi, A. S., Fatahi, B., & Samali, B. (2014). Assessment of soil pile-structure interaction influencing seismic response of mid-rise buildings sitting on floating pile foundations. *Compt Geotech, 55*(1), 172-186.

Fatahi, B., Hokmabadi, A., & Samali, B. (2014). Seismic Performance Based Design for Tall

Buildings Considering Soil-PileStructure Interaction. *Advances in Soil Dynamics and Foundation Engineering*, 1-10. Retrieved from ascelibrary.org,53-58.

Abdelraheem, S. E., Ahmed, M. M., & Alazrak, T. M. (2014, November 29). Evaluation of soil– foundation–structure interaction effects on seismic response demands of multi-story MRF buildings on raft foundations. *International Journal of Advanced Structural Engineering, 5*, 1-18. doi:10.1007/s40091-014-0078-x, 32-37.

Bagheri, M., Jamkhaneh, M. E., & Samali, B. (2018). Effect of Seismic Soil–Pile–Structure Interaction on Mid-and High-Rise Steel Buildings Resting on a Group of Pile Foundations. *International Journal of Geomechanics*. doi:10.1061/(ASCE)GM.1943-5622.0001222,*15-72.*

Bungale Taranath (1988).Structural analysis and design of tall buildings, *The McGraw-Hill Companies, Inc.,127-186.*

NORMS

Comité Européen de Normalisation. (2002). *Eurocode 0: Basis of structural design. Norm EN 1990.* Brussels: Comité Européen de Normalisation.

Comité Européen de Normalisation. (2002). *Eurocode 1: Actions on structures. Norm EN 1991.* Brussels: Comité Européen de Normalisation.

Comité Européen de Normalisation. (2002). *Eurocode 2: Design of concrete structures. Norm EN 1992.* Brussels: Comité Européen de Normalisation.

Comité Européen de Normalisation. (2002). *Eurocode 7: Geotechnical design. Norm EN 1997.* Brussels: Comité Européen de Normalisation.

Comité Européen de Normalisation. (2002). *Eurocode 8: Design of structures for earthquake resistance.* Brussels: Comité Européen de Normalisation.

FEMA. (2009). NEHRP Recommended Seismic Provisions for New Buildings and Other Structures. *The Building Seismic Safety Council of the National Institute of Building Sciences for the Federal Emergency Management Agency. Washington, DC: FEMA P750/2009 Edition.*

PROCEEDINGS

Ancheta, T., Stewart, J., & Abrahamson, N. (2011). Engineering characterization of earthquake ground motion coherency and amplitude variability. *4th International Symposium on Effects of Surface Geology on Seismic Motion.* University of California Santa: IASPEI / IAEE.

THESIS

Arefi, J. (2008). Effects of Soil-Structure Interaction on the Seismic Response of Existing R.C. Frame Buildings. *Master's thesis*. *Università degli Studi di Pavia.*

Moustapha Housseni. (2019). Influence of foundation type on the seismic response of buildings considering soil-structure interaction*. (Master Thesis). National Advanced School of Public Works.*

Djeukoua Nathou, G. L. (2018). Comparative analysis of seismic protection system.*(Master Thesis). National Advanced School of Public Works.*

Goyez, L. G. (2017). Soil-Structure Interaction Effects on the Seismic Response of Low-Rise Eccentrically Braced Frames (Vol. 2398). *Master's thesis*. University of Arkansas.

ANNEXES

ANNEX A: Tables for the methodology

Table A1. Categories of use of the building (EC 1 Part 1)

Category	Specific Use	Example
A	Areas for domestic and residential activities	Rooms in residential buildings and houses; bedrooms and wards in hospitals; bedrooms in hotels and hostels kitchens and toilets.
B	Office areas	
C	Areas where people may congregate (with the exception of areas defined under category A, B, and D[1])	**C1**: Areas with tables, etc. e.g. areas in schools, cafés, restaurants, dining halls, reading rooms, receptions. **C2**: Areas with fixed seats, e.g. areas in churches, theatres or cinemas, conference rooms, lecture halls, assembly halls, waiting rooms, railway waiting rooms. **C3**: Areas without obstacles for moving people, e.g. areas in museums, exhibition rooms, etc. and access areas in public and administration buildings, hotels, hospitals, railway station forecourts. **C4**: Areas with possible physical activities, e.g. dance halls, gymnastic rooms, stages. **C5**: Areas susceptible to large crowds, e.g. in buildings for public events like concert halls, sports halls including stands, terraces and access areas and railway platforms.
D	Shopping areas	**D1**: Areas in general retail shops **D2**: Areas in department stores

[1] Attention is drawn to 6.3.1.1(2), in particular for C4 and C5. See EN 1990 when dynamic effects need to be considered. For Category E, see Table 6.3

NOTE 1 Depending on their anticipated uses, areas likely to be categorised as C2, C3, C4 may be categorised as C5 by decision of the client and/or National annex.

NOTE 2 The National annex may provide sub categories to A, B, C1 to C5, D1 and D2

NOTE 3 See 6.3.2 for storage or industrial activity

Table A2. Imposed loads on floors, balconies and stairs in buildings (EC 1 Part 1)

Categories of loaded areas	q_k [kN/m^2]	Q_k [kN]
Category A		
- Floors	1,5 to2,0	2,0 to 3,0
- Stairs	2,0 to4,0	2,0 to 4,0
- Balconies	2,5 to 4,0	2,0 to 3,0
Category B	2,0 to 3,0	1,5 to 4,5
Category C		
- C1	2,0 to 3,0	3,0 to 4,0
- C2	3,0 to 4,0	2,5 to 7,0 (4,0)
- C3	3,0 to 5,0	4,0 to 7,0
- C4	4,5 to 5,0	3,5 to 7,0
- C5	5,0 to 7,5	3,5 to 4,5
category D		
- D1	4,0 to 5,0	3,5 to 7,0 (4,0)
- D2	4,0 to 5,0	3,5 to 7,0

Table A3. Recommended values of Ψ factors for buildings (EC 0 Part 1)

Action	ψ_0	ψ_1	ψ_2
Imposed loads in buildings, category (see EN 1991-1-1)			
Category A : domestic, residential areas	0,7	0,5	0,3
Category B : office areas	0,7	0,5	0,3
Category C : congregation areas	0,7	0,7	0,6
Category D : shopping areas	0,7	0,7	0,6
Category E : storage areas	1,0	0,9	0,8
Category F : traffic area, vehicle weight ≤ 30kN	0,7	0,7	0,6
Category G : traffic area, 30kN < vehicle weight ≤ 160kN	0,7	0,5	0,3
Category H : roofs	0	0	0
Snow loads on buildings (see EN 1991-1-3)*			
Finland, Iceland, Norway, Sweden	0,70	0,50	0,20
Remainder of CEN Member States, for sites located at altitude H > 1000 m a.s.l.	0,70	0,50	0,20
Remainder of CEN Member States, for sites located at altitude H ≤ 1000 m a.s.l.	0,50	0,20	0
Wind loads on buildings (see EN 1991-1-4)	0,6	0,2	0
Temperature (non-fire) in buildings (see EN 1991-1-5)	0,6	0,5	0
NOTE The ψ values may be set by the National annex. * For countries not mentioned below, see relevant local conditions.			

Table A4. Values of Minimum cover, C_{min},, requirements with regard to durability for reinforcement steel (EC2)

Environmental Requirement for $c_{min,dur}$ (mm)							
Structural Class	**Exposure Class according to Table 4.1**						
	X0	XC1	XC2 / XC3	XC4	XD1 / XS1	XD2 / XS2	XD3 / XS3
S1	10	10	10	15	20	25	30
S2	10	10	15	20	25	30	35
S3	10	10	20	25	30	35	40
S4	10	15	25	30	35	40	45
S5	15	20	30	35	40	45	50
S6	20	25	35	40	45	50	55

ANNEX B: Architectural plans of the building.

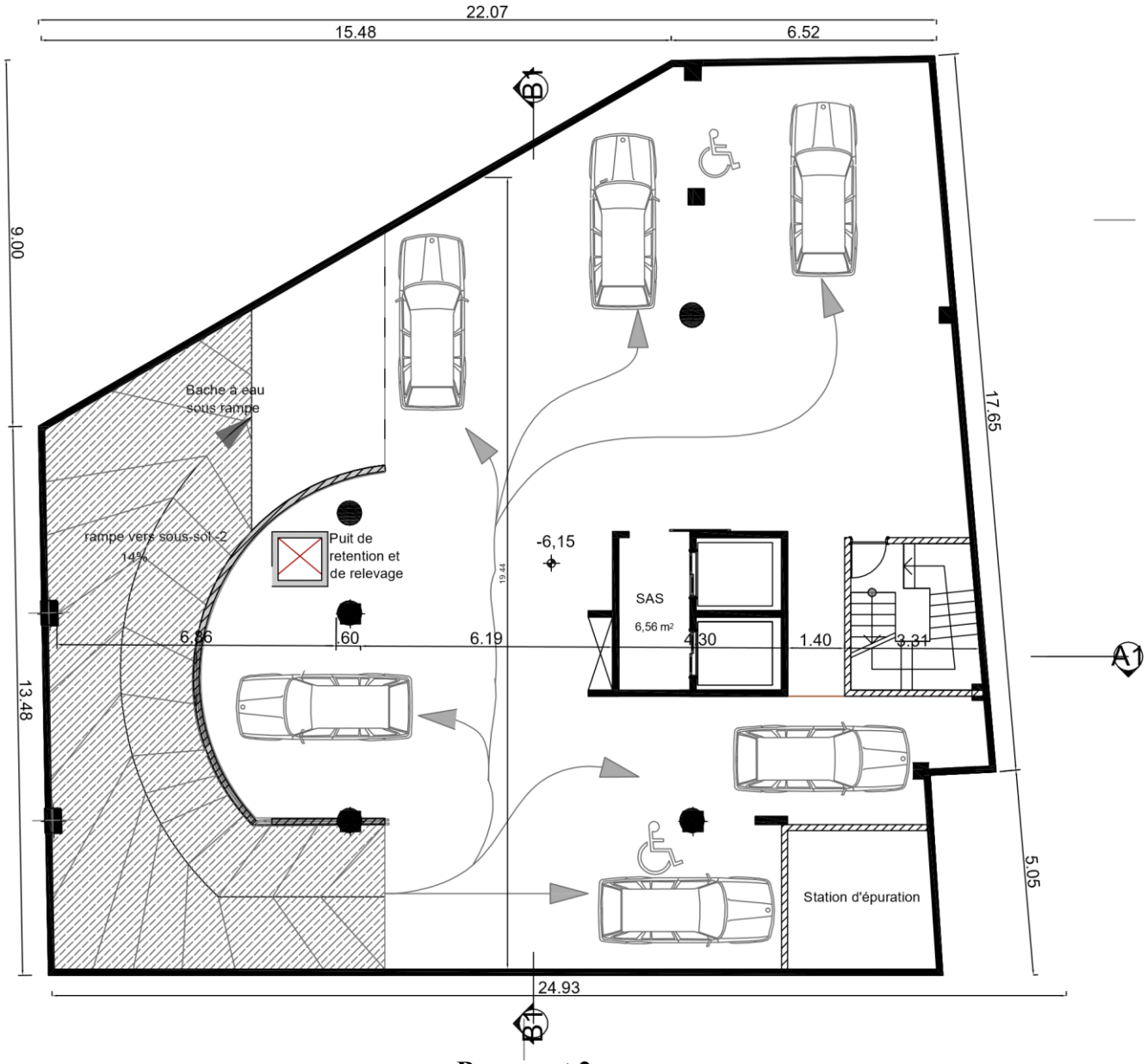

Basement 2

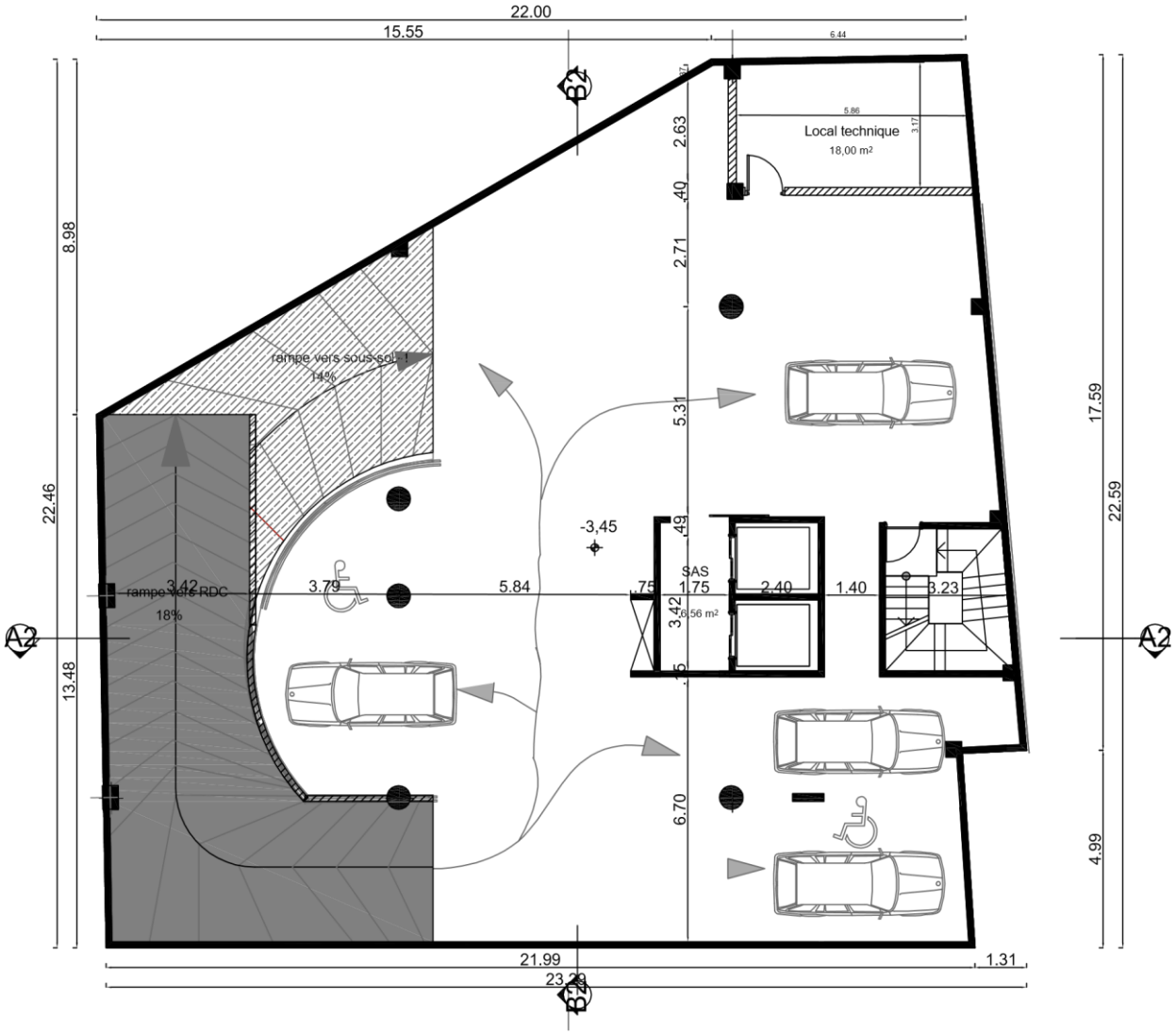
22.00
15.55
6.44
Local technique
18,00 m²
5.86
3.17
2.63
.40
2.71
5.31
.49
.75
SAS
1.75
2.40
1.40
3.23
3.42
6.56 m²
.75
6.70
8.98
22.46
13.48
17.59
22.59
4.99
rampe vers sous-sol
14%
rampe vers RDC
18%
3.42
3.79
5.84
-3,45
A2
21.99
1.31
23.30

Basement 1

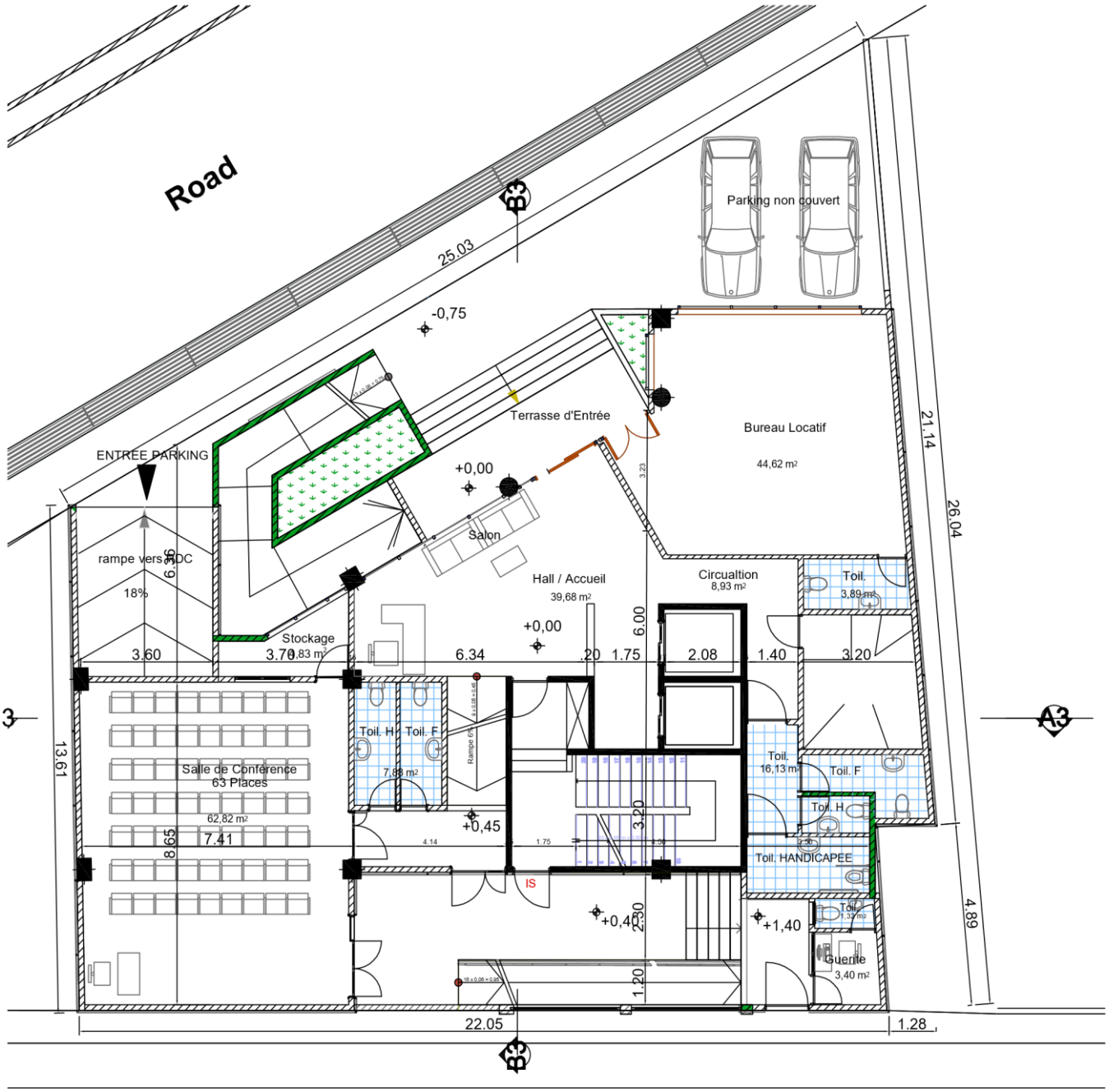

Ground floor

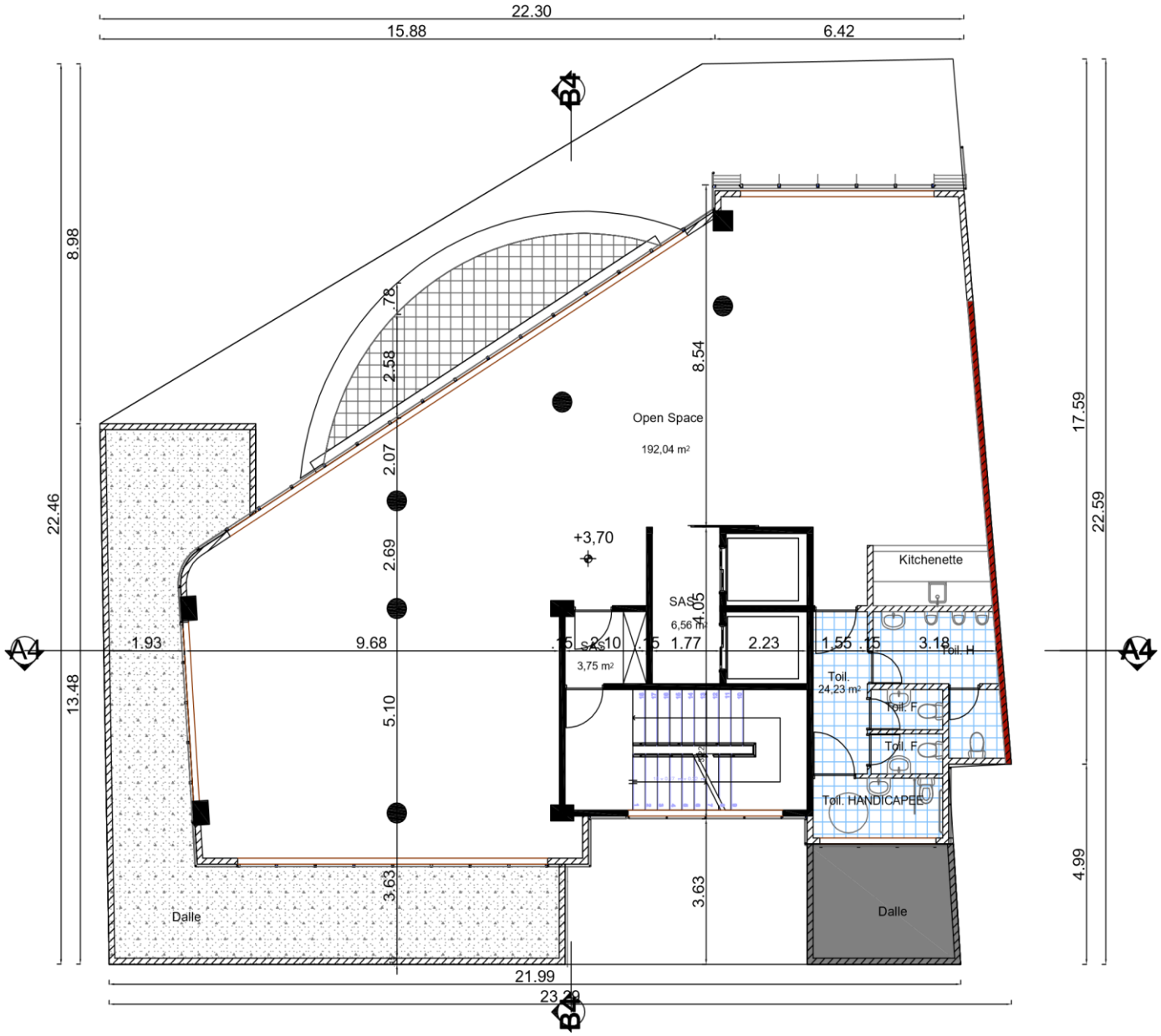
22.30
15.88
6.42
B4
8.98
22.46
13.48
17.59
22.59
4.99
A4
A4
2.78
2.58
2.07
2.69
5.10
3.63
8.54
3.63
Open Space
192,04 m²
+3,70
SAS
6,56 m²
SAS
3,75 m²
4.05
1.93
9.68
.15
2.10
.15
1.77
2.23
1.55
.15
3.18
Kitchenette
Toil. H
Toil.
24,23 m²
Toil. F
Toil. F
Toil. HANDICAPEE
Dalle
Dalle
21.99
23.29
B4

Level 1

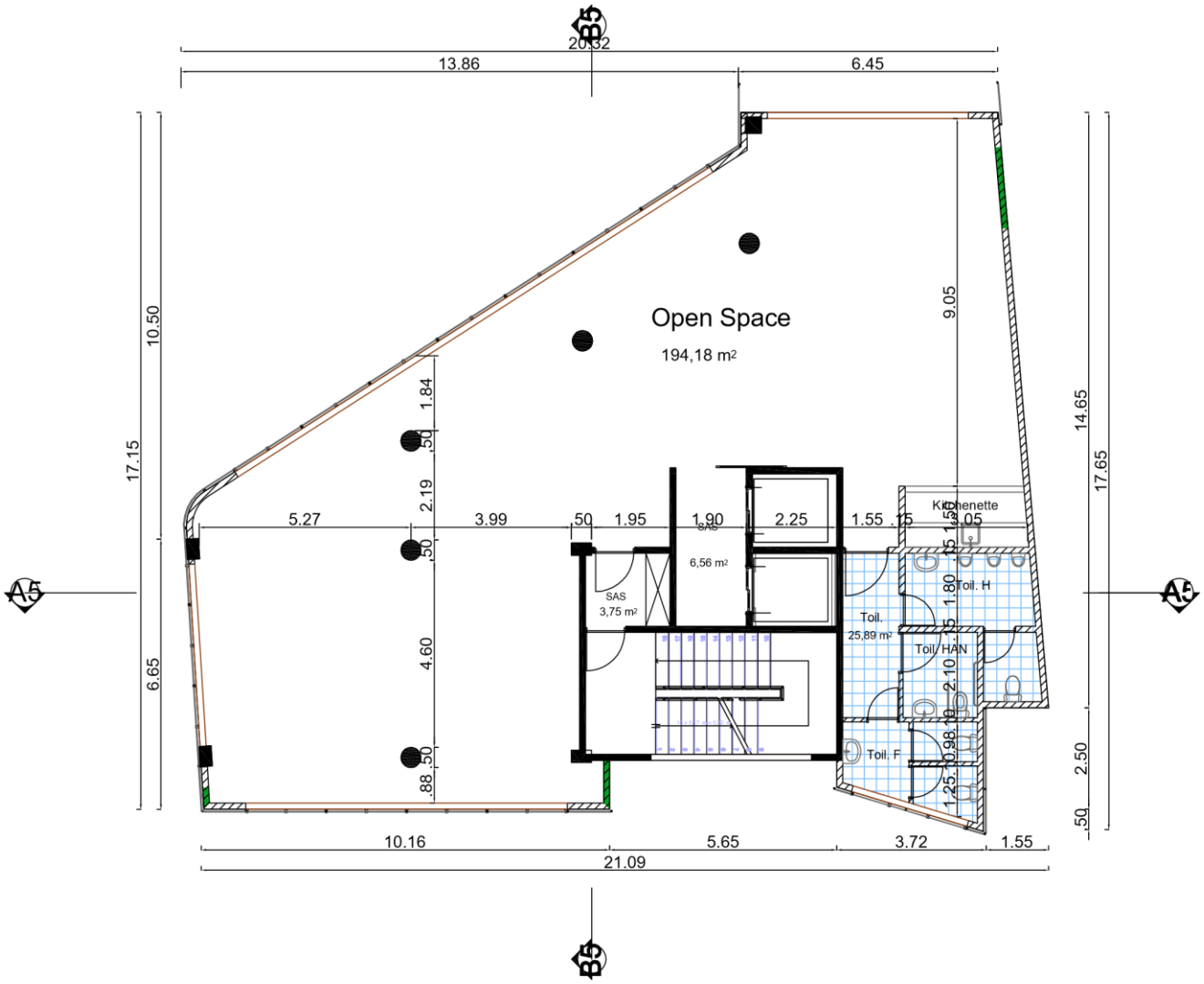
B5
20.32
13.86
6.45
Open Space
194,18 m²
9.05
10.50
17.15
14.65
17.65
1.84
.50
2.19
.50
4.60
.50
.88
6.65
2.50
.50
5.27
3.99
.50
1.95
1.90
2.25
1.55
.15
3.05
SAS
6,56 m²
SAS
3,75 m²
Kitchenette
Toil. H
Toil.
25,89 m²
Toil. HAN
Toil. F
1.80
2.10
.98
1.25
10.16
5.65
3.72
1.55
21.09
A5
A5
B5

Level 2, 3&4

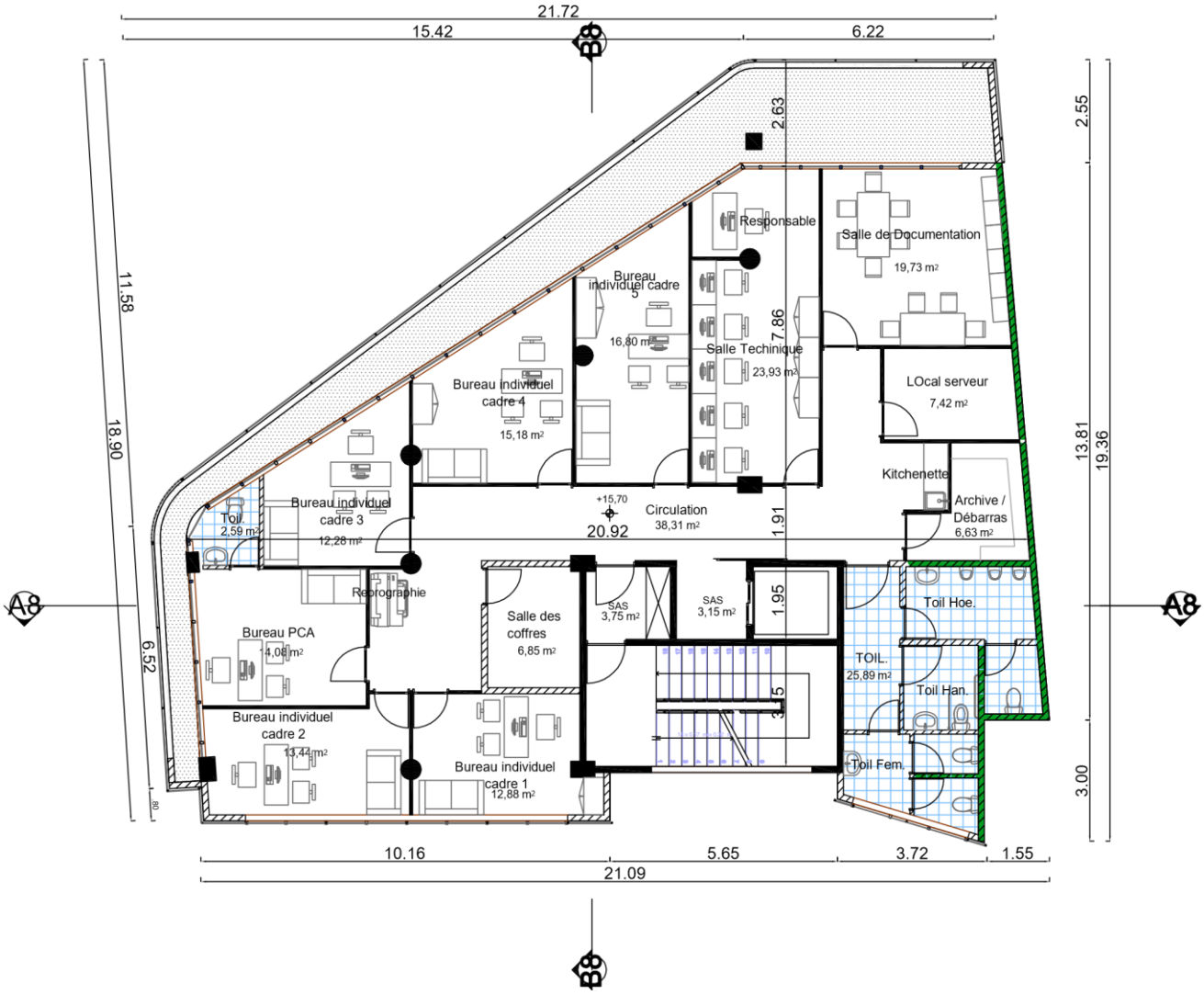
21.72
15.42
6.22
B8
2.63
2.55
11.58
18.90
6.52
80
13.81
19.36
3.00
A8
A8
Responsable
Salle de Documentation
19,73 m²
Bureau individuel cadre 5
16,80 m²
Salle Techinique
23,93 m²
7.86
Bureau individuel cadre 4
15,18 m²
LOcal serveur
7,42 m²
Kitchenette
Archive / Débarras
6,63 m²
Toil
2,59 m²
Bureau individuel cadre 3
12,28 m²
+15,70
20.92
Circulation
38,31 m²
1.91
Reprographie
Salle des coffres
6,85 m²
SAS
3,75 m²
SAS
3,15 m²
1.95
Toil Hoe.
Bureau PCA
4,08 m²
TOIL.
25,89 m²
Toil Han.
3.15
Bureau individuel cadre 2
13,44 m²
Toil Fem.
Bureau individuel cadre 1
12,88 m²
10.16
5.65
3.72
1.55
21.09
B8

Level 5

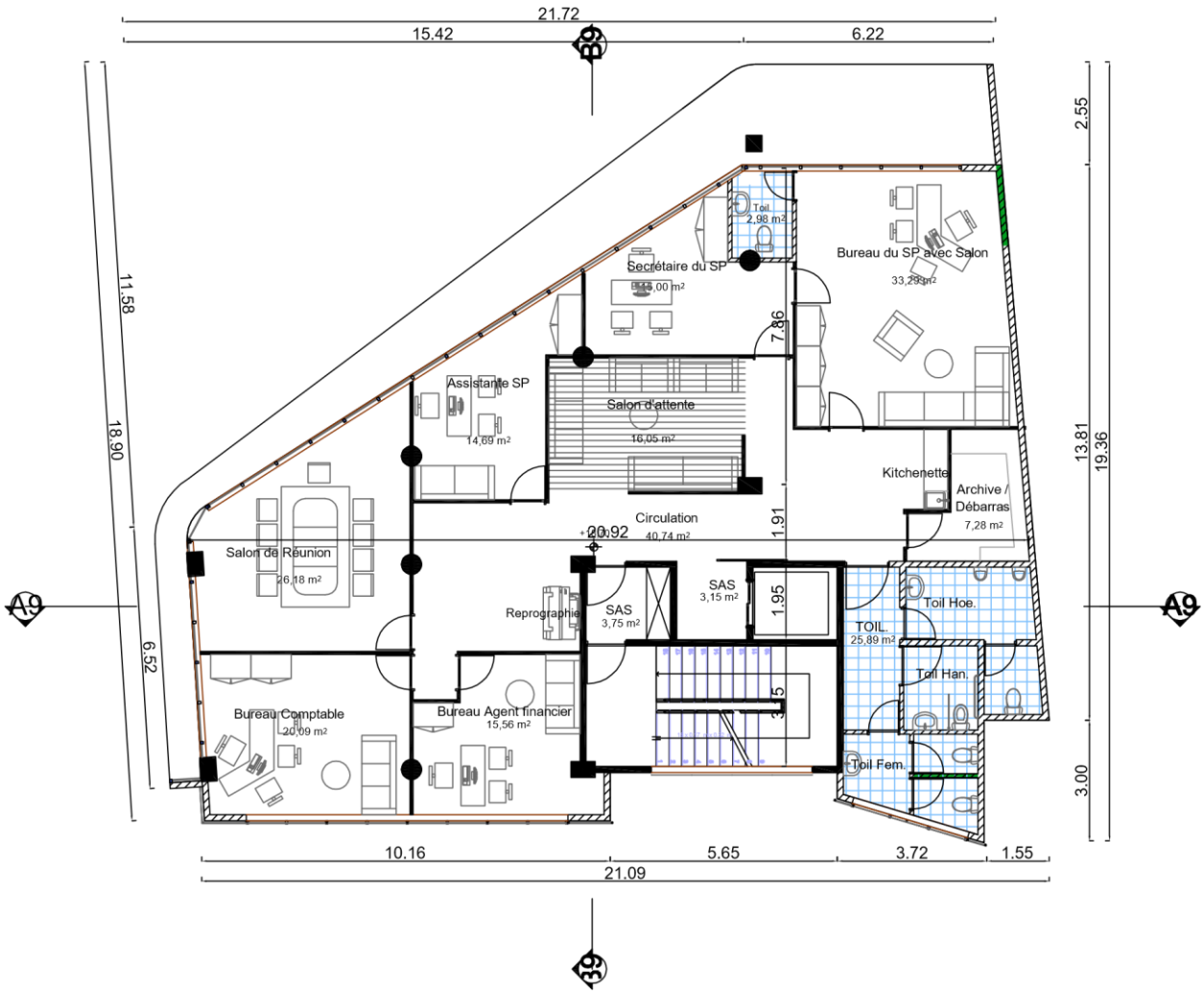
21.72
15.42
6.22
11.58
18.90
6.52
2.55
13.81
19.36
3.00
Téil.
2,98 m²
Secrétaire du SP
Bureau du SP avec Salon
33,29 m²
7.86
Assistante SP
14,69 m²
Salon d'attente
16,05 m²
Kitchenette
Archive /
Débarras
7,28 m²
Circulation
40,74 m²
+20.92
1.91
Salon de Réunion
26,18 m²
Reprographie
SAS
3,75 m²
SAS
3,15 m²
1.95
Toil Hoe.
TOIL.
25,89 m²
Toil Han.
Bureau Comptable
20,09 m²
Bureau Agent financier
15,56 m²
Toil Fem.
A9
A9
10.16
5.65
3.72
1.55
21.09

Level 6

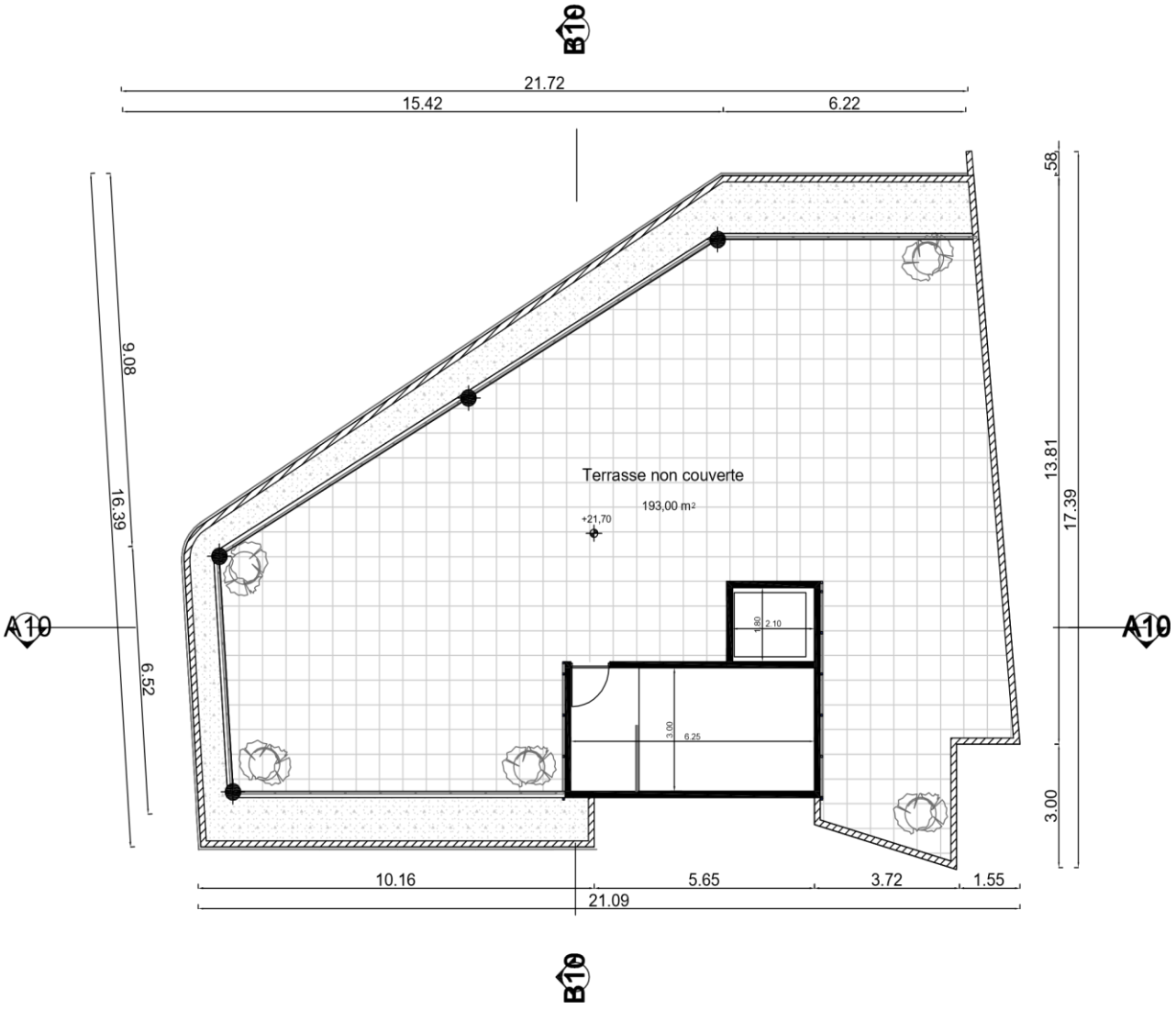
B10
21.72
15.42
6.22
9.08
16.39
6.52
58
13.81
17.39
3.00
Terrasse non couverte
193,00 m²
+21,70
A10
A10
1.60
2.10
3.00
6.25
10.16
5.65
3.72
1.55
21.09
B10

Roof